Concentration-Dependent Effects of Cadmium on Mouse Angiogenesis *In Vitro*

A Thesis Submitted to the Committee on Graduate Studies in Partial Fulfillment of the Requirements for the Degree of Science in the Faculty of Arts and Science

TRENT UNIVERSITY

Peterborough, Ontario, Canada

Environmental and Life Sciences M.Sc. Graduate Program

June 2024

ABSTRACT

Concentration-Dependent Effects of Cadmium on Mouse Angiogenesis *In Vitro*

Caitlyn Knight

Cadmium is a toxic metal that has detrimental effects on blood vessel development and function. To examine the effect of varying concentrations of cadmium on angiogenesis, two *in vitro* assays were used. First, developing yolk sac blood vessels were studied in gestation day 8 mouse embryos exposed to medium alone, 1.25, or 1.75 μM cadmium chloride ($CdCl_2$). Embryos exposed to 1.25 μM cadmium experienced a significant increase in the number of vessels formed; however, they were smaller in size. Vessel morphology and signalling pathways were also investigated using the mouse aortic ring assay, with exposures of 0.0, 0.5, 1.0, 5.0, or 10.0 μM $CdCl_2$. Samples exposed to 10 μM experienced a significant increase in vessel length. However, no significant differences in phosphorylated PTEN and AKT were observed. The results of this study suggest that low levels of cadmium may disrupt angiogenesis, particularly the development of the embryonic vasculature in the yolk sac.

Key Words: Angiogenesis, Vasculogenesis, Cadmium, Vascular Development, Blood Vessels, AKT, PTEN, VEGF, VEGFR, Embryonic Development, Teratogenicity, Fluorescent Staining, Image Analysis, Western Blotting

ACKNOWLEDGEMENTS

As I wrap up this chapter of my life, I would like to extend my sincere gratitude to a number of individuals whose invaluable contributions have made it all possible.

First and foremost, I would like to express my profound appreciation to my supervisor, Dr. Carolyn Kapron, for her guidance and continuous support throughout this research journey. Your expertise and mentorship has been instrumental in shaping the direction of this thesis and my academic growth. I would also like to thank the members of my committee, Dr. Robert Huber and Dr. Stephanie Tobin, for their insightful feedback and valuable suggestions. I am also thankful to Debbie Lietz for her assistance with microscopy and to Jason Allen for his dedicated support in animal care.

I would especially like to thank my family and friends for their unwavering love, encouragement, and understanding throughout this challenging yet rewarding journey. To my parents, thank you for always reminding me that with determination, I can achieve anything I set my heart on and reach for the stars. Kennedy, thank you for always being my number one fan; I know I can always turn to you in moments of doubt. Your belief in me has been a constant source of motivation. To my friends, while I know I may not have been a walk in the park, I could always count on you for the laughter and joy you brought me. Whether through late nights at DNA, endless rants and discussions, ice cream trips, or being there for me during moments of tears (or crying with me), your presence has made this experience infinitely richer and more meaningful.

To all mentioned and those unmentioned, I extend my heartfelt thanks for being a part of this remarkable journey.

TABLE OF CONTENTS

LIST OF FIGURES

LIST OF APPENDICES

LIST OF ABBREVIATIONS

Aβ – Amyloid β
Ang-1 – Angiopoietin 1
Apaf-1 – Apoptotic Protease-Activating Factor
APS – Ammonium Persulfate
BAD – Bcl-2 Family Protein
bFGF – Basic Fibroblast Growth Factor
BSA – Bovine Serum Albumin
CAM – Chorioallantoic Membrane
CLS – Capillary-Like Structures
Cyto c – Cytochrome-c
DLL4 – Delta-Like Ligand 4
DMT1 – Divalent Metal Transporter 1
DNA – Deoxyribonucleic Acid
EC – Endothelial Cell
GLUT – Glucose Transporter
HIF-1α – Hypoxia-Inducible Factor 1α
HUVEC – Human Umbilical Vein Endothelial Cells
IAR – Intussusceptive Arborization Remodelling
IBR – Intussusceptive Branching Remodelling
IMG – Intussusceptive Microvascular Growth
JNK – c-Jun N-Terminal Kinase
NO – Nitric Oxide
MAPK – Mitogen-Activated Protein Kinase
MDM2 – Murine Double Minute 2
MLK3 – Mixed Lineage Kinase 3
MMP – Matrix Metalloproteinases
MT – Metallothionein
MVD – Microvascular Density
mTORC1 – Mammalian Target of Rapamycin Complex 1
PDGF-B – Platelet Derived Growth Factor B
PDK1 – 3-Phosphoinositide-Dependent Protein Kinase 1
PDK2 – 3-Phosphoinositide-Dependent Protein Kinase 2
PECAM-1 – Platelet Endothelial Cell Adhesion Molecule
PI3K – Phospatidylinositol-3 Kinase
PIP2 – Phosphatidylinositol (3,4)-Bisphosphate
PIP3 – Phosphatidylinositol (3,4,5)-Trisphosphate
PTEN – Phosphate and Tensin Homolog
RA – Rheumatoid Arthritis
RNA – Ribonucleic Acid

ROS – Reactive Oxidative Species
TGF-β – Transforming Growth Factor-β
TSC1 – Tumour Suppressor Protein Tuberous Sclerosis 1
TSC2 – Tumour Suppressor Protein Tuberous Sclerosis 2
t-SNARE –Target Membrane-Soluble N-Ethylmalemide Attachment Protein Receptor Syntaxin-6
VEGF – Vascular Endothelial Growth Factor
VEGFR – Vascular Endothelial Growth Factor Receptor
WEC – Whole Embryo Culture
ZIP8 – 8-Transmembrane Zinc-Related Iron-Related Protein

1 INTRODUCTION

1.1 Cadmium: Properties, Routes of Exposure, and Toxicology

Some heavy metals, such as iron and zinc, are essential nutrients with important biological functions (Rengel, 1999). However, cadmium is highly toxic heavy metal that has no known biological function. Natural sources of cadmium are one of the main contributors to cadmium body burden. Natural emissions include weathering rocks, airborne soil particles, forest and bushfires, sea salt, volcanic emissions, and meteoric dust (Kubier et al., 2019). Anthropogenic sources also contribute to toxicity with cadmium emission resulting from non-ferrous metal production, fossil fuel combustion, phosphate fertilizer manufacturing, road dust, iron, steel, and cement production, and municipal and sewage sludge incineration (Kubier et al., 2019; Pacyna and Pacyna 2001). Although cadmium emissions have decreased over the past 50 years, natural and anthropogenic cadmium pollution is a worldwide problem affecting food and drinking resources, primarily in Asia and Africa (Kubier et al., 2019). In Canadian and American populations, cadmium blood concentrations are similar, with highest levels found in adult females (Akesson et al., 2002; Berglund et al., 1994). Women tend to have a greater frequency of iron deficiency and smaller stores, which can increase gastrointestinal cadmium absorption and, ultimately, lead to higher blood cadmium levels (Kubier et al., 2019; Smereczański and Brzóska, 2023). Iron deficiency increases divalent metal transporter 1 (DMT1), which is a common transporter for both iron and cadmium, thus individuals with low iron stores are more likely to have an increased affinity for cadmium (Leazer et al., 2002; Tallkvist et al., 2001). This being said, individuals working in careers in automotive or industrial occupations are particularly at risk (Kim et al., 2012; Prozialeck et al., 2006). Exposure varies geographically, with Asian countries having

higher industrial exposure rates than European and North American countries, predominantly due to their larger production stores (Chunhabundit, 2016).

Cadmium toxicity was identified before the end of the 19th century, but the risk associated with cadmium in soil was not discovered until the endemic bone disease itai-itai, which results in fractures and severe pain, appeared in Japan (Smolders and Mertens, 2013). This endemic was linked to rice paddies irrigated with cadmium-contaminated water drained from a metal mining area. Cadmium toxicity causes kidney tubular dysfunction, leading to increased calcium excretion and, ultimately, osteomalacia (Smolders and Mertens, 2013). Cadmium is naturally present in all soils; however, current concentrations are higher than historical geogenic values (Kubier et al., 2017; Liu et al., 2017). Cadmium exists in soil as a divalent cation and is enriched by human activities related to atmospheric deposition, phosphate fertilizers, and sewage sludge (Kim et al., 2012; Smolders and Mertens, 2013; Wei et al., 2017; Xiong et al., 2021). Although cadmium is unlikely to affect the chemistry of the soil, its long-term effects on the ecosystem are pronounced because of its persistent toxicity and bioavailability (Smolders and Mertins, 2013). Similar to rice, tobacco accumulates higher levels of cadmium. Cadmium-filled smoke is efficiently absorbed by the lungs, increasing the amount of cadmium in the body. Thus, cadmium exposure can also arise from non-occupational routes, including tobacco smoke and crop ingestion (Kim et al., 2012; Wei et al., 2017; Xiong et al., 2021).

Non-occupational routes of exposure generally involve chronic exposure to low concentrations; however, cadmium has a biological half-life of 15-30 years (Kim et al., 2012; Prozialeck et al., 2006). Due to its non-biodegradable nature and long biological half-life, cadmium can accumulate in environmental organic matter, ultimately

contaminating the food chain and environment. Cadmium can also bioaccumulate over time in humans, increasing the total burden on the body. The provisional maximum tolerable daily intake defined by the World Health Organization is 25 ug/kg body weight per month (62 ug/day for a 70 kg person) (FAO/WHO, 2021). For an average diet, cadmium intake is 4.63 μg per day, but tobacco smokers, individuals living in contaminated areas or those with a higher cadmium dietary intake may surpass the recommended tolerable intake (Hanson et al., 2012; Kim et al., 2018). Blood cadmium concentrations, which vary depending on gender and socioeconomic conditions, typically range from 0 μM to 0.05 μM (Branca et al., 2018). For example, rice consumption is one of cadmium's major routes of exposure to humans, with East Asia, China, and Japan holding the highest grain cadmium levels, while Western countries had lower levels (Shi et al., 2020; Smolders and Mertens, 2013).

Cadmium absorption takes place primarily through the respiratory and gastrointestinal tracts. Following absorption, it is transported into the bloodstream, where it binds to albumin and other thiol-containing proteins (Genchi et al., 2020). These cadmium-associated proteins are then able to enter erythrocytes through transport proteins such as DMT1, metal transport protein 1, calcium channel proteins, and the 8-transmembrane zinc-related iron-related protein (ZIP8) (Klaassen et al., 2009; Wang et al., 2016). Cadmium bound to erythrocytes is brought to the liver via blood, where it begins to accumulate and induce the synthesis of metallothionein (MT) (Sabolić et al., 2010). Cadmium becomes bound to MT and is mainly stored in the liver; however, trace amounts are released into the blood, and redistribution to the kidney occurs (Mezynska and Brzóska, 2018; Sabolić et al., 2010). Subsequently, cadmium-MT complexes are filtered by the renal glomeruli and pass into the tubular fluid. Inside the renal tubules,

cadmium ions are released from the cadmium-MT complexes and are reabsorbed by the proximal tubule cells. Cadmium cannot be detoxified once bound to the MT protein, causing it to accumulate (Bharathiraja et al., 2013; Genchi et al., 2020; Mezynska and Brzóska, 2018; Prozialeck and Edwards, 2012; Wang et al., 2016). Trace amounts of cadmium are transferred from the renal tubule and excreted via feces and urine; however, the majority becomes trapped in the tissue (Nordberg and Nordberg, 2022). With initial exposure, cadmium concentrations are the highest in the liver, but over time, cadmium is redistributed to the kidney, where it begins to build up (Klaassen and Liu, 1997; Klaassen et al., 2009). This is because of the long biological half-life of cadmium, causing it to accumulate in the kidney cortex and liver. With constant accumulation during the human lifespan and increased exposure, liver and kidney dysfunction may arise (Ferraro et al., 2010; Nordberg and Nordberg, 2022; Järup, 2002; Zhu et al., 2022). Accumulation of cadmium generally occurs predominantly in the kidneys and liver but is also associated with damage to the reproductive, cardiovascular, respiratory, and renal systems (Figure 1) (Fagerberg et al., 2012; Järup, 2002; Thompson & Bannigan, 2008). Cadmium-linked neurotoxicity is another common side effect of exposure with its relation to neurodegenerative diseases such as Alzheimer's and Parkinson's disease (Figure 1) (Buée et al., 1994; Notarachille et al., 2014; Rahimzadeh et al., 2017).

Cadmium complexes are taken up through various channels and carriers where they accumulate intracellularly, disrupting gene regulation and intracellular signalling networks (Thévenod et al., 2019). Cadmium affects cell cycle progression, proliferation, and repair, as well as the regulation of apoptotic pathways (Bertin and Averbeck, 2006; Dong et al., 2001; Fang et al., 2002; Oh and Lim, 2006; Yang et al., 2004a). Various concentrations cause different cytotoxic effects. At elevated cytotoxic concentrations,

DNA, RNA, and protein biosynthesis is inhibited. Although not directly genotoxic, cadmium indirectly induces single-strand breaks and mutagenic lesions in DNA through a decrease in cellular antioxidants and an increase in oxidative stress (Figure 1) (Bertin and Averbeck, 2006; Mikhailova et al., 1997; Waalkes, 1984; Waisberg et al., 2003). It can also induce lipid peroxidation and chromosome aberrations (Beyersmann and Hechtenberg, 1997; Branca et al., 2018; Mendez-Armenta and Ríos, 2007).

Cadmium exposure is known to increase the risk of cancer due to its oncogenic properties and its role in the dysfunction of critical signalling pathways (Figure 1) (Wei et al., 2017). Non-genotoxic effects of cadmium include an upregulation in intracellular signalling pathways (Beyersmann and Hechtenberg, 1997). This can increase mitogenesis, cell proliferation, and DNA synthesis by stimulating the expression of various types of genes, including proto-oncogenes. Such carcinogenic properties are induced through multifactorial processes, including the upregulation of mitogenic signalling pathways and the indirect effects of genotoxicity (Beyersmann and Hechtenberg, 1997).

Cadmium has been found to exert toxic effects through diverse mechanisms including DNA damage, changes in gene expression, oxidative stress and apoptosis (Đukić-Ćosić et al., 2020). Studies addressing this issue have noted cadmium's biochemical, metabolic, and cytotoxic effects on the vascular network. The vascular network plays a vital role in the diffusion exchange of metabolites and nutrients, and it is therefore important to understand how cadmium interferes with vascular development (Adair and Montani, 2010; Carmeliet and Jain, 2000).

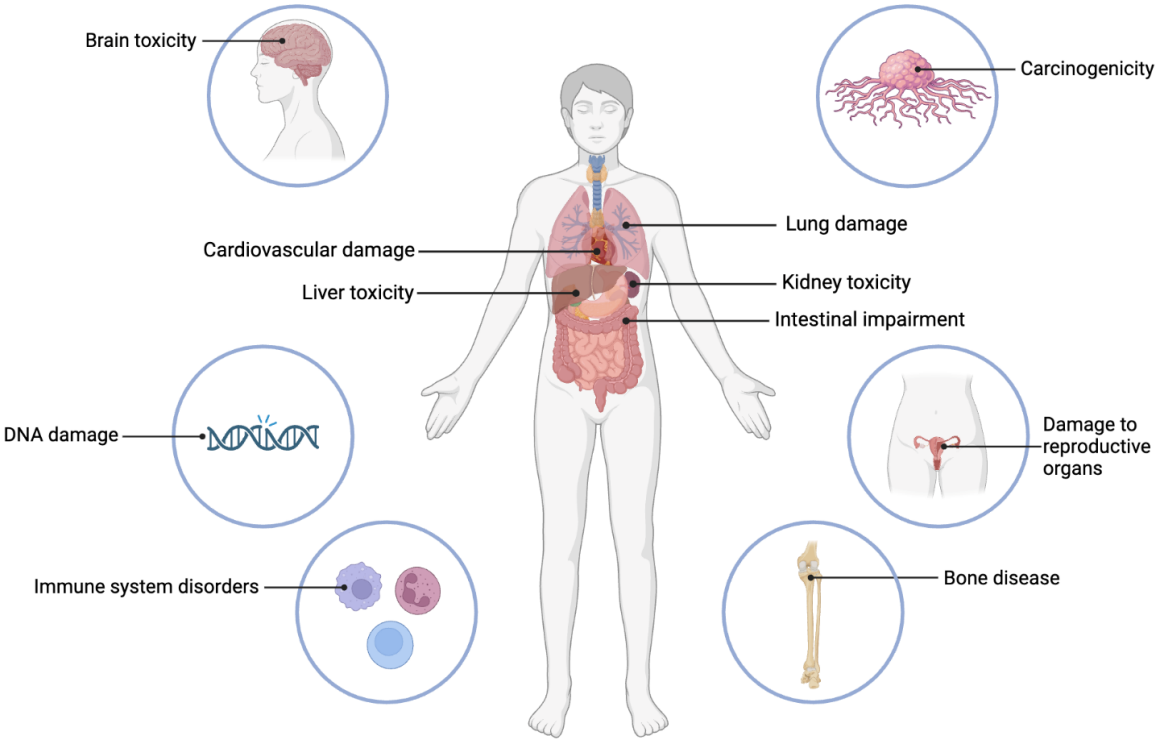

Figure 1. Possible outcomes of cadmium toxicity on different organ systems in the human body. Image adapted from Peana et al., (2023). Created with Biorender.com

1.2 Vasculogenesis and Angiogenesis

1.2.1 The importance of angiogenesis

A better understanding of cadmium toxicity may reside in determining its effects on angiogenesis, the development of capillaries from pre-existing vessels. Angiogenesis is a crucial element in the physiological processes of neovascularisation, which refers to the normal development of blood vessels (Adair and Montani, 2010). It is required in embryogenesis, cardiovascular maturation, tissue repair and regeneration processes. Due to the importance of the diffusion exchange of metabolites and nutrients, metabolically active tissues are no more than a few micrometres away from capillaries (Adair and Montani, 2010; Bremnes et al., 2006; Carmeliet and Jain, 2000; Risau and Flamme, 1995). However, the angiogenic process needs to maintain a delicate balance during

embryonic development and adulthood, as dysregulated angiogenesis may contribute to pathological conditions such as cancer, macular degeneration, and retinopathy, as well as impaired repair of ischemic tissues (Bremnes et al., 2006; Carmeliet, 2005; Risau and Flamme, 1995; Sewduth and Santoro, 2016; Tonini et al., 2003).

For new blood vessels to arise, expression of pro-angiogenic growth factors is required, including vascular endothelial growth factor (VEGF). The physiological effects of VEGF are mediated through its interaction with its receptor, vascular endothelial growth factor receptor (VEGFR) (Lugano et al., 2020; Marmé and Fusenig, 2008; Risau and Flamme, 1995). Under hypoxic situations, VEGF is upregulated, which orchestrates blood vessel formation via activation of VEGFR and downstream signalling pathways. This leads to specific endothelial responses, promoting vascular permeability, cell proliferation, migration, and differentiation (Lugano et al., 2020; Marmé and Fusenig, 2008; Risau and Flamme, 1995). Thus, this process increases oxygen delivery and ultimately promotes vascularization.

1.2.2 Sprouting angiogenesis

The cellular mechanisms governing angiogenesis are well documented. Interactions among endothelial cells orchestrate this process, primarily through sprouting angiogenesis. Sprouting angiogenesis is initiated in poorly perfused tissues under hypoxic conditions, stimulating the need for new blood vessels (Chen et al., 2019; Sewduth and Santoro, 2016). During angiogenic sprouting, endothelial cells compete with one another for a leading tip position. This competitive nature is regulated by the Notch-VEGFR negative feedback loop and is associated with two types of endothelial cells: tip cells and stalk cells. Tip cells express higher amounts of VEGFR and rely on Delta-like Ligand 4

(DLL4)-Notch signalling, which is important for their specification (Chen et al., 2019; Sewduth and Santoro, 2016). Since tip cells have a greater abundance of VEGFR, they are more likely to receive a greater abundance of VEGF and thus express higher levels of DLL4. Conversely, adjacent endothelial cells have lower levels of DLL4. Therefore, they cannot activate Notch signalling nor turn into stalk cells (Figure 2) (Chen et al., 2019; Sewduth and Santoro, 2016).

Endothelial tip cells guide the developing capillary sprout toward the VEGF stimulus via long, thin cellular processes known as filopodia. Filopodia are heavily endowed with VEGFR, allowing them to sense different VEGF concentrations, ultimately giving the sprouting phenotype to these cells (Chen et al., 2019; Sewduth and Santoro, 2016). VEGF signalling induces the expression of DLL4, which activates Notch signalling in neighbouring stalk cells. This causes the downregulation of VEGFR expression, giving stalk cells a non-sprouting quiescent phenotype (Figure 2) (Blanco and Gerhardt, 2013). This phenotype is vital for stalk cells because of its importance in acquiring barrier formation and polarity. Additionally, the Notch pathway interacts with the Wnt pathway, which is essential in inducing the transcription of Platelet-Derived Growth Factor B (PDGF-B), leading to the recruitment of mural cells (Chen et al., 2019; Sewduth and Santoro, 2016). This pathway is also responsible for stabilizing tight junctions and maintaining the polarity of the vessel through the apicobasal polarization of endothelial cells. Polarization is vital for vessel lumenization since one side of the endothelial cell is in contact with blood flow while the other is attached to the basement membrane (Chen et al., 2019; Sewduth and Santoro, 2016).

The competitive nature of these two endothelial cell types continues throughout angiogenesis since endothelial cells are constantly migrating and elongating, primarily

guided by lamellipodia and filopodia. Tip cells are challenged and replaced during this process by migrating stalk cells (Chen et al., 2019). Since non-neighbouring stalk cells do not receive inhibitory signals from tip cells, they can replace tip cells, sending the pre-existing tip cell to the basement membrane and causing its conversion to a stalk cell. Shuffling during sprouting angiogenesis allows intricate branching and sprouting, leading to a robust network formation (Chen et al., 2019). The proliferation of endothelial cells enables the capillary sprout to elongate. When tip cells of adjacent capillary sprouts meet at the source of VEGF, they fuse, creating a continuous lumen (Figure 2) (Adair and Montani, 2010). This creates a space where oxygenated blood can flow, supplying tissues with adequate amounts of oxygen. Once this process is complete, VEGF levels return to normal, and the capillaries are stabilized with the recruitment of pericytes to encase the vessel (Adair and Montani, 2010; Bremnes et al., 2006; Carmeliet and Jain, 2000; Chen et al., 2019; Kolte et al., 2016; Lugano et al., 2020; Potente et al., 2011; Rajabi and Mousa, 2017).

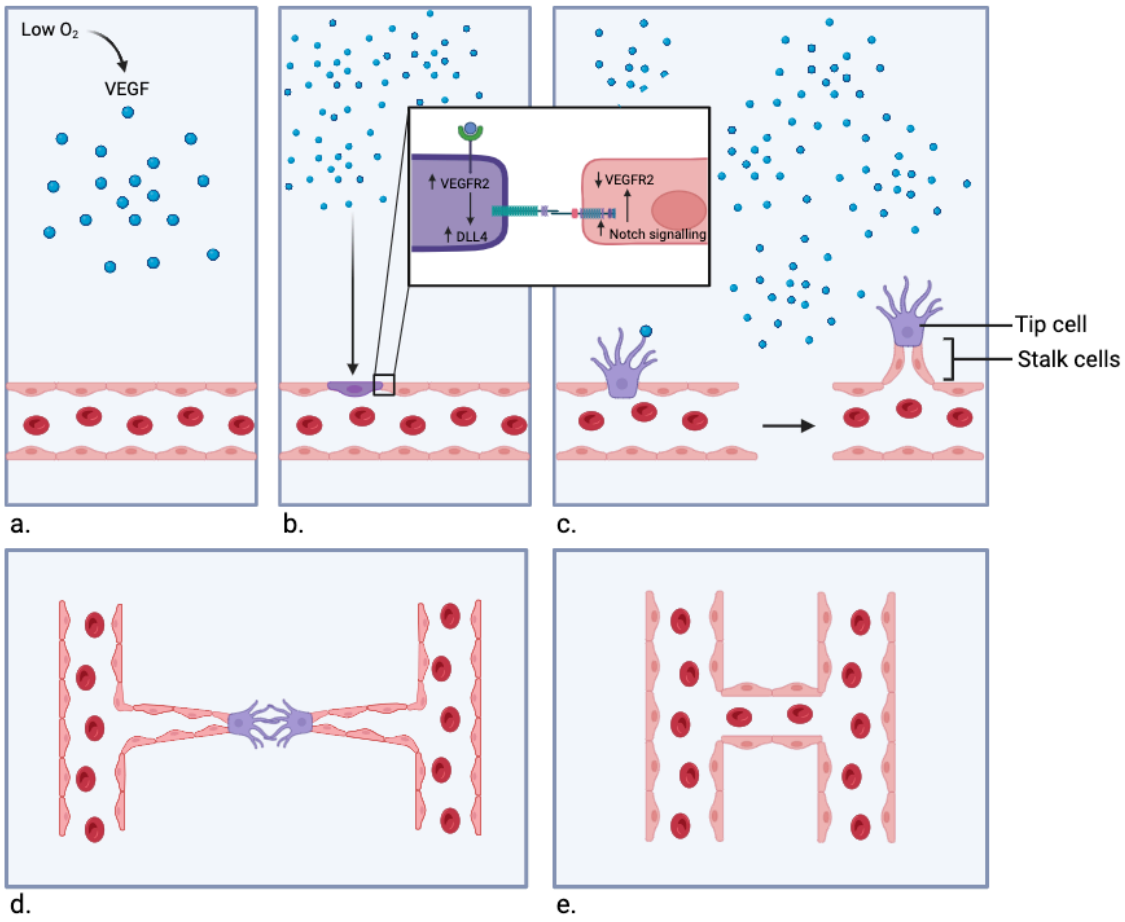

Figure 2: Graphic sequence demonstrating the process of sprouting angiogenesis. The following stages are illustrated: (a) Angiogenesis is stimulated in regions of low oxygen, inducing VEGF production and quiescent endothelial cells (pink); (b) once stimulated, quiescent endothelial cells convert into a tip cell phenotype (purple) and tip cell competition occurs via DLL4-notch signalling. Tip cells produce filopodia that are densely packed with VEGFR, enabling tip cells to extend toward the source of VEGF through cell division; (d & e) through VEGF signalling and the rearrangement in tight junctions, two luminal segments integrate to create the anastomosis. Image adapted from Hendriks and Ramasamy (2020). Created with Biorender.com

1.2.3 Intussusceptive angiogenesis

Initially, sprouting angiogenesis was thought to be the only process of angiogenesis; however, intussusceptive angiogenesis was discovered for its role in vascular remodelling (De Spiegelaere et al., 2012). Intussusceptive angiogenesis is also commonly referred to as splitting angiogenesis because it results in a single vessel being

divided into two. This occurs through the extension of the vessel wall into the lumen, allowing it to split (Adair and Montani, 2010). There are three forms of intussusceptive angiogenesis: intussusceptive microvascular growth (IMG), intussusceptive arborization remodelling (IAR), and intussusceptive branching remodelling (IBR) (Karthik et al., 2018).

Intussusceptive microvascular growth initiates the expansion of the primordial capillary network, increasing surface area and establishing organ angioarchitecture (Vasudev and Reynolds, 2014). The reorganization of endothelial cells invades surrounding interstitial tissue, pericytes, and myofibroblasts and deposits collagen fibrils. Collagen deposits lead to the subsequent expansion during IAR (Makanya, 2009). After IMG expands the vascular network, IAR adapts the vasculature into a typical vascular tree pattern by altering branching (De Spiegelaere et al., 2012). The original pattern of vessels from vasculogenesis or sprouting angiogenesis lacks the organization and meshwork resembling the tree-like arrangement of matured vasculature (Vasudev and Reynolds, 2014). The arborization of these vessels creates the structure of the vascular tree. Connective tissue columns, or tissue pillars, vertically form in rows in the lumen. Subsequent rows of these pillars increase the density of the vascular network and create generations of future vessels for feeding and draining (Djonov and Makanya, 2005, Vasudev and Reynolds, 2014). After expansion and remodelling, IBR prunes the vascular network to optimize perfusion and minimize the presence of unnecessary vessels (Djonov et al., 2003). Branching remodelling is accomplished through the insertion of transluminal pillars at the branching points of the horizontal pillars (Djonov et al., 2002). This allows the branching points to relocate and change blood flow properties, creating eccentric

pillars. The target branch increases in size and fuses, resulting in the ablation of the vessel and, ultimately, vascular pruning (Djonov et al., 2002).

Intussusceptive angiogenesis only occurs on pre-existing vasculature and is crucial in remodelling. It is faster and more efficient in comparison to sprouting angiogenesis. Since it reorganizes existing endothelial cells rather than relying on endothelial proliferation and migration, it appears more economical from an energetic and metabolic perspective (Burri and Djonov, 2002). It occurs during embryonic development, as well as in pathological conditions, such as tumorigenesis, and physiological adaptations commonly demonstrated in exercised muscles (Djonov et al., 2003; Garcia and Larina, 2014; van Royen et al., 2001). The stimuli for this type of angiogenesis can be physiological adaptations such as shear stress or local biochemical alterations (Milkiewicz et al., 2008; van Royen et al., 2001). Endothelial cells can sense shear stress and transduce a molecular signal leading to transcriptional proteins, including eNOS and other angiogenic factors (Fisher et al., 2001; Osawa et al., 2002; Zakrzewicz et al., 2002).

1.2.4 Gestational development of mice

The allocation of extraembryonic lineages in mouse embryos is a critical step in their early development. This is important for maternal-fetal communication as well as nutrient exchange. Embryonic fate during pre-implantation stages relies on cell polarization, establishing cell-cell junctions, and acquiring an epithelial state (Rivera-Pérez and Hadjantonakis, 2015; Viotti et al., 2011). During the late implantation stage of the blastocyst (E4.5), the embryo consists of three lineages: trophectoderm, primitive endoderm, and epiblast. The trophectoderm gives rise to trophoblastic tissues, such as the

chorion, ectoplacental cone and extraembryonic ectoderm. The primitive endoderm generates the endoderm of the visceral and parietal yolk sacs (Rivera-Pérez and Hadjantonakis, 2015; Viotti et al., 2011). The visceral yolk sac is crucial in fulfilling embryonic nutrition and protection until the chorioallantoic placenta is established. Lastly, the epiblast helps establish adult mouse tissues and the fetal portion of the placenta (Rivera-Pérez and Hadjantonakis, 2015; Viotti et al., 2011).

Within the epiblast, the primitive streak forms, defining the future posterior of the embryo (E6.5). This is also the site of gastrulation, where the epiblast generates the mesoderm, ectoderm and definitive endoderm. During gastrulation, epithelial cells undergo epithelial-mesenchymal transition, facilitating the migration and invasion of mesenchymal cells into the space between the visceral endoderm and epiblast (Rivera-Pérez and Hadjantonakis, 2015; Viotti et al., 2011). The primitive streak elongates distally, stopping when it reaches the tip of the embryo (E7.5). Cell fate is determined during this period depending on where and when they leave the streak. The first lineages to emerge from the streak are the mesoderm of the yolk sac, the chorion, and blood islands (Figure 3) (Rivera-Pérez and Hadjantonakis, 2015; Viotti et al., 2011).

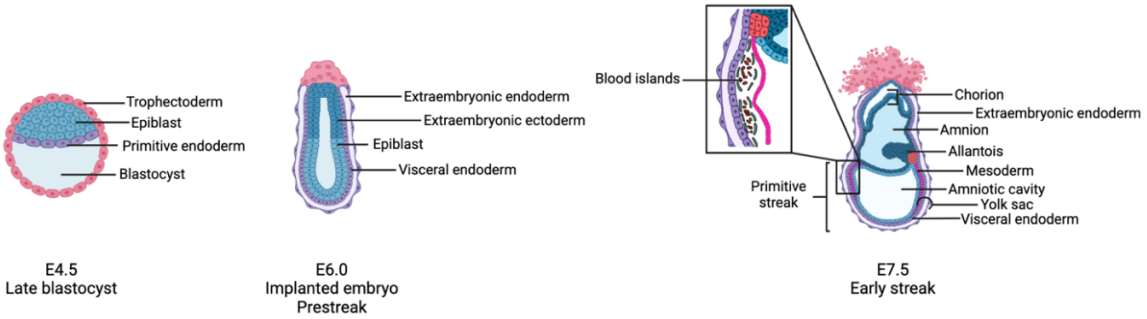

Figure 3: Schematic representation of mouse embryo development prior to and after implantation. Shortly after implantation, the blastocyst elongates to form an egg cylinder resembling a bilaminar cup-shaped epithelial structure, with the visceral endoderm encapsulating the epiblast and extraembryonic endoderm (E5.5). By E7.5, the primitive streak elongates, forming the primitive streak and mesoderm of the yolk sac. Image adapted from Kafer and Cesare (2020) and Ferkowicz and Yoder (2005). Created with Biorender.com

By day 8 of gestation (E8), embryos can be identified by the presence of 1-7 pairs of somites, and a visible allantois, connecting maternal circulation to embryonic blood vessels of the placenta. However, vasculogenesis of the yolk sac begins at E7.5, in which the aggregation of angioblasts creates blood vessels. Mesodermal cell masses proliferate and differentiate to form both the vitelline veins and blood islands (Figure 3) (Ferkowicz and Yoder, 2005). Blood islands begin forming in the proximal yolk sac, primarily near the site of maternal attachment. Shortly after, growing blood islands are partially covered by endothelial cells, which begin to divide and remodel the blood islands into blood-filled capillary beds (Ferkowicz and Yoder, 2005). By day 9 of gestation, the embryo starts turning and by E9.5, the embryo has successfully turned and is fully encapsulated by both the yolk sac as well as the amniotic and exocoelomic cavities (Figure 4) (San Roman et al., 2016; Viotti et al., 2011; Xu et al., 2021).

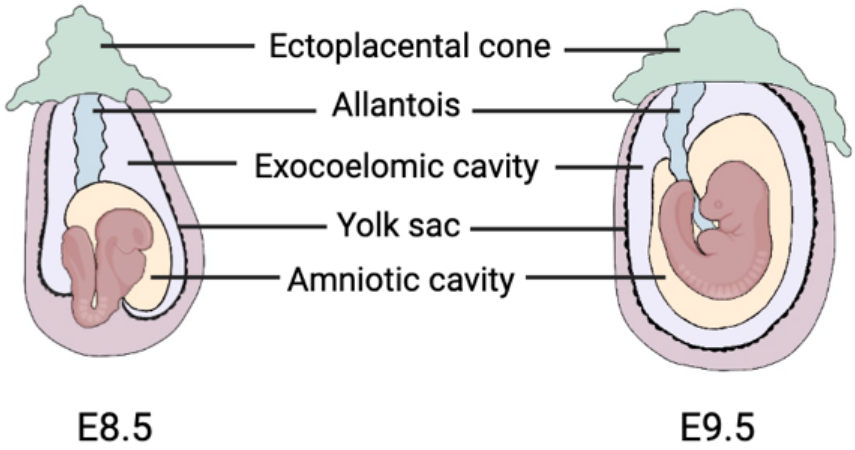

Figure 4: Simplified diagram illustrating the conformational turning of the embryo. At 8.5 days of gestation, 8-10 somites are present before embryonic turning and inversion of extraembryonic membranes. During day 9, the embryo turns, resulting in the inversion of germ layers. The once inner ectoderm is now the outer aspect of the embryo, while the endoderm is on the inner part, with the mesoderm separating the two. The midgut, once continuous with the yolk sac endoderm, is formed during this process. Due to its new positioning on the embryo's inner side, the vitelline duct's subsequent formation follows. The amnion and yolk sac encapsulate the embryo with the newly turned position. Image adapted from Kafer and Cesare (2020).

1.2.5 The importance of vasculogenesis in embryonic development

During embryonic development, blood vessels form through vasculogenesis and angiogenesis. Vasculogenesis refers to the aggregation of angioblasts, creating a blood vessel. In the first phase of vasculogenesis, cells migrate from the primitive streak to the ventral mesoderm, where they become hemangioblasts (Drake and Fleming, 2000; Risau and Flamme, 1995; Shalaby et al., 1997). By mouse embryonic day 7.5, hemangioblasts in the splanchnic mesoderm condense into aggregations called blood islands, which is where the first stage of vasculogenesis begins (Gilbert, 2000; Shalaby et al., 1997). Next, hemangioblasts give rise to angioblasts and hematopoietic cells. The outer cells, or angioblasts, differentiate into endothelial cells, ultimately creating the vasculature needed

to feed the embryo. The inner cells, hematopoietic cells, give rise to the red blood cell population in the developing embryo (Gilbert, 2000). This process starts in extraembryonic tissues and is established by mouse embryonic day 8.5 (3 to 5 somites) when the network of vessels is rapidly undergoing morphological changes to fulfill the demands of the growing yolk sac and embryo (Drake and Fleming, 2000; Shalaby et al., 1997). Subsequently, intraembryonic vasculogenesis occurs, forming the dorsal aorta and other vessels to connect with capillary networks. As the blood islands grow, they merge to form the capillary network, draining into two vitelline veins. These veins are responsible for transporting food and blood cells (Gilbert, 2000).

Next, the process of angiogenesis remodels the primary network into distinct arteries, veins, and capillary beds (Drake and Fleming, 2000; Garcia and Larina, 2014; Gilbert, 2010). This process, known as vascular remodelling, occurs between embryonic days 8.5 and 9.5, creating an organized vascular network. During this time, established vessels expand and increase in diameter, while smaller vessels fuse to form the larger vessels of the yolk sac and embryo (Garcia and Larina, 2014). Thus, vessels undergo intussusception, rearranging branch points and creating new vessel sprouts from pre-existing vessels. This results in a hierarchically branched and organized vascular network, allowing vessels to become conduits for blood, oxygen, nutrients, and waste transportation (Garcia and Larina, 2014). Once vascular remodelling is complete, the vasculature of the yolk sac and embryo are subdivided into distinguishable arteries and veins. Arterial or venous fate can depend on differential effects of hemodynamic force and subsequential cell signalling as well as molecular markers on endothelial cells (le Noble et al., 2004; Wang et al., 1998).

1.2.6 The formation of primordial vessels

Three growth factors are critical in the initiation of vasculogenesis: basic fibroblast growth factor (bFGF), VEGF, and angiopoietins. bFGF is required for the transition of mesodermal cells into hemangioblasts. A knockout inactivation of bFGF results in an accumulation of epiblast cells due to their inability to migrate through the primitive streak, and ultimately, they fail to form mesoderm (Drake and Fleming, 2000; Garcia and Larina, 2014; Gilbert, 2010). bFGF signalling promotes the expression of VEGFR. VEGF is secreted by mesenchymal cells near the blood islands, and its receptors are located on hemangioblasts and angioblasts. Once VEGFR is upregulated, mesodermal precursors can respond to VEGF. VEGF enables the differentiation of angioblasts and regulates their multiplication to form primordial vessels. This growth factor promotes the expansive growth of blood vessels; without it, blood islands would fail to appear (Drake and Fleming, 2000; Garcia and Larina, 2014; Gilbert, 2010). The final family of proteins involved are angiopoietins produced by perivascular and mural cells. Angiopoietin 1 (Ang-1) mediates the interaction between endothelial cells and pericytes, which acts on the receptor Tie-2 expressed on endothelial cells. This is crucial for the association between endothelial cells and the surrounding matrix, ultimately supporting the integrity of the vessel. Mutations associated with angiopoietins lead to malformed blood vessels due to abnormal smooth muscles that normally encase them (Drake and Fleming, 2000; Garcia and Larina, 2014; Gilbert, 2010).

1.3 Cell Signalling Pathways: p-AKT, p-PTEN, and p-VEGFR2

1.3.1 p-AKT

Serine-threonine kinases are crucial mediators of vascular development, with considerable progress being made in the understanding of their role in angiogenesis specifically. AKT, also known as Protein Kinase B, is a serine/threonine-specific protein kinase that is frequently active in many cancers and plays a fundamental role in cell proliferation, survival, and growth (Abeyrathna and Su, 2015; Shiojima and Walsh, 2002). In unstimulated cells, AKT exists in the cytoplasm; however, once the cell is stimulated by growth factors and activated receptors, phosphoinositide-3-kinase (PI3K) triggers the conversion of phosphatidylinositol (3,4)-bisphosphate (PIP2) to phosphatidylinositol (3,4,5)-trisphosphate (PIP3), recruiting AKT to the plasma membrane by binding PIP3 (Abeyrathna and Su, 2015). AKT can now be phosphorylated by upstream kinases 3-phosphoinositide–dependent protein kinase 1/2 (PDK1 and PDK2), yielding a fully activated kinase. Once activated, AKT is now available to phosphorylate downstream substrates (Figure 5) (Abeyrathna and Su, 2015; Shiojima and Walsh, 2002).

A fundamental and widely accepted role of AKT is the mediation of cell survival, mainly through inhibiting apoptosis. One way AKT inhibits apoptosis is through the phosphorylation of caspase-9, inhibiting its activation (Abeyrathna and Su, 2015; Zhao et al., 2015). This ultimately results in negative regulation of cytochrome-c (Cyto c) and apoptotic protease-activating factor (Apaf-1). AKT is responsible for phosphorylating several other apoptotic molecules (Abeyrathna and Su, 2015). For example, BAD is a protein in the Bcl-2 family, and its phosphorylation inhibits apoptotic effects. AKT also plays a role in regulating p53 degradation by phosphorylating murine double minute 2

(MDM2). Degradation of p53 promotes cell cycle transition and survival, allowing cells to proliferate (Figure 5) (Abeyrathna and Su, 2015; Zhao et al., 2015).

Cell survival can additionally be mediated through mitogen-activated protein kinase (MAPK) and c-Jun N-terminal kinase (JNK) pathways (Abeyrathna and Su, 2015; Zhao et al., 2015). These pathways are commonly regarded as stress-activated protein kinase pathways, both playing a role in the activation of apoptosis (Abeyrathna and Su, 2015). AKT inhibits mixed lineage kinase 3 (MLK3), a kinase from the MAPK family, subsequently inhibiting downstream JNK and halting apoptosis (Figure 5) (Abeyrathna and Su, 2015; Zhao et al., 2015).

Cell growth and proliferation are further stimulated through the interplay between AKT and c-Myc. AKT further increases the production of growth factors, which increases the transcription of c-Myc and reduces its degradation, positively regulating cell cycle progression (Abeyrathna and Su, 2015). Another important regulator of cell growth is the mammalian target of rapamycin complex 1 (mTORC1). mTORC1 is an mTOR complex responsible for regulating cell growth and metabolism. This complex is activated by AKT through the inhibition of tumour suppressor protein tuberous sclerosis 1/2 (TSC1 and TSC2) (Figure 5) (Paplomata and O'Regan, 2014).

Furthermore, AKT plays a role in mediating angiogenesis by stimulating the secretion of VEGF. Through the activation of the TSC1–TSC2/mTORC1 pathway in endothelial cells, protein levels of hypoxia-inducible factor 1α (HIF-1α) increase, ultimately stimulating VEGF release (Figure 5) (Abeyrathna and Su, 2015). Moreover, VEGF-induced endothelial cell migration occurs through the AKT-PI3K pathway. Proper matrix attachment of endothelial cells also depends on the indirect interactions between

AKT and integrin $\alpha_v\beta_3$, found on the surface of endothelial cells and pericytes (Silva et al., 2008). After integrins bind to the extracellular matrix, they become clustered and associate with the actin filaments of the cytoskeleton (Abeyrathna and Su, 2015; Shiojima and Walsh, 2002). This further promotes the clustering, leading to the formation of focal adhesions and activation of intracellular signalling. The binding of endothelial cells to the extracellular matrix via $\alpha_v\beta_3$ is essential in VEGF's activation of AKT, which is crucial in preventing cell detachment-induced apoptosis (Shiojima and Walsh, 2002). Cell attachment via extracellular matrix and integrin interactions activate intracellular AKT survival pathways, which maintain endothelial cell viability. Intracellular signalling causes stimulated endothelial cells to express higher levels of the $\alpha_v\beta_3$ integrin (Shiojima and Walsh, 2002). It has been demonstrated that $\alpha_v\beta_3$ interacts with VEGFR, further activating AKT activation. A decrease in AKT activity causes decreased integrin-dependent AKT activation induced by cell detachment (Bachelder et al., 2001; Eliceiri, 2001; Shiojima and Walsh, 2002). Therefore, integrin signalling is mediated via cell attachment, and, ultimately, the PI3K/AKT pathway is a crucial synergistic regulator of endothelial cell survival and angiogenesis. Furthermore, VEGF's induction of integrin signalling is imperative in AKT's cooperative and synergistic activation (Abeyrathna and Su, 2015; Shiojima and Walsh, 2002).

Small GTPases of the Rho family govern the regulation of endothelial cell migration by acting in response to VEGFR2 activation. RhoA is known for its phosphorylation of VEGFR2 and activation of PI3K, regulating cell motility (Lamalice et al., 2007). Once the PI3K pathway has been activated, PDK1 is further phosphorylated, leading to AKT activation (Figure 5). PI3K has been implicated to play a role in the

directional control of cell migration by responding to the chemoattractant gradient (Lamalice et al., 2007; Shiojima and Walsh, 2002). Nitric oxide (NO) is also an important regulator of cell migration and is produced by eNOS. eNOS is activated downstream of the VEGFR2/PI3K/AKT pathway, ultimately activated by VEGF (Figure 6) (Williams et al., 2000). NO serves as an important messenger for VEGFR2 in regulating angiogenesis by expanding the surface area of endothelial cells, allowing for a greater response to angiogenic and promigratory agents (Lamalice et al., 2007; Rouusseau et al., 2000).

Low levels of cadmium induce angiogenesis and trigger the activation of AKT and its downstream effectors in human epithelial cells (Jing et al., 2012). Active AKT causes HIF mRNA unwinding, promoting HIF translation. Elevated HIF levels further increase VEGF transcription. As a result, VEGF-mediated angiogenesis is upregulated by AKT-dependent and independent mechanisms (Figure 7) (Jiang and Liu, 2009; Karar and Maity, 2011; Wei et al., 2017).

1.3.2 p-PTEN

Phosphatase and tensin homolog (PTEN) is commonly referred to as a tumour suppressor protein, acting as a phosphatase on both lipids and proteins. PTEN is frequently found to be deleted, downregulated, or mutated in malignancies, and these events profoundly affect tumour susceptibility (Carracedo et al., 2011; Hopkins et al., 2014). Thus, a loss of function of this homolog can lead to defects in normal cell homeostasis. This protein acts as a signal to cease cell division and trigger apoptosis by antagonizing the PI3K pathway. It inhibits the transformation of PIP2 to PIP3 and, in turn, blocks PI3K signalling and downstream processes, such as the activation of AKT (Figure 5). Therefore, cell survival, growth and proliferation are inhibited by blocking

AKT (Hopkins et al., 2014). PTEN is thus crucial for the inhibition of oncogenic transformation. With a loss of PTEN, AKT is upregulated, and VEGF expression is elevated, increasing pro-angiogenic mechanisms (Hopkins et al., 2014; Jiang and Liu, 2009; Karar and Maity, 2011; Rodriguez and Huynh-Do, 2012).

PTEN has been described to have PIP3-independent functions; more specifically, PTEN phosphatase activity is crucial for inhibiting cellular migration (Leslie et al., 2007). Furthermore, migration is reduced by the dephosphorylation of adhesion kinases by PTEN, limiting the spread of fibroblasts (Leslie et al., 2007; Raftopoulou et al., 2004; Tamura et al., 1998).

PTEN has also demonstrated anti-oncogenic functions through p53 expression, another major tumour suppressor. Similar to PTEN, p53 is responsible for regulating cell proliferation and death. In the absence of stress, p53 levels are maintained through a constant proteasome-dependent degradation (Trotman and Pandolifi, 2003). Degradation of this protein is mediated by MDM2, an oncoprotein that controls tumorigenesis and is upregulated in situations such as oxidative stress. MDM2 regulates p53 by blocking its transcriptional activity and promoting its degradation (Freeman et al., 2003; Trotman and Pandolifi, 2003; Nakanishi et al., 2014). Additionally, PTEN plays a role in regulating p53 by antagonizing PI3K (Figure 5). When AKT is activated, MDM2 is phosphorylated, which results in its nuclear import. Nuclear MDM2 then tags p53 for proteasomal degradation (Freeman et al., 2003; Mayo and Donner, 2001; Ogawara et al., 2002). Since PTEN is an antagonist of AKT, its phosphatase activity can prevent p53 degradation by keeping AKT inactive. Furthermore, a transcriptional target of p53 is PTEN. Thus, in stressful environments, when there is an increase in p53, PTEN transcription also increases. This creates a positive feedback loop in which PTEN protects p53 and, in turn,

regulates its transcription levels (Figure 5) (Freeman et al., 2003; Trotman and Pandolifi, 2003; Nakanishi et al., 2014).

High cadmium concentrations have been found to increase pro-apoptotic proteins, causing cell damage and, ultimately, cell death. Consequently, signalling pathways essential for vascular maintenance and growth are disrupted, and the availability of HIF, VEGF, and VEGFR is reduced (Kim et al., 2012; Wei et al., 2017). With disrupted HIF and VEGF expression, pro-angiogenic mechanisms are interrupted, increasing the cytotoxic effects on the vascular endothelium (Figure 7) (Carmeliet and Jain, 2011; Gheorghescu and Thompson, 2016; Gheorghescu et al., 2015; Jing et al., 2012; Kim et al., 2012; Wei et al., 2017; Xiong et al., 2021).

1.3.3 p-VEGFR2

VEGFR2 is an important regulator of angiogenesis and has been demonstrated to be the first molecule expressed in mesodermal cells to give rise to angioblasts (Risau 1998). VEGF is upregulated in hypoxic situations, which orchestrates blood vessel formation via the activation of VEGF receptors and initiating signalling pathways (Figure 6). This leads to specific endothelial responses such as proliferation, migration, invasion, and vascular permeability (Lugano et al., 2020; Marmé and Fusenig, 2008; Risau and Flamme, 1995). The physiological effects of VEGF are mediated through its interaction with its receptor, VEGFR. The three main VEGF receptors are VEGFR1, VEGFR2, and VEGFR3 (Liao and Johnson, 2007). VEGFR1 and VEGFR2 are responsible primarily for regulating angiogenesis and vascular permeability, whereas VEGFR3 regulates lymphangiogenesis (Liao and Johnson, 2007).

VEGFR2 is a transmembrane glycoprotein mainly distributed in vascular endothelial cells and allows the signal transduction of downstream pathways such as PI3K/AKT. By binding to VEGFR2, VEGF can mediate endothelial cell proliferation, migration, invasion, and survival, which are key to angiogenesis (Shibuya, 2011; Wang et al., 2020a; Wang et al., 2020b). The phosphorylation of AKT can subsequently activate signalling pathways, further promoting blood vessel formation by inhibiting apoptotic activity. VEGF-activated VEGFR2 regulates vascular permeability by activating eNOS to produce NO (Figure 6). The release of NO from endothelial cells can further activate the PI3K/AKT pathway, changing vascular permeability (Shibuya, 2011; Wang et al., 2020a; Wang et al., 2020b).

VEGF stimulates the release of inactive VEGFR2 from the Golgi apparatus of endothelial cells. The endosome then undergoes intracellular trafficking and is brought to the plasma membrane. The binding of VEGF to VEGFR2 also stimulates the trafficking of intracellular VEGFR2 within recycling endosomes. This allows VEGFR2 to return to the plasma membrane, in addition to the trafficking of newly synthesized VEGFR2 (Basagiannis and Christoforidis, 2016; Manickam et al., 2011; Simons, 2012). Thus, the balance between endocytosis and exocytosis of VEGFR2 signalling is vital in regulating VEGFR2 levels. VEGFR2 trafficking is controlled by the Golgi-localized target membrane-soluble N-ethylmalemide attachment protein receptor (t-SNARE) syntaxin-6. Reduced levels of syntaxin-6 have been correlated with decreased VEGF-induced angiogenesis and permeability (Basagiannis and Christoforidis, 2016; Manickam et al., 2011; Simons, 2012).

Cadmium increases cancer risk and developmental abnormalities (Wei et al., 2017). For a tumour to grow and metastasize, vasculature is needed. In normal

vasculature, pro- and anti-angiogenic factors are in balance. However, cancerous cells are stimulated when blood vessel formation is induced, and pro-angiogenic signalling dominates (Carmeliet and Jain, 2000; Lugano et al., 2020). It is important to note that such effects of cadmium on cell survival and protein expression are concentration-dependent. At low concentrations (< 1 μM), cadmium evokes an upregulated HIF response, and endothelial cells demonstrate a resistance to cadmium toxicity (Jing et al., 2012; Kim et al., 2012; Wei et al., 2017). Thus, low concentrations appear to stimulate VEGF, which protects cells from cell death and damage. With the upregulation of VEGF, endothelial cells are vigorously active and multiplying. As tumour cells begin to outgrow the capacity of their vasculature, hypoxia is further stimulated. VEGF is expressed more aggressively, initiating rapid growth of malignant cells, and releasing tumours from dormancy (Figure 7) (Liao and Johnson, 2007; Tonini et al., 2003). Therefore, the upregulation of VEGF permits tumour expansion and invasion into surrounding tissues.

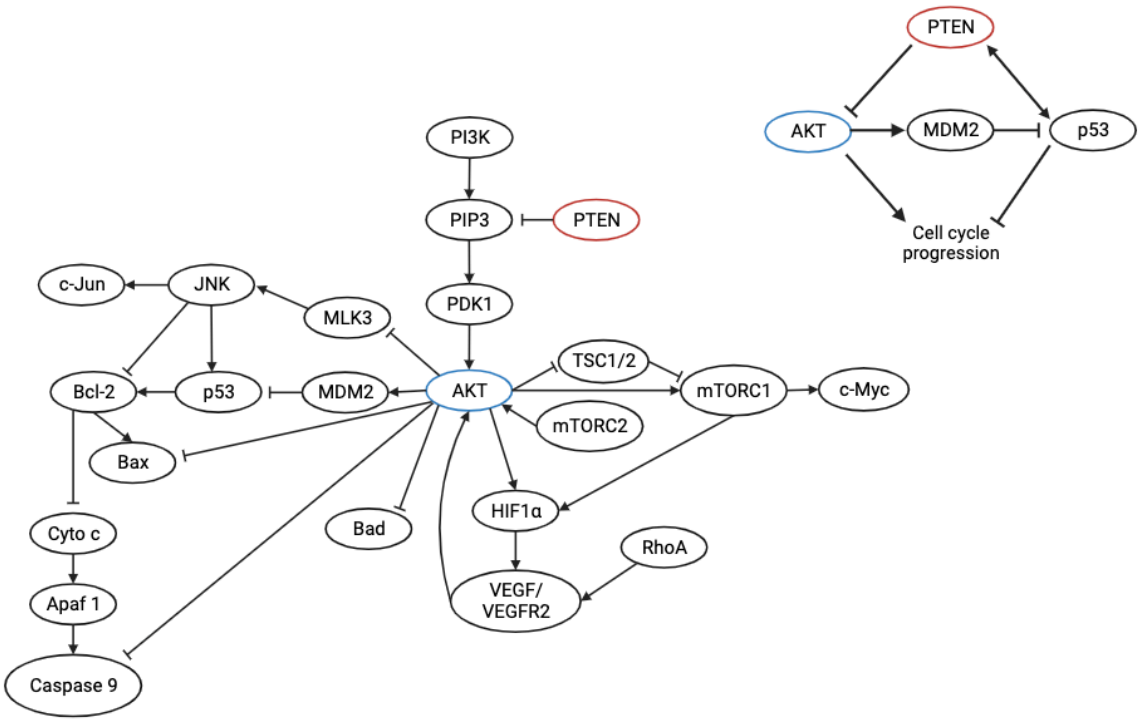

Figure 5: Angiogenic pathways demonstrating the interactions between the PI3K/AKT pathway. Receptor tyrosine kinases activate PI3K, which triggers the conversion of PIP2 to PIP3, activating AKT via PDK1. This conversion can be inhibited by PTEN, which triggers the conversion of PIP3 to PIP2. mTORC2 can influence AKT activity by phosphorylating AKT and subsequently inhibit TSC1/2, allowing mTORC1 and c-Myc to be activated. HIF1α is activated by both AKT and mTORC, ultimately stimulating VEGF and VEGFR2 release, which furthers AKT phosphorylation. AKT regulates the inhibition of several apoptotic molecules such as BAD, caspase 9, Bcl-2, and Bax. p53 is regulated by the degradation of MDM2; however, AKT can prevent p53 degradation by keeping AKT inactive. p53 inhibition is furthered by AKT inhibiting MLK3 and subsequently JNK and c-Jun, respectively. Image adapted from PI3K Akt Pathway (2016) and Nakanishi et al., (2014).

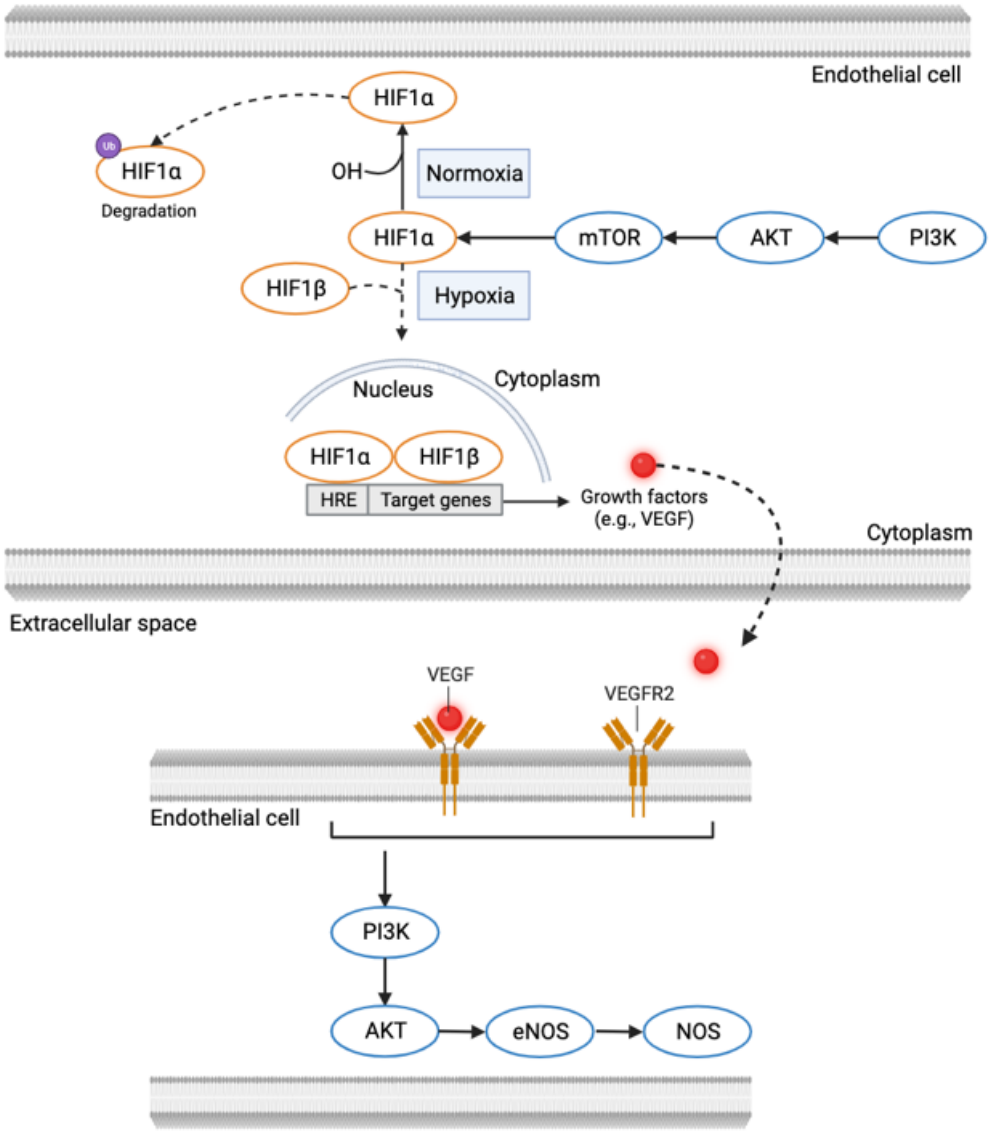

Figure 6: Angiogenic pathways focusing on VEGF regulation under hypoxic situations. With ample oxygen supply, HIF-1α is activated via PI3K signalling and then ubiquitinated for degradation. However, under hypoxic environments, nuclear binding of HIF-1α and HIF-1β occurs in the cytoplasm, which initiates transcriptional stimulation of growth factors in the nucleus. Growth factors, such as VEGF, bind to VEGFR2 on the surface of endothelial cells, which activates downstream signalling of the PI3K/AKT pathway. Image adapted from Welsh et al., (2013). Created with Biorender.com

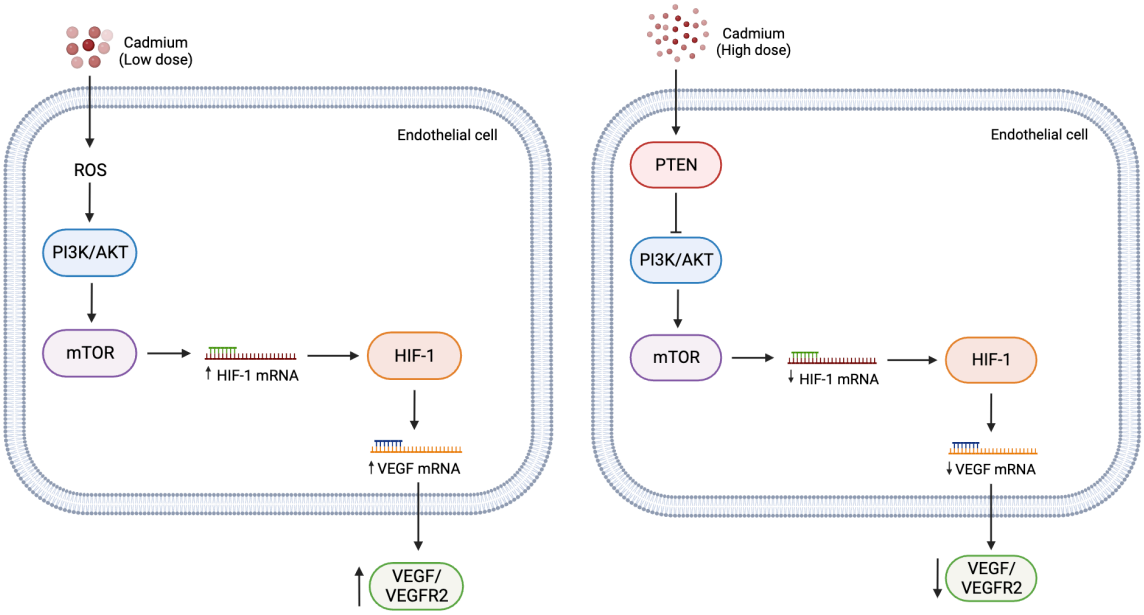

Figure 7: The effects of low and high cadmium concentrations on various signalling pathways. Low cadmium concentrations cause an increase in ROS inside endothelial cells, stimulating mTOR via PI3K/AKT pathways. HIF-1 mRNA transcription is upregulated, causing an increase of HIF and, subsequently, VEGF mRNA and VEGF/VEGFR2 production. High concentrations of cadmium inhibit the VEGF/VEGFR2 signalling through PTEN upregulation. PTEN production inhibits the PI3K/AKT pathway and its downstream effectors. Image adapted from Wei et al., (2017). Created with Biorender.com

1.4 Cellular and Physiological Implications of Angiogenesis

Given the role of VEGF in angiogenesis, abnormalities in its expression have the potential to be important in disease pathology. Without adequate blood supply, tissues become hypoxic, inducing the expression of VEGF and its receptors via hypoxia-inducible factor-1α (HIF-1α) (Nishida et al., 2006). This process is known as pathological angiogenesis. With increased transcription of VEGF mediated by HIF-1α, there is an increased production of other growth factors and receptors, including VEGFR. This creates new capillary networks via sprouting angiogenesis (Liao and Johnson, 2007; Marmé and Fusenig, 2008; Nishida et al., 2006). Conversely, aging tissues experience

defects in capillary density due to a lack of hypoxia-inducible factor activation and, ultimately, VEGF expression. This causes a decrease in endothelial migration and proliferation (Lähteenvuo and Rosenzweig, 2012; Villar-Cheda et al., 2009; Watanabe et al., 2020).

1.4.1 Age-related diseases and conditions

With aging, there is a significant reduction in microvascular density (MVD), a phenomenon known as microvascular rarefaction. This age-related process affects capillaries in all organs and is induced by hypoxia. HIF-1α induces VEGF production, promoting the formation of new blood vessels, which is indispensable in replenishing MVD changes (May et al., 2008). With decreased capillary density, there is an increase in senescent endothelial cells. This results in age-related changes in endothelial cells, including reduced proliferation, which limits the capacity of tissues to create new blood vessels (Lähteenvuo and Rosenzweig, 2012).

Reduced VEGF production in aged populations is likely due to decreased HIF-1α production. During the aging process, less HIF-1α results in repressed mitochondrial biogenesis, impairing energy-dependent cellular processes, such as increasing ROS levels and cellular apoptosis (Forsythe et al., 1996; Kim et al., 2006; Zhang et al., 2007). This leads to decreased cellular and tissue repair, further increasing hypoxic microenvironments (Carmeliet and Jain, 2000; Lähteenvuo and Rosenzweig, 2012; Watanabe et al., 2020). VEGF signalling insufficiency and inadequate MVD lead to reduced tissue oxygenation and perfusion, as well as compromised mitochondrial activity and metabolic alterations (Grunewald et al., 2021).

1.4.2 Disorders of the immune system

The immune system becomes less efficient with age, causing the body to experience widespread dysfunction and decreased ability to respond to immune challenges. This process is illustrated through age-related autoimmune conditions such as rheumatoid arthritis (RA) (Elshabrawy et al., 2015; Paleolog, 2002). RA is an inflammatory joint disease typically affecting peripheral joints. The synovial membrane becomes inflamed, causing it to increase in size. Hypoxia is induced because of increased metabolic demand and the increasing number of leukocytes recruited to the joint. This causes an accumulation of HIF-1α (Elshabrawy et al., 2015; Paleolog, 2002). The formation of blood vessels plays an important role in the pathogenesis of RA. Signals are sent to generate new blood vessels in the hypoxic synovial environment. The upregulation of VEGF furthers the vascular permeability of the joint, increasing edema and, thus, joint swelling (Paleolog, 2002). As the synovium grows and synovial cells proliferate, HIF-1 α accumulates. With increased metabolic demand, angiogenesis of the synovial membrane is signalled, allowing chronic inflammation by transporting inflammatory cells to the inflamed tissue (Marrelli et al., 2011). One study demonstrated the importance of VEGF in developing joint destruction by stimulating collagen-induced arthritis in genetically susceptible mice. Mice treated with a soluble form of the Flt-1 VEGFR experienced reduced joint pain and inflammation as well as minimal bone and cartilage destruction compared to untreated animals. This suggests that the blockade of VEGF may be beneficial in the therapeutic relief of RA (Miotla et al., 2000).

1.4.3 Cognitive dysfunction and neurodegeneration

Microvascular rarefaction is associated with the age-related decline of the vascular plexus, contributing to cognitive dysfunction and neurodegeneration. Vascular damage of nervous tissue is the initial result of aging, disrupting the blood-brain barrier. This disruption impairs brain perfusion, contributing to neuronal injury (Emerich et al., 2007; Villar-Cheda et al., 2009; Watanabe et al., 2020). Perfusion deficits contribute to the pathogenesis of neurodegenerative diseases and chronic ischemia (Villar-Cheda et al., 2009). In Alzheimer's disease, amyloid β (Aβ) directly and indirectly reduces capillary density. Aβ not only accumulates on capillaries inhibiting angiogenesis but also binds to circulating VEGF in the brain (Kalaria et al., 1998; Paris et al., 2004; Yang et al., 2004b). Reduced vascularity in the brain leads to hypoxia, causing the upregulation of VEGF (Kalaria et al., 1998). This stimulates the upregulation of pro-angiogenic factors and endothelial cell activation. Despite an increase in pro-angiogenic factors, there is a lack of increased angiogenesis in the aging brain (Buee et al., 1994; Buee and Delacourte, 1997; Edelber and Reed, 2003; Jellinger, 2002). Thus, activated endothelial cells elicit an inflammatory response and increase protease activity, which may promote neuronal death (Grammas et al., 2011). Increased blood-brain barrier dysfunction furthers neurodegenerative diseases due to neuroinflammation (Kim et al., 2006). Villar-Cheda et al. (2008) studied age-related changes in substantia nigra compacta vascularization and VEGF expression while also investigating how exercise influences these changes in a rat model. The results showed an age-dependent decrease in microvessels in the substantia nigra, with the most significant response in the oldest rats. Similarly, they found that VEGF mRNA levels also declined with increased age. The authors also noted that treadmill running increased VEGF mRNA levels in middle-aged and aged rats. This study

suggests that exercise is a potential therapeutic benefit for individuals suffering from neurodegenerative disorders by increasing circulating VEGF in the brain.

Grunewald et al. (2021) investigated whether VEGF might correct capillary loss and ultimately increase lifespan and health outcomes by increasing circulatory VEGF through genetic manipulation from early adulthood onward in mice. This study found that mice treated with VEGF lived longer with an extended health span due to increased protection against capillary loss and compromised perfusion. This was reflected by, but not limited to, reduced abdominal fat accumulation, reduced skeletal muscle mass and bone loss, as well as a reduction in liver steatosis and the burden of spontaneous tumours (Grunewald et al., 2021). To conclude, increased VEGF might help with pathological conditions associated with aging (Grunewald et al., 2021). However, it is important to note that excess VEGF is associated with tumorigenesis. Thus, despite its positive effect on aging-related diseases, increasing VEGF expression may allow cancer cells to develop and spread more easily (Lugano et al., 2020; Rajabi and Mousa, 2017).

1.4.4 Tumorigenesis

For a tumour to grow and metastasize, vasculature is needed. Since oxygen plays a pivotal role in cell growth, malignant cells reside close to blood vessels (Lugano et al., 2020; Rajabi and Mousa, 2017). In growing cancers, endothelial cells are vigorously active due to the release of pro-angiogenic factors, such as VEGF. For this to occur, there must be an 'angiogenic switch.' When pro- and anti-angiogenic factors are in balance, the body experiences vascular homeostasis. Vascular homeostasis promotes quiescent vasculature and non-proliferative endothelial cells. However, when blood vessel formation is induced and pro-angiogenic signalling dominates, there is an angiogenic

switch (Carmeliet and Jain, 2000; Lugano et al., 2020). As tumour cells begin to outgrow the capacity of their vasculature, hypoxia is stimulated. This occurs early in tumour development and, as a result, VEGF is expressed more aggressively, initiating rapid growth of malignant cells and releasing tumours from dormancy (Liao and Johnson, 2007; Tonini et al., 2003).

In cancerous environments, the basement membrane is locally injured due to the partial detachment of pericytes from endothelial cells, which causes the basement membrane to be structurally abnormal and unequally distributed (Baluk et al., 2003). This causes increased vessel fragility as well as chaotic blood flow through poorly organized and malformed vessels, creating a hypoxic environment and ultimately stimulating VEGF (Baluk et al., 2005). VEGF upregulation permits tumour expansion and invasion into surrounding tissue. This process occurs through an increased production of matrix metalloproteinases (MMPs), which causes the breakdown of the extracellular matrix. Matrix destruction permits the migration of endothelial cells into surrounding tissue, eventually evolving into a mature network of blood vessels for the tumour to feed on (Bremnes et al., 2006; Nishida et al., 2006; Risau and Flamme, 1995). Dysregulation of VEGF leads to vascular hyper-permeability, which may lead to interstitial pressure and impaired therapeutic delivery. Additionally, the new and leaky vasculature promotes the escape of tumour cells into the bloodstream, promoting the establishment of distant metastasis (Lugano et al., 2020).

The ordered division of the vascular tree is vital for efficient circulation; however, vascular remodelling occurs in the presence of dominant pro-angiogenic signalling (Lugano et al., 2005). The tumour signals for a new vascular network; however, the newly formed vessels may fail to mature and prune. This causes disorganization and

uneven blood flow. This process causes persistent or intermittent hypoxia, furthering the tumour's heterogeneous and chaotic blood flow (Baluk et al., 2005; Lugano et al., 2020). This is partly due to the structurally and functionally abnormal architecture of blood vessels. Such vessels are uneven in diameter, with excessive branching and shunts. This is most likely due to the irregular release of VEGF (Lugano et al., 2020).

The chaotic structure of tumour vasculature also disrupts blood flow, hindering therapeutic effectiveness. Endothelial junctions are disrupted, and pericytes lining the vessels partially detach. This process further reduces the efficacy of cancer therapy; irregular vessels may lead to leakiness, making it difficult for cancer drugs to reach all parts of the tumour (Awad et al., 2023; Carmeliet and Jain, 2000; Lugano et al., 2020). Tumours can also lack functional lymphatics. It is thought that excess VEGF at the periphery of the tumour causes lymphatics to enlarge (Kim et al., 2006). This causes a buildup of interstitial fluid and metastatic cells. With increased vascular permeability, tumour vessels become leaky, releasing cancer cells from the tumour surface and facilitating lymphatic metastasis (Kim et al., 2006). Abnormal lymphatics may contribute to interstitial hypertension, which can interfere with the delivery of some cancer treatments. Future therapeutic agents must overcome the pressure barrier created by tumours to block lymphatic metastasis (Kim et al., 2006).

1.4.5 Teratogenicity

A critical first step in embryonic development is the formation of the cardiovascular circulatory system, allowing the delivery of oxygen and nutrients to newly forming organ systems and tissues. If there is an abnormality in the network's

establishment, organ development and the embryo's viability can be impacted (Drake and Fleming, 2000; Garcia and Larina, 2014).

Birth defects result from alterations in embryonic or fetal development, and one way in which this occurs is through exposure to teratogens. Teratogenic agents include physical and infectious agents, drugs, maternal health, and environmental factors such as cadmium (Tymchuk et al., 2022). Large amounts of this heavy metal can adversely affect the reproductive system and cause embryotoxic effects. Ambient air pollution has been associated with an increase in the number of complications during pregnancy. Their offspring experience several physical and cognitive disabilities, as well as decreased birth rates and increased physical and intellectual disabilities (Pedersen et al., 2013; Tymchuk et al., 2022).

The placenta is often referred to as the barrier that prevents the passage of harmful substances to the developing embryo; however, it has become evident that the placenta itself is insufficient to prevent the passage of all teratogens (Molina-Mesa et al., 2022). The placenta, in part, works as a barrier to limit the movement of cadmium to the fetus, and teratogenic effects may be associated with placental damage. Placental cadmium concentrations are known to be higher than in fetal tissue. To elaborate, with continuous exposure to cadmium from maternal osmotic minipumps starting after implantation and continuing throughout pregnancy, embryos had the highest fetal concentration on day 12 of gestation before complete placental development, reducing slightly by day 15 in mice (Mahalik et al., 1995). The placenta can synthesize cadmium-bound metallothionein, preventing it from reaching the fetus. However, during the early phases of development, the amount of metallothionein in the placenta is relatively low, resulting in larger amounts of cadmium reaching the fetus. During the later stages, metallothionein synthesis of the

placenta is increased, reducing the amount of cadmium that can reach the fetus. This can be seen by a decrease in fetal cadmium concentrations by day 15; however, this could be due to the growing embryo's increase in tissue mass when the placenta is less permeable to cadmium (Mahalik et al., 1995). Furthermore, during the final stages of gestation, the placenta is the main target for cadmium toxicity rather than the fetus. With exposure, the teratogen accumulates in the placenta, eventually impairing placental function and consequently fetal development (Geng and Wang, 2019; Mahalik et al., 1995; Lopez Fernádez de Villaverde, 2005).

The impact of teratogens on development is often associated with the type of teratogen, dose, duration, and time of exposure. Moreover, the dosage and time of exposure are critical during the period of organogenesis. At this time, developing embryos are maximally sensitive (Hovland et al., 1999; Lopez Fernádez de Villaverde, 2005). Exposure to teratogens, such as cadmium, has demonstrated specific patterns in abnormalities associated with organ formation correlated to the time of administration. The timing of organogenesis is species-specific, occurring between days 8-10 of gestation in mice (Cao et al., 2019). Early in the organogenesis stage, before the placenta has formed, the embryonic gut endoderm, specifically the anterior visceral endoderm, is a target site for cadmium accumulation. Due to its proximity to the maternal environment and the later vitelline duct, cadmium is easily transported to the embryo (Dencker, 1975; Lopez-Fernádez de Villaverde, 2005). However, this is a gestational stage-dependent effect occurring only until day 9, when the vitelline duct closes. After this point, cadmium accumulates in the placenta and yolk sac and can be followed by a shift in teratogenic malformations, including but not limited to deformities of limbs, heart, and spinal column (Dencker, 1975; Hovland et al., 1999; Lopez Fernádez de Villaverde, 2005).

Cadmium is known to induce oxidative stress, including the production of reactive oxidative species (ROS), such as the hydroxyl radical, superoxide radical, and nitric oxide (Nemmiche, 2017). Cadmium's ability to interfere with sulfhydryl groups interferes with the redox status of the cell and ultimately affects the cellular levels of redox-active species (Gobe and Crane, 2010). This alters the transcriptional levels of HIF-1α, activating various downstream proteins, including VEGF. Vascular development is critical in the homeostatic response to toxicant exposure, and derangement in the angiogenic process can be associated with malformations (Gheorghescu et al., 2015). Thus, some teratogenic properties of cadmium may stem from its ability to disrupt angiogenesis, leading to inadequate oxygenation of embryonic tissues and developing structures (Gheorghescu et al., 2015). The accumulation of cadmium can occur as early as the four-cell stage; however, it can happen later, depending on maternal exposure (Thompson and Bannigan, 2008). If dosage exposure is high during early developmental stages, the growth of the embryo may be halted altogether before it reaches the blastocyst stage. Furthermore, if the embryo reaches the blastocyst stage, exposure could result in cell apoptosis before implantation due to decompaction and degeneration (Thompson and Bannigan, 2008). The effects of cadmium exposure after implantation are stage- and dose-dependent, with major consequences, including craniofacial, cardiovascular, neurological, gastrointestinal, genitourinary, and limb abnormalities (Geng and Wang, 2019; Gundacker and Hengstschlager, 2012).

In humans, cadmium has also been noted to alter the expression of related functional genes in the placenta, which affects the morphology and function of various cells. This reduces the proliferation and migration of trophoblast cells by inhibiting

transforming growth factor-β (TGF-β) (Brooks and Fry, 2017). An inhibition in this signal transduction process can delay placenta formation and size, ultimately limiting normal development. Furthermore, the accumulation of cadmium ions promotes apoptosis, further delaying placental development (Saedi et al., 2023). Cadmium accumulation is also responsible for embryonic malformations caused by excess apoptosis. ROS-induced p53 production is one way in which apoptosis is upregulated. p53 regulates apoptosis by halting the cell cycle of damaged cells in fertilized chick embryos. More specifically, cadmium-induced activation of this protein is implicated in teratogenic embryonic development via its induction of other apoptotic proteins (Zhu et al., 2024). With increased p53, downstream effectors are upregulated, including BAX, BAD, cytochrome c, APAF1, and caspase 9, executing programmed cell death (Jacobson, 1997; Lopez Fernádez de Villaverde, 2005; Robertson and Orrenius, 2000; Sionov and Haupt, 1999). This pathway is essential for the normal development of the central nervous system, illustrating one way in which apoptosis causes malformations. Overall, this pathway leads to cell cycle arrest and death, leading to teratogenic results (Lopez Fernádez de Villaverde, 2005; Zhu et al., 2024). Lastly, cadmium exposure has been correlated with epigenetic alterations, specifically changes in DNA methylation. Some epigenetic alterations include DNA hypermethylation, gene silencing, and hypomethylation in human prostate epithelial cells and embryo lung fibroblasts (Benbrahim-Tallaa et al., 2007; Jiang et al., 2008). Placental development is reliant on DNA methylation, and changes to this mechanism early in life can cause sex-specific cadmium toxicity (Kippler et al., 2013; Vilahur et al., 2015). Kippler et al. (2013) analyzed cadmium concentration in children's urine and the associated methylation in

their blood. They found a sex-specific association in which girls had an overrepresentation of methylation changes associated with organ development, morphology, and bone mineralization. Comparatively, boys had increased cell death-related genes (Kippler et al., 2013).

Cadmium entering the placenta can result in fetal growth restriction. This is further associated with delayed fetal development and altered birth anthropometry, such as birth weight, head circumference, birth height and Apgar scores, assessing for signs of hemodynamic compromise (Zhang et al., 2018). There is still a lack of knowledge surrounding the exact mechanisms by which cadmium restricts fetal growth. Still, cadmium exposure has been linked to a decrease in the expression of carrier proteins (Geng and Wang, 2019). These carrier proteins are associated with nutrient transport, and a reduced nutritional supply to the embryo may play a role in delayed development. Moreover, the early stages of development require large amounts of glucose and other energy substances to support copious amounts of cell proliferation and growth (Geng and Wang, 2019). A lack of energy molecules may delay embryonic development by interfering with this growth process. One family of nutrient transporters involved in this process are glucose transporters, GLUTs. It has been observed that the expression of GLUT3 was downregulated in cadmium-exposed mice, reducing placental glucose transport and decreasing the amount of energy and nutrient supply the fetus receives, leading to fetal growth restriction (Xu et al., 2016). Furthermore, studies show that fetal growth restriction is more commonly associated with high cadmium concentrations (Geng and Wang, 2019; Xu et al., 2016).

Cadmium-associated abnormalities could be caused by damage to embryonic vasculature. Studies have demonstrated decreased length, size, and junction density of

chick yolk sac blood vessels when embryos were exposed to cadmium. Likewise, there was a decrease in the amount of hemoglobin and angioblast activation compared to control groups (Veeriah et al., 2015; Vimalraj et al., 2017). Studies have also indicated that heavy metals, including cadmium, can induce apoptosis and deregulate the cell cycle of vascular cells. Toxic levels are known to mediate ROS-mediated endoplasmic reticulum stress, decrease cell proliferation, and enhance apoptosis in the placenta (Fish et al., 2008). Together, these properties inhibit yolk sac vascular development, leading to embryonic deformities and death (Geng and Wang, 2019; Veeriah et al., 2015; Vimalraj et al., 2017).

1.5 Types of Assays Used for the Study of Vascular Development

Angiogenesis is a mix of complex cellular and molecular activities, and the most important yet difficult challenge when studying angiogenesis is selecting an appropriate assay. *In vitro* and *in vivo* assays both model and simulate different aspects of the angiogenic process (Staton et al., 2004).

In vitro assays target specific behaviours of endothelial cells (ECs) and often focus on the molecular mechanisms of angiogenesis. They are also commonly used to validate the effects of certain compounds on angiogenesis (Chávez et al., 2016). These tests open the opportunity to isolate the study's objective and control variables, essentially minimizing covariates that may be associated with a response. *In vitro* assays focus on the response of ECs to inhibitory and stimulatory agents, as assessed by their migration, proliferation, and tubule formation. They can be carried out at both a two-dimensional and three-dimensional level, which allows mechanisms and molecular interactions to be studied at normal and pathological levels (Medina-Leyte et al., 2020). In a two-

dimensional model, vessels develop on the surface of the substrate, whereas in three-dimensional assays, vessels invade a biogel matrix (Vailhé et al., 2001). The development of *in vitro* models has increasingly broadened our understanding of many diseases and processes and led to the development of novel diagnostic methods and techniques.

1.5.1 Two-dimensional models in the study of angiogenesis

Two-dimensional models begin with ECs being seeded onto an adhesively coated culture dish. When sensed by the cells, the substrate triggers mechanical signals, stimulating cells to reorganize to form a lumen and create capillary-like structures (CLS) in a two-dimensional fashion (Vailhé et al., 2001). The two-dimensional model can be further classified as short- or long-term. Short-term models portray the morphogenesis steps of angiogenesis but are not representative of proliferative and migratory actions. In comparison, long-term models are less representative for screening angiogenic molecules and thus lack strong reproducibility. This is due to the sparse number of cells undergoing morphological differentiation, and thus, CLS are not reliably observed in long-term cultures (Vailhé et al., 2001). These models provide a convenient observation of stable tubular structures that form slowly over the culture period. Another strength of this model is the specific analysis of angiogenic cells, allowing one to study molecular and cellular characteristics (Vailhé et al., 2001).

In theory, two-dimensional models are a relatively simple way of isolating cells *in vitro* and studying the activity of angiostatic molecules. By working in two dimensions, one may better understand the cellular organization from intussusceptive, or remodelling, aspect rather than sprouting (Vailhé et al., 2001). However, this model lacks the third dimension and does not reflect all physiological steps associated with angiogenesis.

Three-dimensional models replicate in vitro conditions more closely, allowing ECs to invade the three-dimensional substrates. This preserves vessel architecture, closely replicating an *ex vivo* model. Through manipulation, more angiogenic steps can be accounted for, and depending on the composition of the culture media, cells can sprout, proliferate, migrate, and/or differentiate (Vailhé et al., 2001).

1.5.2 The use of in vitro assays in the study of angiogenesis

Certain *in vitro* assays can be selected to represent a singular aspect of angiogenesis (Chávez et al., 2016; Staton et al., 2004). For example, cell proliferation assays are one way in which EC proliferation can be studied and evaluated in response to a test substance. Cell proliferation assays are relatively straightforward and highly reproducible, making this a rather precise quantification. This assay can assess if ECs are triggered to divide and proliferate when exposed to a specific stimulus (Chávez et al., 2016). However, a problem with this method is that cells may behave differently when exposed to still versus flowing cultures (Staton et al., 2004). Another disadvantage is the uncertainty of whether decreased proliferation is associated with cytotoxic or cytostatic effects of the test substance; however, this assay can be used in combination with a cell death assay to give a more accurate picture of the endothelial response (Staton et al., 2004).

Migration assays measure EC motility as the cells move along a gradient of angiogenic stimulatory factors through chemotaxis (Chávez et al., 2016; Staton et al., 2004). In this type of assay, ECs are plated on a filter in the upper portion of the chamber, and they migrate in response to the test substance plated in the bottom. An advantage of this assay is its high sensitivity to minor differences that may occur in concentration

gradients (Falk et al., 1980; Staton et al., 2004). However, difficulties arise with the setup and problems with maintaining trans filter gradients over a prolonged period (Staton et al., 2004). Issues also arise with obtaining accurate cell counts when cells begin crossing the filter.

In vitro models that use human umbilical vein endothelial cells (HUVEC) can recapitulate many aspects of human physiology. While this model fails to include all endothelial cell types, it is advantageous for developing a greater understanding of vascular endothelial properties and pathways involved in its functioning (Medina-Leyte et al., 2020). HUVEC cultures are ideally composed of ECs isolated from the umbilical vein of full-term infants with healthy mothers. The ECs are then subjected to growth in a medium, allowing the study of metabolic and other physiological functions. This method's strength is the ability to use cords derived from subjects with certain diseases. This opens the possibility to study the role of genetic, epigenetic, and proteomic factors (Medina-Leyte et al., 2020). HUVEC cultures can form capillary-like structures which are useful as angiogenic models; however, they do not reflect all the physiological steps associated with angiogenesis. In addition to evaluating CLS, the role of adhesion molecules in tubular morphogenesis, blood vessel maturation and the synthesis of extracellular proteins can be studied with this *in vitro* method (Medina-Leyte et al., 2020). However, cultured HUVEC can experience limitations in proliferation as the culture reaches confluence (Medina-Leyte et al., 2020). HUVEC cultures have a lifespan of approximately ten passages; however, there is a loss in their primary characteristics and a lack of stimuli response after the 6^{th} passage. Thus, HUVEC models hold the disadvantage of having a relatively short lifespan, making this model unsuitable for long-term experiments (Medina-Leyte et al., 2020).

1.5.3 The use of in vivo assays in the study of angiogenesis

In vivo models aim to assess vascular development in a region of a whole animal in response to pro- and anti-angiogenic factors and tend to focus on an overall outcome rather than specific associated processes such as proliferation (Chávez et al., 2016). Currently, *in vitro* assays fail to include supporting cells, the extracellular matrix, and circulating blood. While *in vivo* assays include these components, limitations arise depending on the microenvironment, organ site, and the administration of test variables (Staton et al., 2004). An obvious advantage of studying angiogenesis *in vivo* is that several cell types can be analyzed to observe how pro- and anti-angiogenic processes affect blood vessel formation. Although there is a great benefit to studying angiogenesis *in vivo*, a major disadvantage is that experiments are relatively expensive, and other cell types can confuse the results. This can be attributed to the involvement of inflammatory agents and responses, which can cloud the discrimination of responses from blood vessel cells and paracrine effects (Norrby, 2006). For example, the presence of tumour cells may induce a non-specific inflammatory reaction that could cause varying angiogenic responses and connective tissue infiltration. A similar response could be seen with wounds or when a foreign material is involved (Norrby, 2006).

Differentiation assays can closely mimic i*n vivo* situations when studying lumen formation. Differentiation assays, also known as tubule formation assays, study the assembly of ECs to form capillary-like structures (Chávez et al., 2016; Staton et al., 2004). This is accomplished by culturing ECs on matrices that consist of fibrin, collagen or Matrigel. This allows tubules to form through the attachment, migration, and differentiation of ECs. However, a problem associated with these matrices is that it is unclear whether the tubes possess a lumen (Donovan et al., 2001). Using this assay in the

third dimension allows one to study the formation of capillary networks inside a matrix resembling extracellular components, making it more representative of *in vivo* microenvironments (Chávez et al., 2016). Nevertheless, it can be challenging to analyze tubule formation and the quantification of cell behaviours (Staton et al., 2004).

Another type of *in vivo* assay is the chorioallantoic membrane (CAM) assay. The chorioallantoic membrane is a highly vascularized membrane initially responsible for gas exchange in the avian embryo. The CAM assay allows angiogenic inhibitors and stimulants to be studied in a vascularized environment (Chávez et al., 2016; Norrby, 2006; Staton et al., 2004). Tissue grafts are created with pro- or anti-angiogenic agents and placed directly on the chorioallantoic membrane. This assay is performed *in ovo*, but an alternative method uses CAM explants in petri dishes to measure angiogenic growth (Norrby, 2006; Staton et al., 2004). This method allows a greater quantification of blood vessels studied over a greater region of the CAM than is possible *in ovo*. There are, however, downfalls associated with this method. The CAM is a susceptible area, and any irritant, including shell dust created when opening the shell, can produce an inflammatory angiogenic reaction (Jakob et al., 1978; Knighton et al., 1991). Furthermore, the membrane is also sensitive to changes in oxygen tension (Chávez et al., 2016; Norrby, 2006). This makes sealing the shell a particularly challenging task (Auerbach et al., 2000; Norrby, 2006).

Mouse models are also commonly used to study angiogenic processes because their physiology is most like that of humans. This is valuable when testing angiogenic factors concerning human diseases and studying the role of angiogenesis (Chávez et al., 2016; Jensen et al., 2012). Researchers can also genetically manipulate mice to generate important genes for angiogenesis and vascular biology.

1.5.4 The use of organ culture assays in the study of angiogenesis

Organ culture assays are another type of model that is more closely representative of *in vivo* situations. Segments, disks, or sections of the studied tissues are cultured, and once plated on a matrix, the length and number of microvessel outgrowths are measured. Problems can arise with quantifying the outgrowths due to vessel clustering in the matrix (Auerbach et al., 2000; Staton et al., 2004). This assay is the closest to mimicking *in vivo* environments because it includes non-endothelial cells and the supporting matrix. Another strength of this model is that quiescent ECs respond and become proliferative, then migrate to differentiate tubules, which is representative of angiogenesis *in vivo* (Staton et al., 2004). However, species differences can be problematic when comparing and referencing studies. Thus, using non-human tissues can be challenging when testing the response of a substance, as the reaction could be species-specific (Staton et al., 2004).

Two well-known organ culture assays are fetal metatarsal and aortic ring assays. The metatarsal assay is an *ex vivo* assay that uses metatarsals extracted from 17-day-old mouse embryos to observe vessel outgrowth (Staton et al., 2004). Once plated onto tissue culture plates, vessel outgrowth is quantified by measuring the vessel length, area, and the number of vessel branch points (Goodwin, 2007). Unlike other *in vitro* assays, the metatarsal method allows one to observe the formation of tubule lumen as well as the development and recruitment of supportive cells. Thus, this method enables the complex microenvironment and its interactions to be studied. Limitations of this assay include a lack of blood flow; however, this feature is common to all *in vitro* and *ex vivo* models (Song et al., 2015).

The aortic ring assay is a common organ culture model that uses mouse or rat aorta segments to demonstrate vessel growth (Goodwin, 2007). Segments of the aorta are

embedded in a collagen gel, and the outgrowth can be quantified using immunohistochemical analysis or phase microscopy. Like the metatarsal assay, leftover adventitia on the vessel can influence vessel outgrowth (Goodwin, 2007). Variability in handling, age and strain of mice can lead to varying responses in vessel outgrowth (Zhu et al., 2003). On a final note, as this assay occurs in three dimensions, photography and quantification can prove challenging. Compared to cell-based assays, the two listed organ cultures have advantages, which include supporting cells, such as pericytes, playing an essential role in neovessel stability (Baker et al., 2012; Song et al., 2015). Although these two models have their presented disadvantages, organ culture models work to bridge the gap between *in vivo* and *in vitro* models by providing an economical middle way.

The rodent whole embryo culture (WEC) is an assay that is similar to organ cultures in the sense that the experimenter can direct observation and manipulation that is representative of *in vivo*. The ex-utero technique grows post-implantation mouse or rat embryos through the period of organogenesis, typically between embryonic days 7.5 and 13.5 (New, 1978). Cultures are generally viable for up to 5 days, where somite number, axial rotation, developmental progression, and protein content can be assessed. Essentially, the WEC allows mammalian embryos to be grown and observed outside the confinement of the maternal uterus (New, 1978; Piersma, 1993; Webster et al., 1997). Advantages of this technique include the ability to screen and control the exposure of test chemicals without maternal interference (e.g., absorption, metabolism, distribution, and excretion) (Webster et al., 1997). Another advantage of this method is reduced animal use as well as reduced cost and time. Since embryos can be cultured individually, one litter can be exposed to multiple test concentrations and substances (Piersma, 1993; Webster et al., 1997). However, this process includes higher technical skill to ensure that the

embryos are not damaged and ultimately alter the test chemical's response. The main disadvantage of this assay is the limited period of embryogenesis and restricted culture duration, which limits the range of abnormalities that could be observed (Webster et al., 1997). Lastly, the artificial route of administration and absence of maternal factors give rise to the disadvantage of studying adult/maternal toxicity (Piersma, 1993; Webster et al., 1997).

Due to the heterogeneity and complexities of angiogenic tissues, no single assay best embodies all situations. Thus, angiogenesis studies heavily rely on considering the advantages and drawbacks of multiple assays to select the most efficient method appropriately. An ideal model should be specific, repeatable, precise, and reliable; however, these tend to be common limitations in current models (Norrby 2006). It is important to realize that, when possible, both *in vitro* and *in vivo* assays should be used to complement one another in study (Norrby, 2006; Staton et al., 2004). Given the presented limitations and advantages, the aortic ring assay and whole embryo culture were used to complement this investigation. In combination, these assays demonstrate the short-term effects of cadmium on the vasculature system in both adulthood and during the sensitive period of embryogenesis.

1.6 Objectives, Hypotheses and Predictions

Many studies have identified cadmium as either an inhibitor or a stimulator of angiogenesis (Gheorghescu et al., 2015; Jing et al., 2012; Kim et al., 2012; Majumder et al., 2008; Majumder et al., 2009; Prozialeck et al., 2006; Woods et al., 2008). Cadmium has been found to increase oxidative stress in the body, causing the inactivation of tumour suppressor proteins and the activation of oncogenes, including AKT and VEGF,

stimulating angiogenesis. However, cadmium has also been identified for its anti-angiogenic properties, which are linked to an upregulation of pro-apoptotic proteins, reducing VEGF signalling (Gheorghescu et al., 2015; Zhao et al., 2015). The fact that cadmium does not have a linear dose-dependent effect presents a critical gap in knowledge. Angiogenesis is an essential homeostatic regulator in response to toxin exposure, and its dysfunction is involved in a range of pathophysiological processes. Thus, despite knowledge about dose-dependent toxicity, little is known about the angiogenic mechanisms governing such toxicity. The apparent lack of knowledge is demonstrated in multiple stages of development, including embryogenesis and pathophysiological processes in adulthood. This study aims to address this gap in knowledge by investigating the effects of various cadmium concentrations on both embryonic and adult angiogenic processes in mice.

In this thesis, I examined whether changes in blood vessel development and signalling pathways were correlated with cadmium exposure at different concentrations. I hypothesized that cadmium would disrupt vascular development and signalling in a non-linear concentration-dependent manner. In the whole embryo culture model, I predicted that samples exposed to cadmium *in vitro* from day 8 to 9 of gestation would demonstrate a concentration-dependent decrease in yolk sac vessel size and development compared to control samples. Thus, embryos treated with 1.75 μM would exhibit a greater decrease in angiogenesis compared to 1.25 μM. In the aortic ring assay, I predicted that samples treated with lower levels of cadmium (< 5 μM) would demonstrate an increase in angiogenesis. More specifically, samples would exhibit an increase in the number of vessels and vessel branch points as well as an increase in vessel length, accompanied by an increase in AKT and VEGF signalling. Conversely, samples treated with higher levels

of cadmium (≥ 5 μM) would experience a decrease in the number of vessels, vessel branch points and vessel length through an upregulation of PTEN.

The results of this study will help establish the specific mechanisms of cadmium's effect on cell proliferation, differentiation, and growth of *in vitro* vascular cultures. Additionally, they will provide information on how this heavy metal causes abnormal blood vessel outgrowth at different concentrations and provide insight into how it may affect vessel development at a developmental and teratogenic level. These results can increase our understanding of pro- and anti-angiogenic molecules that could be used to treat angiogenic-regulated diseases through experimental manipulation in three dimensions rather than two, more closely mimicking *in vivo* processes.

2 METHODS

2.1 Image Analysis of Histological Sections of Cultured Mouse Embryos

The effect of cadmium on yolk sac blood vessel development was studied using histological sections of cadmium-treated and control-cultured mouse embryos prepared by Scroggie (1996), according to the method described in Appendix A. The slides used for this study contained serial sections of whole mouse embryos with intact yolk sacs that had been cultured in the absence or presence of 1.25 or 1.75 μM cadmium chloride for 24 hours, starting on day 8 of gestation (3 to 5 somites). These concentrations were selected based on the results from Nakashima et al., (1988), which found that embryo viability began to decrease at 2 μM. For this thesis, image analysis was performed on every 13th cross-section for embryos sectioned transversely. Cross-sections were analyzed manually and using Fiji/ImageJ to examine the morphological and quantitative differences of yolk sac blood vessels between treatment groups (Schindelin et al., 2012). The total number of

yolk sac blood vessels per embryo was calculated using the sum of the number of vessels per cross-section for the whole embryo. Furthermore, the average number of yolk sac blood vessels was determined by taking the average value to account for potential differences in yolk sac size (Figure 8). Using the Measure tool in Fiji/ImageJ, the average perimeter (μm) of the yolk sac (Figure 9) and the average cross-sectional area (μm²) of the whole conceptus (embryo plus yolk sac) (Figure 10) were determined using every 13th section. The same measurements were taken for yolk sac blood vessels of the three middle cross-sections. Lastly, the relative vascular density for each treatment group was calculated and expressed as the number of blood vessels per μm² of the yolk sac cross-sectional area.

Figure 8: Histological analysis outlining the blood vessels found within the yolk sac of the mouse embryo cross-section. The total number of yolk sac blood vessels per embryo was counted using a light microscope, and the average number of vessels per section was calculated. Using the measure tool in Fiji/ImageJ, the perimeter (μm) and cross-sectional area (μm²) of blood vessels were calculated.

Figure 9: Histological analysis outlining the yolk sac of the mouse embryo cross-section. Using the measure tool in Fiji/ImageJ, the perimeter (μm) of the yolk sac was calculated.

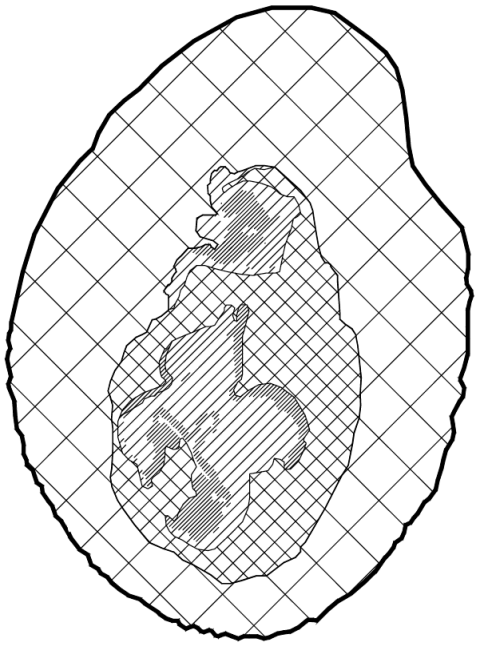

Figure 10: Cross-sectional area of the yolk sac of the mouse embryo cross-section. Using the measure tool in Fiji/ImageJ, the cross-sectional area (μm²) of the whole conceptus (embryo plus yolk sac) was measured, as indicated by cross-hatching.

2.2 Mouse Dissection and Aorta Explant

CD1 mice purchased from Charles River Laboratory were housed in positive pressure rooms at Trent Animal Care Facility. Males and females were caged separately on a 12-hour light/dark cycle with constant access to Lab Diet 5012 and municipal water. All work was completed in compliance with the Trent University Animal Use Protocol.

Mice were sacrificed using cervical dislocation at ages ranging from 8 weeks to 26 months. Following euthanasia, the aorta was detached from the spinal column and cut just before the artery branches into the abdominal iliacs. Once separated, the aorta was placed into Gibco Opti-MEM with GlutaMax supplement (Baker et al., 2012; Kapoor et al., 2020). The aorta was then cleaned by removing excess tissue and cut into 1 mm rings in Opti-MEM under a dissecting microscope, ensuring it did not dry out. The rings were kept on ice until they were ready to be embedded.

Following the methodology of Baker et al. (2012) and Kapoor et al. (2020), one aortic ring was embedded per well of a 96-well plate (Sigma-Aldrich) using a 1 mg/mL collagen type-I matrix (Gibco) in Opti-MEM, neutralized with NaOH. 50 µl of the collagen matrix was transferred to each well of the 96-well plate and left for 30 minutes at 37 °C/5% CO_2, during which time the collagen began to gel. Next, the aortic rings were carefully transferred to the collagen with forceps. The last 25 µl of the collagen matrix was added on top of the rings, and the plates were left undisturbed for 10-15 minutes at room temperature and then incubated at 37 °C/5% CO_2 for 30 minutes.

Lastly, Opti-MEM culture medium was prepared by adding 2.5% (vol/vol) FBS, 30 ng/ml VEGF recombinant protein (Gibco) and 1% (vol/vol) penicillin-streptomycin (Gibco). The medium was warmed to 37 °C, and 150 µl was carefully added to the wells. The plate was then placed in a humidified incubator at 37 °C and 5% CO_2.

2.3 Cadmium Treatment of Aortic Cultures

The first media change occurred on day 3, in which 130 µl of old media was removed, and 150 µl of new, warmed complete media was added to all wells. At this time, aortic ring viability was assessed by phase contrast microscopy, and cadmium treatments were initiated. Fibroblasts are a common cell type found throughout the body, supporting endothelial cell sprouting and lumen formation. Thus, to deem an aortic ring viable, cultures had fibroblasts migrating outwards. Treatments were applied to wells that demonstrated fibroblast growth. Control treatments consisted only of culture medium. To test the effects of cadmium, a stock solution of warmed cadmium chloride in Dulbecco's Phosphate Buffered Saline supplemented with 100 mg/L magnesium chloride and 100 mg/L calcium chloride (DPBS) (Gibco) was added to the culture media to obtain concentrations of 0 µM, 0.5 µM, 1 µM, 5 µM and 10 µM (Jing et al., 2012; Mao et al., 2011; Wei et al., 2017). Similarly, 130 µl of old media was removed, and 150 µl of fresh media with or without cadmium chloride was added every other day until the experiment ended on day 10.

2.4 Fluorescent Staining: BS1 Lectin, and DAPI

At the end of the 10-day culture period, aortic rings were stained using DAPI (Invitrogen, catalog # D1306) to identify nuclei and vessels were stained for endothelial cells using BS1 lectin (Sigma-Aldrich, product # L2895) to measure the total vascular network length and area. First, the culture media was removed from all wells, and the whole plate was washed with DPBS. Cells were fixed with 4% formalin in DPBS for 30 minutes at room temperature. After 30 minutes, the fixative was removed, and wells were permeabilized with DPBS + 0.25% (vol/vol) Triton X-100 for two 15-minute incubations

at room temperature. Wells were incubated with blocking buffer (0.5% bovine serum albumin (BSA), 1% Tween 20 and 3% Triton X-100 dissolved in DPBS) for one hour at room temperature with gentle rocking.

Detection reagents were prepared in blocking buffer to a concentration of 0.1 mg/ml for BS1 lectin FITC-conjugate with 50 µl added to each well. Wells were covered and incubated overnight at 4 °C with gentle rocking. The next day, the detection reagent was removed, and wells were washed four times in blocking buffer for 15 minutes. After BS1 lectin staining, the aortic ring cultures were incubated with 50 µl of 400 nM DAPI for one hour. Following DAPI staining, wells were washed with DPBS + $MgCl_2$ + $CaCl_2$.

Vessel outgrowth was viewed using a Nikon Eclipse Ts-2R inverted microscope. BS1 lectin (green) were visualized using a 495 nm FITC filter cube, while DAPI (blue) was visualized using the 358 nm UV filter cube. Outgrowth was photographed and analyzed using Fiji/ImageJ (Schindelin et al., 2012).

2.5 Protein Extraction

On day 10 of the aortic ring culture, protein was extracted for western blotting to determine relative changes in protein amounts by measuring band densities. Proteins of interest included the phosphorylated forms of VEGFR2, PTEN, and AKT. These were compared to a reference protein such as beta-actin or GAPDH (Haberstroh and Kapron, 2006). Media was removed from each well, and the collagen matrix and cells were dissolved using 50 µl of ice-cold RIPA buffer (150 mM of sodium chloride, 50 mM Tris-HCl (pH: 8.0), 1% Triton-X 100, 0.5% sodium deoxycholate, and 0.1% SDS). Samples were placed into 1.5 ml microcentrifuge tubes according to their treatment group. Each sample had a total of three rings pooled together, and there were at least six samples per

treatment group. The remaining liquid from the wells was added to the same microcentrifuge tube (Kapoor et al., 2020).

Samples were vortexed vigorously at 15,000 rpm for 5 minutes, and insoluble aortic rings and collagen were removed. The protein concentration per sample (μg) was measured using an Invitrogen Qubit fluorometer, allowing equal protein loading. Samples were subjected to gel electrophoresis and western blotting protocols or were frozen at -20 °C for later analysis.

2.6 Gel Electrophoresis and Western Blotting

Frozen samples were thawed on ice, and samples were prepared with a 3X loading buffer (3X blue loading and 1/10 volume 30X DTT reducing agent (Cell Signaling). Next, the lysates were boiled for 5 minutes. Samples were spun on a benchtop microcentrifuge at 10,000 rpm for 5 minutes to remove insoluble aortic rings and collagen.

Protein concentration was measured using the Qubit fluorometer, and samples with equal amounts of protein per lane were resolved on a 10% polyacrylamide gel using a Biorad Mini-Protean system. The separating gel was prepared using BioRad 30% acrylamide/bis, 1.5M Tris-HCl (pH: 8.8), 10% SDS, dH_2O, TEMED, and 10% ammonium persulfate (APS). The polyacrylamide solution was mixed gently before being poured into the gel casting device. A small amount of dH_2O was added to the top of the separating gel to minimize bubble formation and create a uniform surface. While the separating gel was solidifying, a 4% stacking gel was prepared. This was done by adding 30% acrylamide/bis, 0.5M Tris-HCl (pH: 6.8), 10% SDS, dH_2O, TEMED, and 10% APS. Once the separating gel solidified, the water previously added was removed, and the

stacking gel was added to the casting frame along with a 10-well comb. The stacking gel was left to solidify for 30 minutes.

Once the prepared polyacrylamide gel had solidified entirely, the gel was removed from the casting frame and placed in the electrophoresis device. The entire chamber was filled with 1X running buffer (250mM tris, 1.92M glycine, and 1% SDS; pH: 8.8). Once assembly was complete, 5 µl of blue pre-stained protein ladder (Cell Signaling) was added to the first well. Samples were loaded with equal amounts of protein in each lane. Once the ladder and samples were added, the SDS-PAGE was run at 130V for 1.5 hours.

After electrophoresis, the samples were transferred from the gel onto a BioRad nitrocellulose membrane by electroblotting with transfer buffer (25mM tris, 192mM glycine, 20% methanol; pH: 8.3) at 90V for 1 hour at 4 °C. Once the transfer was complete, membranes were removed from the transfer sandwich and washed with 1X TBS-T (20 mM Tris, 150 mM NaCl, and 0.1% Tween-20; pH: 7.6) for 5 minutes. After the wash, membranes were incubated with blocking buffer composed of 5% BSA (Tocris) in 1X TBS-T for 1 hour. Following blocking, the membranes were rinsed with TBS-T for three 5-minute intervals. Membranes were incubated and gently rocked overnight at 4°C with primary rabbit monoclonal antibodies to P-PTEN (Cell Signaling, catalog # 9551S), P-AKT (Cell Signaling, catalog # 2965S), and P-VEGFR2 (Cell Signaling, catalog # 2478S) diluted to 1:1000 in TBS-T with 5% BSA. Primary antibodies were removed the following day, and membranes were again rinsed three times with TBS-T. Then, the membrane was incubated for 1 hour in HRP-linked secondary anti-rabbit antibody (Cell Signaling) diluted 1:2000 in blocking buffer. During this incubation, the membrane was shaken slowly for 1 hour. After incubation, three portions of 15 ml of TBS-T were used to wash the membrane three times.

P-PTEN, P-AKT, and P-VEGFR2 protein band densities were visualized using Clarity or Clarity Max chemiluminescence reagents (Bio Rad) and the ChemiDoc imaging system (Bio Rad).

Following imaging, the membrane was rinsed with TBS-T to remove excess chemiluminescent substrate on the membrane, then placed in 15 ml of gentle stripping buffer (0.2M glycine, 35 mM SDS, and 1% tween-20; pH: 2.2), for 10 minutes at room temperature with a gentle rocking motion. Three portions of TBS-T were used to wash the membrane. The membrane was re-blocked, and the methodology was repeated using primary rabbit monoclonal antibodies to GAPDH (Cell Signaling, catalog # 5174S) diluted to 1:1000 in TBS-T with 5% BSA. The following day, GAPDH was removed, and membranes were rinsed 3 times with TBS-T. Next, the membrane was incubated for 1 hour in HRP-linked secondary anti-rabbit antibody (Cell Signaling) diluted 1:2000 in blocking buffer. During this incubation, the membrane was shaken slowly for 1 hour. After incubation, three portions of 15 ml of TBS-T were used to wash the membrane three times.

The ChemiDoc imaging system and Clarity Max were used to observe the newly probed GAPDH at its specified molecular weight. After the images were acquired, Fiji/ImageJ and Excel were used to express standardized band densities as a percentage relative to the control group (Schindelin et al., 2012).

2.7 Statistical Analysis

For the aortic ring assay, treatments were applied to at least six aortic rings, each from a different mouse preparation. Similarly, a range of 8 to 11 embryos, each from different mouse preparations, were used for histological analysis. Western blotting

analysis consisted of two normalizations. First, band densities were standardized through equal protein loading, and second, they were standardized to the housekeeping gene GAPDH. Data for both experiments are represented as a mean ± the standard error of the mean. To determine the significance across treatments and account for multiple comparisons among litters, one-way ANOVA and post-hoc Tukey HSD tests were used. A 95% confidence interval was used in evaluating the significance between treatments. Outliers were identified using the IQR method, and any that were found were excluded from both statistical and data analysis sets (Dash et al., 2023; Sudhakar et al., 2021). Raw values, including outliers, can be found in Appendix B and C. Furthermore, Cohen's f effect size statistics were calculated, where $f < 0.1$ was considered trivial, $f = 0.1 – 0.24$ was considered small, $f = 0.25 – 0.39$ was considered medium, $f \geq 0.40$ was considered large (Cohen, 1988). Cohen's f effect sizes can be found in Appendix E.

3 RESULTS

3.1 The Effects of Cadmium on Vessel Development in Day 8 of Gestation Mouse Embryos

Morphological vascular differences of yolk sac blood vessels treated with 0, 1.25 and 1.75 μM cadmium were examined using the hematoxylin- and eosin-stained cross-sections of mouse embryos. Histological analysis consisted of 9 samples for the control group, 11 for 1.25 μM cadmium, and 11 for 1.75 μM cadmium. Outliers identified using the IQR method were found for the perimeter of the yolk sac as well as for the area of blood vessels (Appendix B).

The response in the quantity of blood vessels in the yolk sac varied depending on the cadmium concentration. ANOVA testing found a significant decrease of 27% in the

average number of blood vessels for embryos treated with 1.75 μM cadmium versus embryos cultured with 1.25 μM, with a p-value of 0.009 and a large effect size. Embryos cultured with 1.25 μM cadmium had a 27% increase in the average number of blood vessels compared to the control (large effect size), whereas those treated with 1.75 μM experienced an 8% decrease (small effect size), although neither of these changes was significant. This is demonstrated in Figure 11, which shows the increase in the average number yolk sac blood vessels solely for embryos treated with low cadmium concentrations. For total number of blood vessels, embryos cultured with 1.25 μM had a 35% increase in the total number of blood vessels per embryo compared to the control ($p=0.033$ and large effect size). Embryos grown in 1.75 μM cadmium were not significantly different from controls. When comparing the two cadmium concentrations, embryos cultured with 1.75 μM had a 30% decrease in the total number of blood vessels per embryo compared to 1.25 μM, with a p-value of 0.0089 and a large effect size. These results can be seen in Figure 12, where embryos treated with 1.25 μM cadmium experienced the greatest increase in the total number of yolk sac blood vessels.

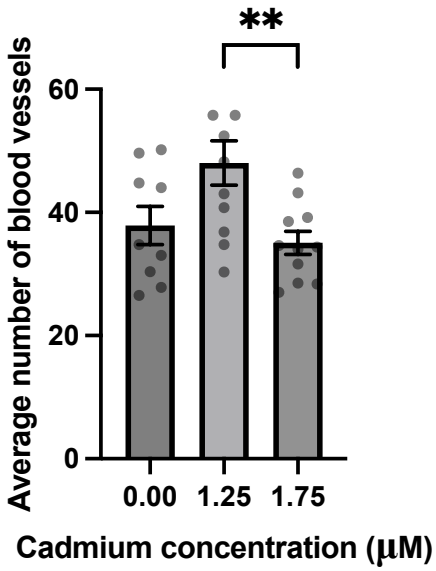

Figure 11. The effect of cadmium on the average number of blood vessels in mouse embryo yolk sacs. Prepared cross-sections were cut transversely and stained with hematoxylin and eosin, n = 9 to 11. Bars represent the mean ±SEM. There was a significant difference in the number of blood vessels in embryos exposed to 1.25 µM compared to those exposed to 1.75 µM, **p<0.01. Overall p-value =0.0088 using one-way ANOVA testing. Overall f-value demonstrated a large effect size (f-value=0.60).

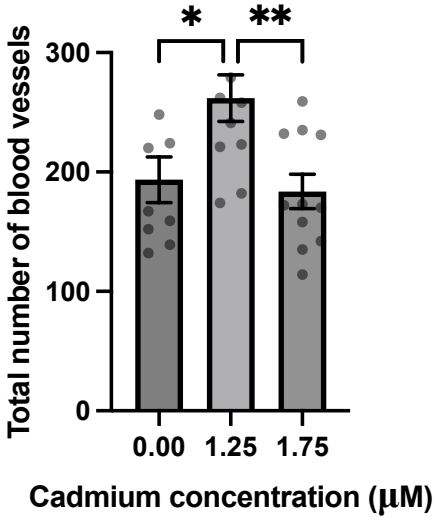

Figure 12. The effect of cadmium on the total number of blood vessels in mouse embryo yolk sacs. Prepared cross-sections were cut transversely and stained with hematoxylin and eosin, n =9 to 11. Bars represent the average ±SEM. Significance was noted for both treatment groups, *p<0.05 and **p<0.01, respectively. Overall p-value=0.0067 using one-way ANOVA testing. Overall f-value demonstrated a large effect size (f-value=0.62).

Yolk sacs exposed to 1.75 μM had a 20% increase in their perimeter compared to the control ($p = 0.013$ and large effect size). Embryos cultured with 1.75 μM also demonstrated a 20% increase in perimeter size compared to 1.25 μM ($p=0.0085$ and large effect size). Figure 13 shows the relative increase in the perimeter for the 1.75 μM treatment group, whereas embryos cultured with 1.25 μM experienced little change. One outlier was found in the perimeter measurements for the control group using the IQR method, and was eliminated from the analysis.

Embryos exposed to 1.75 μM cadmium had an increase in the cross-sectional area of their yolk sac compared to the control and 1.25 μM treatment groups, with a medium effect size; however, no significant differences were found for these data sets. Although insignificant, a small effect size was noted when comparing both treatment groups to the control. The cross-sectional area of the embryo's yolk sac is demonstrated in Figure 14.

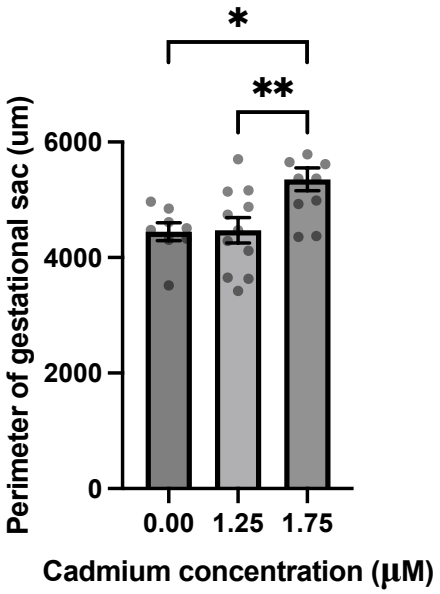

Figure 13. The effect of cadmium on yolk sac perimeter (µm) in mouse embryos. Prepared cross-sections were cut transversely and stained with Hematoxylin and Eosin, n=9 to 11. Bars represent the average ±SEM. A significant difference was noted for both treatment groups, *p<0.05 and **p<0.01, respectively. Overall p-value=0.0039 using one-way ANOVA testing. Overall f-value demonstrated a large effect size (f-value=0.69).

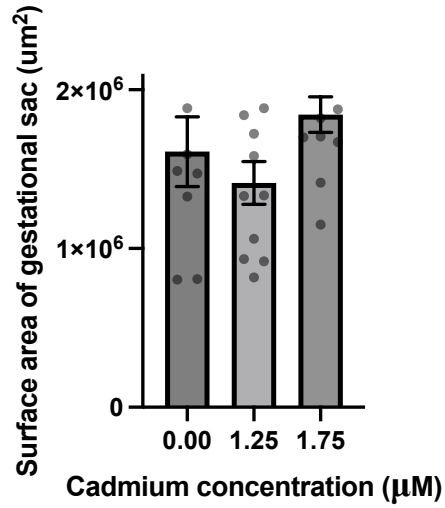

Figure 14. The effect of cadmium on the cross-sectional area (µm^2) of the yolk sac in mouse embryos. Prepared cross-sections were cut transversely and stained with Hematoxylin and Eosin, n = 9 to 11. Bars represent the average ±SEM. No significance was found with an overall p-value=0.14 using one-way ANOVA testing. Overall f-value demonstrated a medium effect size (f-value=0.36).

Both treatment groups had a decrease in the cross-sectional area of yolk sac blood vessels compared to the control (Figure 15). Embryos treated with 1.75 μM cadmium had a greater decrease in size, which was 35% smaller than those not exposed to cadmium ($p=0.015$ and large effect size). The embryos in the 1.25 μM treatment group experienced a similar decrease in size compared to the control, which was 31% smaller in the cross-sectional area of blood vessels ($p=0.02$ and large effect size). As well, both treatment groups experienced a decrease in the perimeter of blood vessels relative to the control; however, only one treatment group was found to be significant (Figure 16). Embryos cultured with 1.25 μM cadmium had blood vessels smaller in their perimeter by 29% ($p=0.0069$ and large effect size), whereas those treated with 1.75 μM decreased by 11% (small effect size). When comparing the two treatment groups, a non-significant medium effect size was observed. Thus, it was observed that embryos for both treatment groups experienced a decrease in blood vessel size (Figures 15 and 16). Four outliers were found using the IQR method, with one outlier in the control group and three in the 1.75 μM treatment group. These were omitted from the analysis.

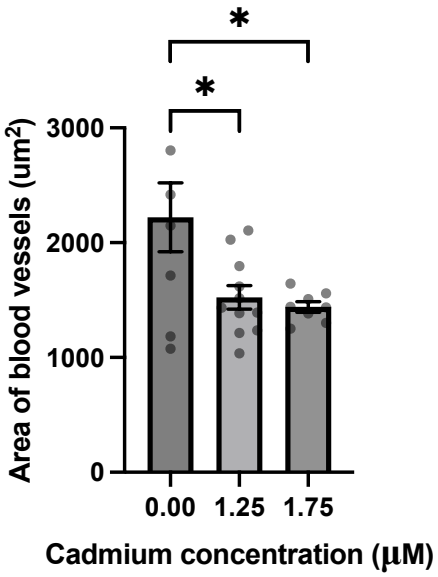

Figure 15. The effect of cadmium on the cross-sectional area (µm^2) of yolk sac blood vessels in mouse embryos. Prepared cross-sections were cut transversely and stained with Hematoxylin and Eosin, n = 9 to 11. Bars represent the average ±SEM. Significance was found for both treatment groups when compared to the control, *p<0.05. Overall p-value=0.0089 using one-way ANOVA testing. Overall f-value demonstrated a large effect size (f-value=0.63).

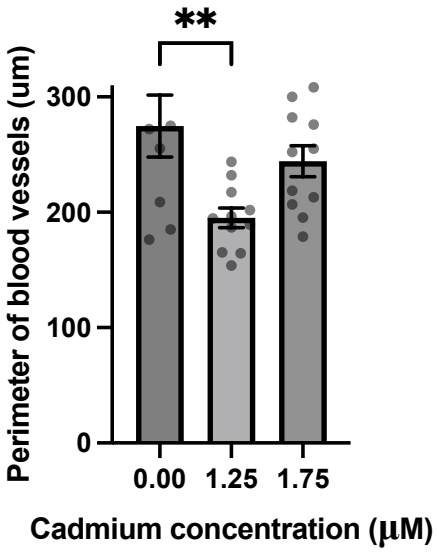

Figure 16. The effect of cadmium on the perimeter (µm) of yolk sac blood vessels in mouse embryos. Prepared cross-sections were cut transversely and stained with Hematoxylin and Eosin, n = 9 to 11. Bars represent the average ±SEM. Results for 1.25 µM were significant when compared to the control group, **p<0.01. Overall p-value=0.0082 using one-way ANOVA testing. Overall f-value demonstrated a large effect size (f-value=0.58).

The blood vessel density was expressed as the number of blood vessels per cross-sectional area (μm^2). The effects of cadmium on the density of blood vessels appeared to be concentration dependent. Embryos exposed to 1.25 µM had a 29% increase (medium effect size), while embryos cultured with 1.75 µM experienced a 30% decrease (medium effect size) in blood vessel density compared to the control. Furthermore, embryos treated with 1.75 µM cadmium experienced a significant decrease by 46% when compared to 1.25 µM, with a p-value of 0.0002 and a large effect size. This trend can be seen in Figure 17, which shows the relative increase in the number of blood vessels per area of the yolk sac when comparing embryos from the 1.25 µM treatment to those grown in 1.75 µM.

In summary, the effects of cadmium on vessel development in day 8 of gestation mouse embryos suggest that embryos exposed to cadmium have more blood vessels that are generally smaller in size compared to the control.

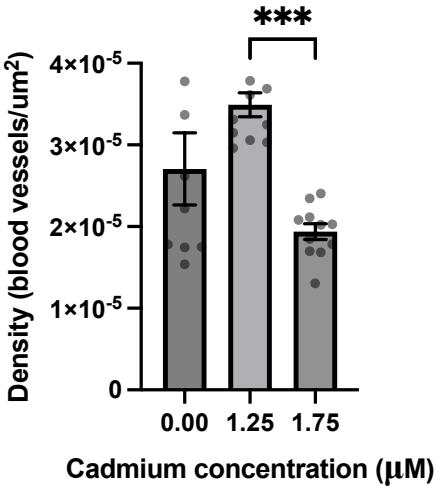

Figure 17. The effect of cadmium on the density of blood vessels in the yolk sac per µm² in mouse embryos. Prepared cross-sections were cut transversely and stained with Hematoxylin and Eosin, n = 9 to 11. Bars represent the average ±SEM. Significance was found when comparing the two treatment groups, ***p<0.001. Overall p-value=0.0004 using one-way ANOVA testing. Overall f-value demonstrated a large effect size (f-value=0.82).

3.2 The Effect of Cadmium on Blood Vessel Outgrowth from Aortic Rings in Culture

The morphology of blood vessels that sprouted in the aortic ring assay was quantified with the aid of fluorescence staining of fibroblasts and blood vessels. Representative images can be found in Appendix F. During the culture period, fibroblasts were noted by phase microscopy to migrate in three dimensions throughout the collagen, away from the aortic ring. The number of fibroblasts appeared to multiply daily, with quantity peaking from days 7 to 10. With an increase in the number of fibroblasts, it appeared that there was an increase in the surface area covered by cells throughout the gel. At the end of the culture period, DAPI-stained nuclei were observed as a blue hue throughout the multiple layers of collagen. Nuclei were seen with and without the presence of vessels by merging images taken with the 495 nm FITC and 358 nm UV filter cubes. When merged, nuclei were seen overlapping lectin-stained vessels. Figures 18 and 19 demonstrate growth-factor-induced vessel outgrowth from mouse aortic rings embedded in collagen. Fluorescent staining highlights endothelial sprouts fluorescing green and nuclei fluorescing blue.

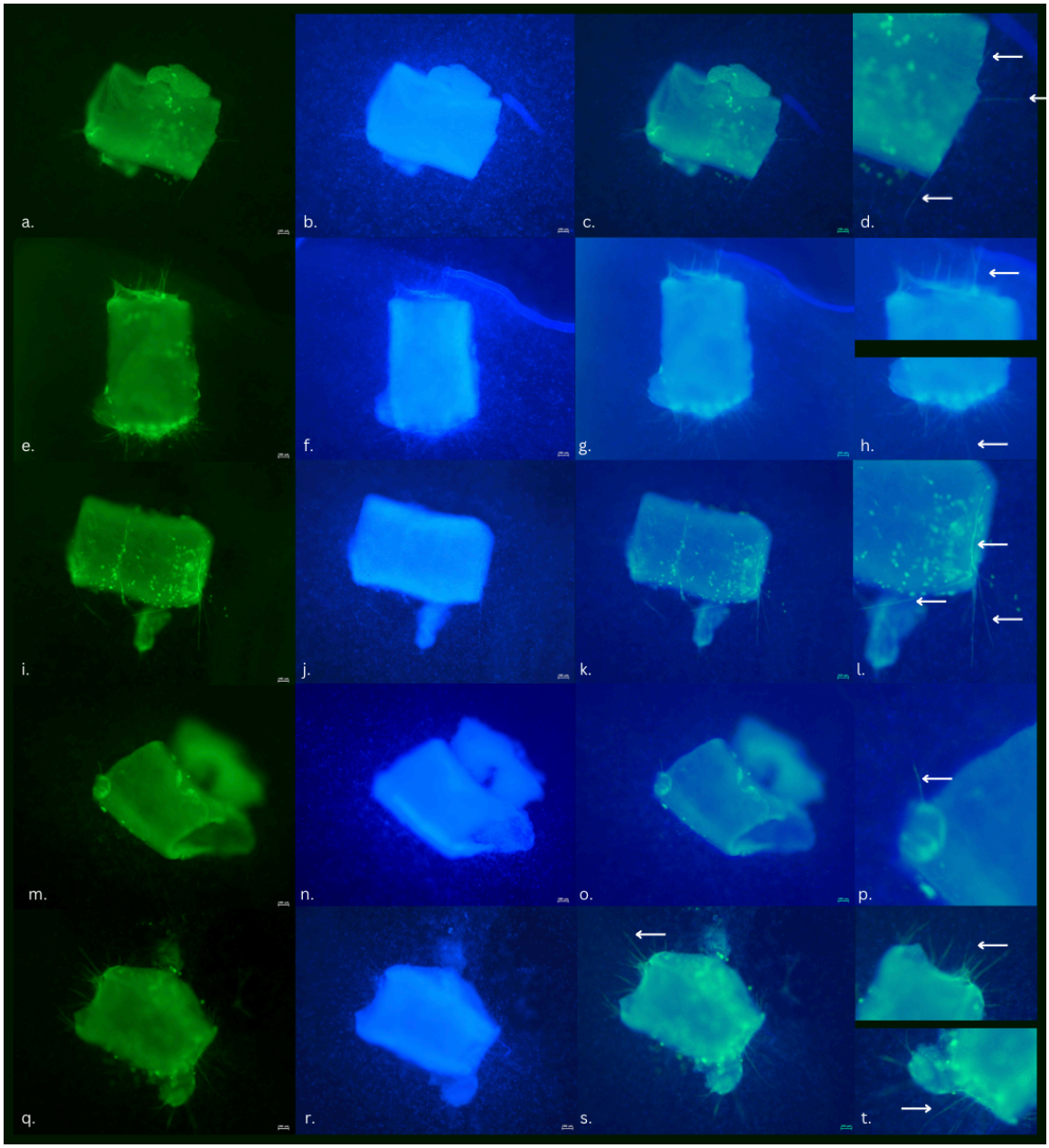

Figure 18. Fluorescent staining of mouse aortic rings exposed to varying cadmium chloride concentrations. White arrows point to growth factor-induced vessel growth in collagen. DAPI (blue) stained nuclei, and BS1 Lectin FITC (green) stained endothelial cells. The third picture in each row demonstrates the FITC and DAPI layers merged. Scale bar 100 µm. (a-d) Aortic ring treated with 0 µM cadmium chloride; (e-h) Aortic ring treated with 0.5 µM cadmium; (i-l) Aortic ring treated with 1 µM cadmium chloride; (m-p) Aortic ring treated with 5 µM cadmium chloride; (q-t) Aortic ring treated with 10 µM cadmium.

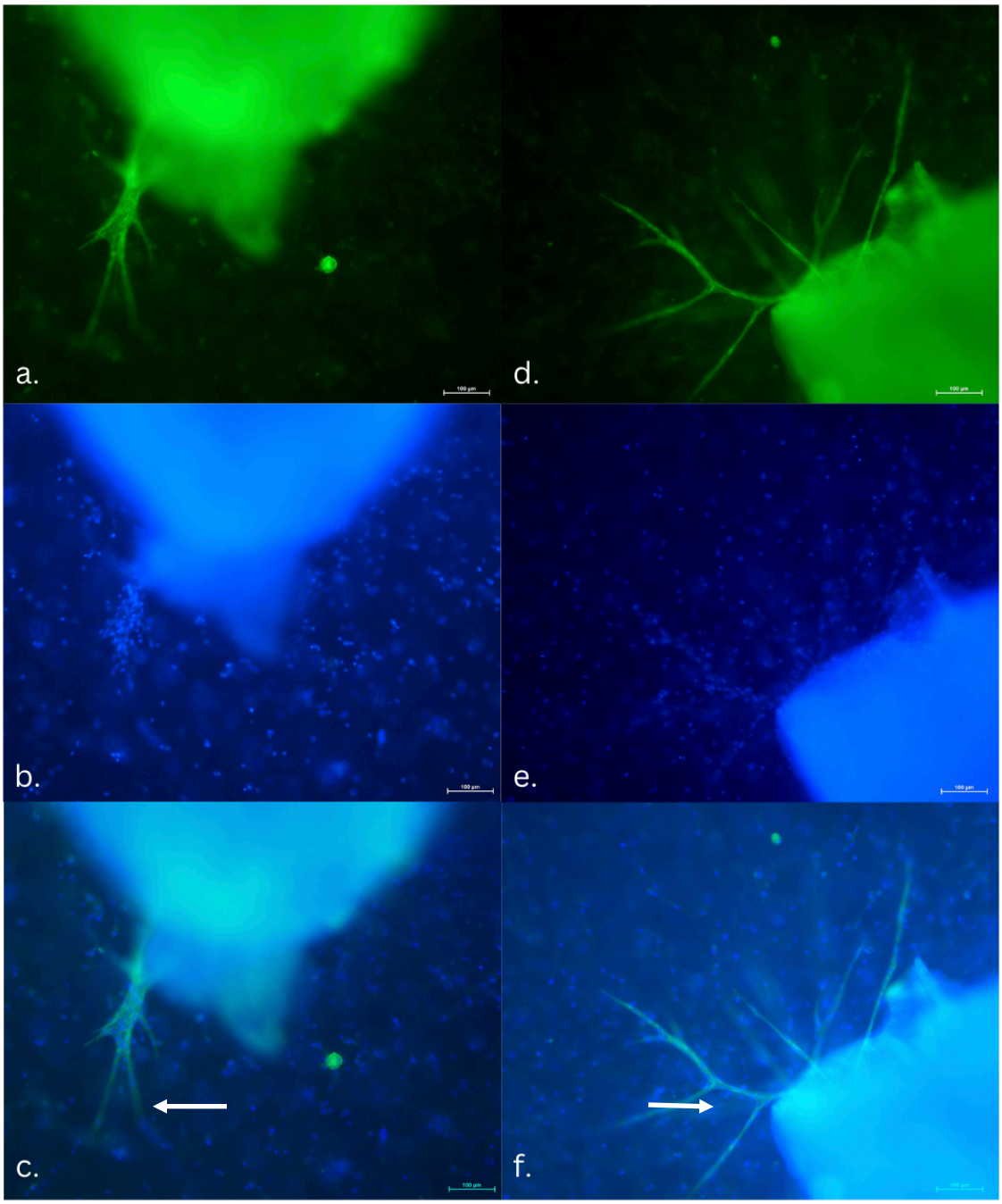

Figure 19. Fluorescent staining of mouse aortic rings exposed to 5 µM cadmium chloride. White arrows point to growth factor-induced vessel growth in collagen. DAPI (blue) stained nuclei, and BS1 Lectin FITC (green) stained endothelial cells. Scale bar 100 µm. (a) Vessel one closeup – endothelial cells staining with BS1 lectin FITC; (b) Vessel one closeup – nuclei staining with DAPI; (c) Vessel one – merged FITC and DAPI layers; (d) Vessel two closeup – endothelial cell staining with BS1 lectin FITC; (e) Vessel two closeup – nuclei staining with DAPI; (f) Vessel two closeup – merged FITC and DAPI layer.

Sample size varied between treatments. Samples consisted of four rings per treatment, excluding 0.5 and 10 μM, which had three each. Furthermore, two rings from the control group had no vessel growth and hence were excluded from branch point and vessel length quantifications. Thus, the sample size was two for the control group. The average number of vessels that sprouted from the rings was increased in all treatment groups compared to the control group (Figure 20). The greatest increases were observed in samples exposed to 0.5 and 1 μM cadmium. These groups experienced an approximate fourfold increase relative to the control (large effect size). Figure 20 illustrates the average number of vessels with 5 μM having the smallest increase, which was three times greater than the control (medium effect size). Additionally, cultures exposed to 5 μM cadmium had a small effect size compared to rings exposed to 0.5 and 1 μM. A large variability in response was observed, and none of the differences were statistically significant. Although statistically insignificant, the increase in the number of blood vessels at 10 μM was found to have a medium effect size. Similarly, all groups experienced an increase in the number of vessel branch points. 1 μM had the highest increase, which was seven times greater than the control (large effect size). Furthermore, a large effect size was also noted for cultures treated with 1 μM compared to 5 μM and a medium effect size compared to 0.5 and 10 μM. Figure 21 demonstrates the greatest increase in branch points at 1 μM, while the other treatment groups experienced a lesser increase; again, these differences were insignificant. However, small effect sizes were noted for 0.5, 5, and 10 μM compared to the control. Vessel length did not experience as drastic of an increase relative to the control group. 10 μM had the greatest increase, yielding 1.5 times increase (small effect size). Vessel length at 10 μM had an average vessel length of 236.6 μm, while the control group averaged 158.3 μm. This trend is

demonstrated in Figure 22, illustrating the relative increase in all treatment groups, with the highest increase at 10 μM. A p-value of 0.0368 was found using a one-way ANOVA when comparing the vessel length of vessels treated with 10 μM compared to the control. This was the only significant difference noted for these observations; however, a small effect size was noted for 10 μM compared to 1 and 5 μM. Additionally, a small effect size was noted for 0.5 μM compared to the control.

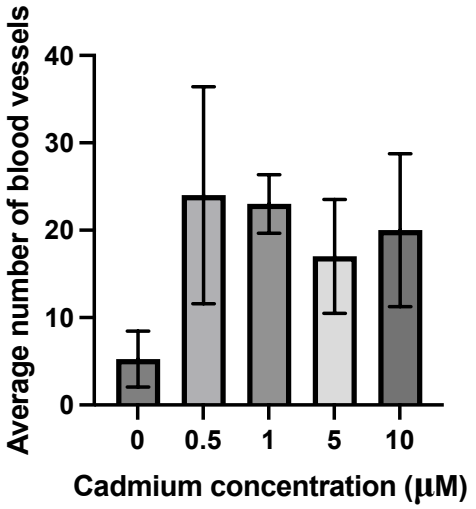

Figure 20. The effect of cadmium on the number of vessels in aortic ring cultures. Vessels were identified using fluorescent staining (BS1 lectin FITC). Sample size consisted of four aortic rings from three different mouse preparations. Bars represent the average ±SEM. Overall p-value=0.32 using one-way ANOVA testing. No significant differences were observed. Overall f-value demonstrated a large effect size (f-value= 0.50).

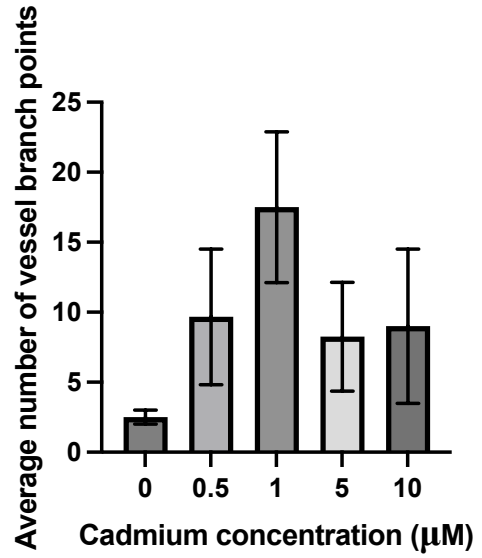

Figure 21. The effect of cadmium on the number of vessel branch points in aortic ring cultures. Vessels were identified using fluorescent staining (BS1 lectin FITC). Sample size consisted of four aortic rings from three different mouse preparations. Bars represent the average ±SEM. Overall p-value=0.39 using one-way ANOVA testing. No significant differences were observed. Overall f-value demonstrated a large effect size (f-value=0.57).

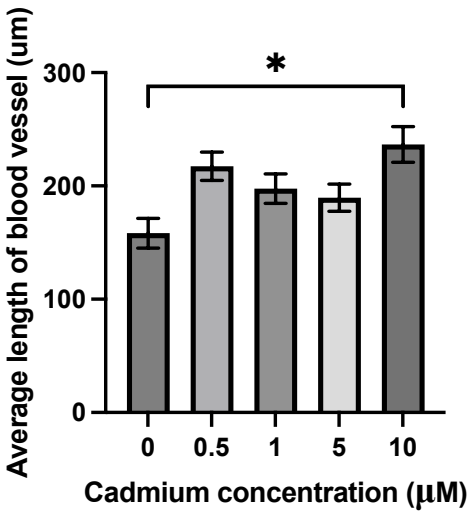

Figure 22. The effect of cadmium on vessel length (µm) in aortic ring cultures. Vessels were identified using fluorescent staining (BS1 lectin FITC). Sample size consisted of four aortic rings from three different mouse preparations. Bars represent the average ±SEM. Overall p-value=0.020 using ANOVA testing. There was a significant increase in vessel length upon treatment with 10 µM cadmium compared to the control group, *p<0.05 using one-way ANOVA and post-hoc testing. Overall f-value demonstrated a small effect size (f-value=0.21).

3.3 The Effect of Cadmium on the Amounts of p-AKT and p-PTEN in the Aortic Ring Assay

Phosphorylated levels of AKT, PTEN, and VEGFR2 were examined using western blotting to study the potential effects of cadmium on cell signalling pathways; however, no results for the amounts of p-VEGFR2 for this assay are presented. Although the reason was not determined, activated VEGFR2 was not detected by western blotting, and thus, band density was not calculated. Band density was used to calculate the amounts of activated AKT and PTEN relative to the control, normalized to GAPDH. Appendix G and H include sample images of western blotting from the aortic ring assay probed for the targeted proteins (Figures 29-31). Figure 23 illustrates a non-significant increase in phosphorylated AKT at 1, 5, and 10 μM cadmium exposures, while 0.5 μM remains relatively unchanged. Although non-significant, phosphorylated AKT levels were found to have a large effect size when comparing 1 μM to the control and 0.5 μM group. Furthermore, a medium effect size was noted when comparing 1 μM to 5 and 10 μM treatment groups, while the remainder were mainly trivial or small in their effect size. The greatest increase was observed in the group exposed to 1 μM, which was two times greater than the control (large effect size). Conversely, phosphorylated PTEN remained relatively unchanged, increasing 1.4 times at 5 μM. Figure 24 demonstrates this increase, and the 0.7 times reduction in band density at 10 μM (small effect size). The effect size for the other treatment groups were mostly trivial or small, apart from 5 μM compared to10 μM, which was found to have a medium effect. However, none of the changes described above were determined to be statistically significant.

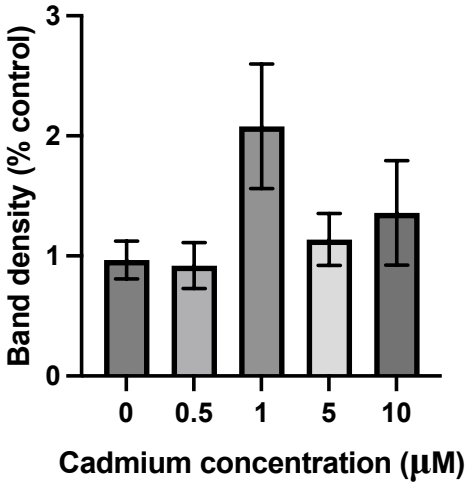

Figure 23. The effect of cadmium on p-AKT amounts in aortic ring cultures. Data was normalized to GAPDH and expressed as mean band density. n=11 for 0 µM; n=6 for 0.5, 1, and 5 µM; n=6 for 10 µM. Bars represent the average ±SEM. Overall p-value=0.082 using one-way ANOVA testing. No significant differences were observed. Overall f-value demonstrated a large effect size (f-value=0.49).

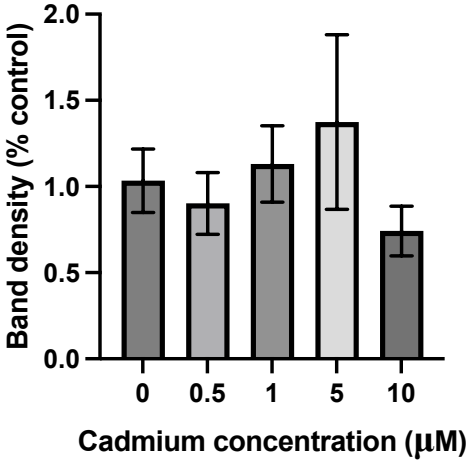

Figure 24. The effect of cadmium on p-PTEN amounts in aortic ring cultures. Data was normalized to GAPDH and expressed as mean band density. n=11 for 0 µM; n=6 for 0.5, 1, 5, and10 µM. Bars represent the average ±SEM. Overall p-value=0.59 using one-way ANOVA testing. No significant differences were observed. Overall f-value demonstrated a medium effect size (f-value=0.28).

4 DISCUSSION

4.1 Morphological Concentration-Dependent Changes: Histological Blood Vessel Analysis

4.1.1 Concentration-dependent response in blood vessel formation

This portion of the study was to observe yolk sac vascular development in embryos exposed to varying cadmium concentrations. The results of this experiment support the hypothesis of this study, in which mouse embryos at day 8 of gestation demonstrate a concentration-dependent angiogenic response to cadmium. The average number of blood vessels was used as an indicator for the number of blood vessels per cross-sectional area, whereas the total number of blood vessels represented the entire count of vessels within the yolk sac. The histological analysis demonstrates that the lower cadmium concentration (1.25 μM) increases angiogenesis based on the observed average and total number of blood vessels within the yolk sac. It was noted that there was a significant increase in the total number of blood vessels in embryos exposed to 1.25 μM versus control. There was also a significantly lower total and average number of vessels for embryos exposed to 1.75 μM compared to 1.25 μM cadmium. This observation is furthered by the results that there was a significantly lower vessel density for embryos exposed to 1.75 μM compared to 1.25 μM cadmium. These results provide novel evidence that cadmium at 1.25 μM has a stimulatory angiogenic response compared to the control and 1.75 μM treatment groups in day 8 of gestation embryos.

Previous studies have also noted cadmium-induced inhibition or stimulation of blood vessel formation in a concentration-dependent manner (Jing et al., 2012; Majumder et al. 2009). These observations have mainly been noted in the vascular bed of CAM assays in chick embryos. Before placenta formation in mammals, the yolk sac plays a

critical role in regulating gas exchange and nutrition to the developing embryo (Donovan et al., 2023). It also factors in establishing the susceptibility to diseases and other later-life health dysfunctions (Parenti et al., 2001). Toxicants may be taken up by the yolk sac following maternal exposure, which results in direct exposure to the embryo (Sant and Timme-Laragy, 2019). Different cadmium concentrations affect blood vessel formation differently. To elaborate, bradykinin is a calcium-mobilizing soluble peptide that can control the angiogenic phenotype of endothelial cells by activating the eNOS pathway (Parenti et al., 2001). Majumder et al., (2009) found that cadmium at 0.1 μM inhibits blood vessel formation in the vascular bed of chick embryos by inhibiting bradykinin. They determined that bradykinin-dependent growth was inhibited by cadmium, further orchestrated by blocked NO production (Majumder et al., 2008; Majumder et al., 2009). Interference in the bradykinin/eNOS/NO production causes endothelial dysfunction, ultimately reducing the formation of vascular networks. In contrast, cadmium concentrations greater than 1 μM have been noted to increase angiogenesis via VEGF upregulation. Jing et al. (2012) found that at 5 μM, cadmium-treated tissues increased vessel formation in a CAM assay. This upregulation was attributed to the activation of AKT signalling through ROS generation and, subsequently, endothelial cell migration.

Attenuation of angiogenesis at high concentrations has been noted in multiple studies, in which a decrease in the formation of the primary plexus in the yolk sac has been observed after exposure to cadmium (Gheorghescu et al., 2015; Gheorghescu and Thompson, 2016; Veeriah et al., 2014). For example, Veeriah et al., (2014) found that 10 μM cadmium decreased vessel formation in the CAM assay, which they attributed to the increase in cadmium-mediated oxidative stress during embryonic development, increasing the vulnerability to teratogenic assault. Vessel formation in the vascular bed of

chick embryos was also noted to be decreased in other studies that examined 50 μM cadmium (Gheorghescu et al., 2015; Gheorghescu and Thompson, 2016).

There are limited studies exploring the effects of cadmium at low concentrations in mouse embryos; however, this could be due in part to the increased embryo lethality and malformations noted with increasing concentrations (Kapron-Bras and Hales, 1991; Nakashima et al., 1988). When exposed to cadmium, day 8 of gestation mouse embryos were found to have significant increases in the number of dead embryos as well as their rate of malformation when exposed to 1.75 and 2.25 μM (Kapron-Bras and Hales, 1991). Similarly, Nakashima et al., (1987) found that teratogenic responses were observed at 1.2 to 2.2 μM in day seven mouse embryos, with embryo lethality obtained at 2 to 2.2 μM. Although embryo survival was not severely impaired until 2 μM, neural tube defects, hemorrhagic heads, and abnormal flexion were induced at 1.2 μM (Nakashima et al., 1988). Kapron-Bras and Hales (1991) also noted increased malformations at 1 μM. In combination, these studies demonstrate the steep dose-response curve suggesting the teratogenic potentials of chronic exposure to cadmium.

Together, these studies demonstrate the complexity of cadmium's teratogenic effect on vessel formation. There is a gap in literature that addresses the relationship between angiogenesis in developing yolk sacs and exposure to cadmium at low concentrations, specifically those under 5 μM. This study examined blood vessel formation at 1.25 and 1.75 μM and found a concentration-dependent response. At 1.25 μM, there was an increase in the total number of vessels compared to the control, as well as an increase in the average and total number of vessels when comparing 1.25 μM to 1.75 μM of cadmium. These results are in alignment with the prediction that lower concentrations may stimulate angiogenesis of the yolk sac, with significance observed for

the control versus the 1.25 μM treatment group. Since the average or total number of vessels was not different in the 1.75 μM concentration versus the control, cadmium at this higher concentration does not appear to have either a stimulatory or an inhibitory effect. Furthermore, based on previous studies, it is thought that as the concentration of cadmium increases, the teratogenic response will also increase and eventually start inhibiting the vascular development of the yolk sac. Similar to other findings, cadmium at low concentrations resulted in an increase in angiogenesis; however, cultures exposed to cadmium concentrations greater than 5 uM may experience a higher magnitude of change in relation to vessel quantity and size. Nonetheless, the concentrations used in this study elicited a stimulatory effect. Future studies should continue to explore the impact of cadmium ranges from 1 to 3 μM, keeping in mind that higher concentrations (> 2.2 μM) might kill all embryos. Additionally, exposure time as a factor that influences teratogenesis could be explored. Due to the critical parameters of organogenesis, future studies could look at acute rather than chronic exposure to cadmium on malformations and embryo lethality. Warner et al., (1984) exposed mouse embryos to 5.35 μg/ml for 0.5 or 1 hour, then allowed the embryos to develop in fresh serum for the remainder of the experiment. They observed numerous malformations in embryos exposed for 0.5 hours, whereas mouse embryos exposed for 1 hour all failed to thrive (Warner et al., 1984). Thus, this study highlights the importance of acute and chronic teratogen exposure in whole embryo cultures.

4.1.2 Increase in yolk sac perimeter of cadmium-exposed embryos

The results of this study revealed an increase in the size of the embryo's gestational/yolk sac at 1.75 μM. This was demonstrated through the significant increase

in the average perimeter of the yolk sac of embryos exposed to 1.75 μM compared to both the control and 1.25 μM groups. There were no significant changes in the cross-sectional area of the yolk sac for both treatment and control groups; however, a medium effect size was found when comparing embryos exposed to 1.25 and 1.75 μM. Furthermore, a small effect size was noted when comparing the other treatment groups. Although the differences were not significant, the observed effect sizes between the two treatment groups could indicate a potential magnitude of change between the two treatments. Further testing with an increased sample size could determine if this difference is real or due to chance (Sullivan and Feinn, 2012). Cadmium is known to disrupt calcium-dependent junctions, which increases the permeability of endothelial and epithelial surfaces (Tobwala et al., 2014). This promotes endothelial leakiness and ultimately results in the loss of the endothelial barrier integrity (Dejana et al., 2009; Fende and Niewenhuis, 1997; Prozialeck et al., 2006; Woods et al., 2008). Increased permeability may cause tissue and yolk sac edema because of fluid leakage across the endothelium and into the extravascular spaces. High cadmium concentrations have been associated with yolk sac edema and neurological, gastrointestinal, cardiovascular, limb and genitourinary abnormalities in placental mammals, as well as axial and somite abnormalities in fish (Aldavood et al., 2020; Cheng et al., 2000; Thompson and Bannigan, 2008). Edema, or swelling of the yolk sac, is likely due to increased permeability and a lack of intravascular volume (Palis and Yoder, 2001). With a lack of intravascular volume, there is less capacity to provide proper drainage and nutrient delivery, which can result in swelling. In addition to this, the vitelline veins provide drainage, and hence, alterations to vascular development may further contribute to the swelling of the yolk sac (Palis and Yoder, 2001). With this knowledge, the result that embryos exposed to cadmium concentrations

of 1.75 μM have an increase in yolk sac perimeter compared to the other treatment groups is in alignment with other literature.

4.1.3 Decreased blood vessel size for cadmium exposed embryos

The size of blood vessels in cadmium-treated embryos decreased, with significant changes in their perimeter and area. Both treatment groups experienced a significant reduction in the cross-sectional area of blood vessels compared to the control, while only embryos exposed to 1.25 μM had a decrease in their perimeter compared to the control group.

Given the results of existing literature, this is not an unexpected result. Vasculogenesis refers to the aggregation of angioblasts, which differentiate into endothelial cells, ultimately creating the vasculature needed for the embryo to grow and survive (Drake and Fleming, 2000; Shalaby et al., 1997). However, cadmium interferes with angioblastic activity and has been associated with defective embryonic vasculature. More specifically, cadmium has been noted to reduce endogenous NO levels of chick embryo angioblast cells. This decreases the cell migration, proliferation, and tube formation of these cells (Veeriah et al., 2015). To elaborate, Veeriah et al., (2015) administered a single dose of cadmium to chick embryos via a hole made in the air sac of each egg. They observed a cadmium-induced decrease in the length and size of chick yolk sac blood vessels, as well as an increase in ROS levels for cadmium-treated angioblast cells. This significantly decreased the viability of these cells compared to controls. Staining and PCR analysis revealed that cadmium was inducing apoptosis through caspase 3 signalling pathways, as well as an increase in p53 compared to the control (Veeriah et al., 2015). Similarly, Kleinzeller and Werner (1939) found that angioblasts

and blood islands lack protection against superoxides and that embryos are particularly vulnerable to cadmium-mediated oxidative stress, increasing the likelihood of teratogenic assault. Thus, an increase in the production of ROS decreases NO production in early embryonic cells. This causes arrested angioblast cell activation and an upregulation in caspase 3 signalling for apoptosis. Together, this inhibits the formation of blood islands and primary plexus formations, as well as vascular maturation, ultimately impairing yolk sac vascular development (Veeriah et al., 2015). These results demonstrate the importance of maintaining NO bioavailability during embryonic development when considering teratogenic assault via ROS-inducing teratogens.

Most research pertaining to embryonic development uses chick models, more specifically, the CAM assay; however, in the current study, mouse embryos were utilized. This is a novel approach and using a mammalian model is beneficial due to the similarities between the mouse and human genomes. For instance, 99% of mouse genes have human homologs, with mouse gene mutations having similar consequences in humans (Waterston et al., 2002). Furthermore, mammalian embryos develop similarly, starting as a one-cell zygote and progressing through the blastocyst stage before implantation or hatching (Taft, 2008). Together, this demonstrates the suitability of using mouse embryos in teratogenicity research and its translation to humans.

Cadmium has been noted to alter placental maturation and is further associated with delayed fetal development, including smaller birth size and weight (Geng and Wang, 2019; Xu et al., 2016). This has been linked to a decrease in the expression of carrier proteins, which are associated with nutrient transport. DMT1 is a transporter that is primarily responsible for cadmium's uptake into the placenta (Klaassen et al., 2009; Wang et al., 2016). Cadmium accumulates in the placenta and affects the network of

maternal and fetal blood vessels, ultimately affecting nutrient and gas exchange. Compromised placental vasculature can result in delayed placental and fetal maturation (Geng and Wang, 2019). Kozlosky et al., (2023) treated day 9 of gestation mouse embryos with cadmium and found that there was reduced fetal and maternal vasculature, as well as a reduction in endothelial progenitor cells. Furthermore, these results were accompanied by a reduction in fetal size after cadmium exposure (Kozlosky et al., 2023). In summary, this study demonstrates cadmium's disruptive effects on yolk sac vasculature development and how its teratogenic effects can result in reduced growth parameters.

4.2 Concentration-Dependent Changes: Aortic Ring Assay

The objective of the aortic ring assay was to examine vessel development in relation to p-AKT and p-PTEN amounts; however, no statistically significant differences were found between treatment groups, thus not supporting my predictions that these proteins would be increased. The results for the mouse aortic ring assay demonstrated that there was a slight increase in phosphorylated AKT band densities at all concentrations of cadmium while phosphorylated PTEN was relatively unchanged, with the exception of the 5 μM treatment, where it was increased. Additionally, the study of the effects of cadmium on vascular development using the aortic ring assay revealed an apparent increase in all vessel measurements; however, the only significant result was an increase in vessel length at 10 μM compared to the control group. Although the majority of the aortic ring results were insignificant, some potential differences warrant methodological refinements for future studies, indicated by calculated effect sizes.

Small to large effect sizes were calculated for the pro-angiogenic response observed in aortic rings treated with cadmium. Regardless of the cadmium concentration, all treatment groups experienced an increase in the number of vessels, vessel branch points and an increase in vessel length. This was accompanied by a slight increase in p-AKT amounts for samples treated with cadmium concentrations greater than 0.5 μM. The pro-angiogenic development in response to cadmium could be beneficial in accounting for oxygen insufficiency and aid in stabilizing the hypoxic environment created (Chen et al., 2019; Sewduth and Santoro, 2016). Although further testing is required to determine if these observed differences were due to chance, non-trivial effect sizes suggest a potential relationship among treatments.

The results for increased vessel length at 10 μM cadmium is a common finding in literature as these concentrations are considered low doses and have been noted to stimulate angiogenesis. Low doses of cadmium induce oxidative stress, elevating reactive oxygen species (Jing et al., 2012). This causes the activation of cell signalling pathways known for upregulating angiogenesis. For example, AKT has been found to be increased in cultures of human bronchial epithelial cells exposed to cadmium (Jing et al., 2012). AKT is a primary target found to be activated in cadmium-induced angiogenesis, and it triggers the activation of downstream effectors such as mTOR, ERK, HIF1, and VEGF (Jing et al., 2012; Kim et al., 2012). Upregulated HIF levels lead to increased VEGF and angiogenesis. Jing et al., (2012) found that the phosphorylation of AKT increased HIF-1α levels in cadmium-exposed epithelial cells. Phosphorylated AKT was found to be increased in a dose-dependent manner when human bronchial epithelial cells were cultured with 5, 10, and 20 μM cadmium (Jing et al., 2012). This study also tested ROS production in response to cadmium and found that there was an increased generation in

cadmium-treated groups, suggesting that cadmium-induced ROS caused increased AKT activation and HIF-1α production.

A similar finding was observed by Kim et al., (2012), who found that HUVEC cell proliferation was increased at 5 and 10 μM cadmium due to increased VEGF secretion. Additionally, there was an increase in activated VEGFR2 at these concentrations. However, they noticed a dose-dependent increase in the expression of caspase 3 and, ultimately, apoptosis. Therefore, existing literature suggests the significant increase in vessel length at 10 μM cadmium that was observed in this study is due to increased pro-angiogenic signalling.

4.3 Limitations and Future Research

The lack of statistically significant differences in the response of tissues exposed to cadmium in the aortic ring assay may be a result of experimental variables, at least in part. One issue this study faced was a small sample size; however, effect sizes suggest that there may be a magnitude of difference between treatment groups. An increase in sample size would have increased the power of analysis and presented a better interpretation of the results and trends. One of the most obvious limitations of this study was the statistically insignificant results of phosphorylated protein amounts from western blotting. This could be due to possible degradation of the sample, incomplete lysis, or not enough protein being loaded. Although sodium orthovanadate was added to inhibit tyrosine phosphatases, other protease and phosphatase inhibitors could have been added to the cell extract to avoid protein degradation and maintain maximum protein yield. Sonication also could have been used in complement to ensure complete cell lysis as well as maximal and consistent protein recovery. This step is particularly important in the

extraction of membrane-bound and organelle-localized targets. This may have been particularly valuable in VEGFR2 expression because of its translocation to the nucleus (Domingues et al., 2011). Given that the studied proteins are expressed in relatively low amounts, future studies could probe for ROS or HIF-1 since they are the main targets of cadmium toxicity. Lastly, the loading control, GAPDH, was inconsistent, suggesting that protein loading amounts may have been inconsistent (Appendix G). The RIPA lysis buffer may have interfered with the reading, contributing to this limitation. When using the Qubit protein assay, the RIPA lysis buffer is not compatible and causes issues with concentration readings. Furthermore, Triton-X and Tris-HCl are also not well tolerated but are used in the RIPA recipe (Qubit Protein Assay User Guide, 2022).

Future studies could address these limitations by using immunoprecipitation assays prior to western blotting. This provides the advantage of allowing antibodies and antigens to react in their native conformation. It also presents the advantage of quantifying proteins at very low concentrations (Thompson, 2009). Since phosphorylated forms of proteins are found in low concentrations, future studies could benefit from this assay. Furthermore, the endogenous levels of total AKT and PTEN antibodies could have been used to complement the quantification of the phosphorylated form. By using the total amount of protein within the culture, an accurate representation of changes in activated protein amounts could be measured.

Future studies could also explore a wider range of cadmium concentrations. This study looked solely at concentrations that have been considered low in other models, since it was expected that the embryo and aorta ex vivo cultures would be more sensitive to the effects of cadmium than cultured cells. Thus, it would be beneficial to look at concentrations greater than 10 μM to gain a greater appreciation of the range of cadmium

effects. Since cadmium exposure in humans is generally chronic and limited to low concentrations, future studies could look to address chronic rather than acute exposure using long-term studies. Furthermore, this could entail chronic exposure to cadmium chloride through inhalation or diet for a longer period of time. Typical blood cadmium levels range from 0 μM to 0.05 μM in humans (Branca et al., 2018); thus, exploring a range of both high and low concentrations would help elucidate the pathological consequences of cadmium. This could be furthered by using different assays to measure cell proliferation, viability, and apoptosis. The use of these assays would allow the growth and death of cells to be monitored through both high and low cadmium exposure. This would provide insight into the cellular effects mediated by cadmium and demonstrate the mechanisms behind increased or decreased angiogenesis and vessel formation.

Further studies could also look at sex differences in response to cadmium exposure. Cadmium, along with other toxic metals, have been found to have varying health effects that are manifested differently in males and females. This is attributed to differences in kinetics, modes of action, or susceptibility (Vahter et al., 2006). This idea became more widespread after the outbreak of itai-itai disease, which mainly afflicted women (Nishijo et al., 2017). Women tend to have higher cadmium blood concentrations, as well as higher concentrations in urine and kidneys (Akesson et al., 2002; Berglund et al., 1994). The main reason for this is the increased absorption of cadmium at low iron stores, with a higher risk for women at a fertile age or during pregnancy (Akesson et al., 2002; Berglund et al., 1994). DMT1 is a common transporter for cadmium, which is also responsible for iron uptake. Individuals with iron deficiency have upregulated DMT1 levels and hence have a higher affinity for cadmium (Leazer et al., 2002; Tallkvist et al., 2001). Cadmium is also known to have estrogenic effects, particularly for its role in

mimicking estrogen in breast cancer cells due to its ability to form high-affinity complexes with estrogen receptors (Garcia-Morales et al., 1994; Stoica et al., 2000). Johnson et al., (2003) also demonstrated its effects in uterine hyperplasia, increased growth and development of mammary glands and the induction of hormone-related genes at low, single doses of cadmium.

5 CONCLUSIONS

The objective of this study was to elucidate the potential non-linear effect of cadmium on angiogenesis in two mouse assays and to better understand its role as an inhibitor and stimulator of angiogenesis. The study further aimed to address the varying effects between embryonic and adult angiogenic processes in these two mouse models. The hypothesis that cadmium would disrupt vascular development and signalling in a non-linear concentration-dependent manner was partially supported. The results of the embryology data found that at low concentrations, cadmium increased vascularization of the yolk sac. However, cadmium decreased the size of vessels, regardless of concentration. The results also demonstrated a significant increase in yolk sac size for embryos exposed to high cadmium concentrations. Although this study failed to gain significant results for much of the aortic ring assay, it was observed that vessel length at 10 μM cadmium exposure in adult cell cultures experienced a significant increase.

Cadmium toxicity is a major concern in our society, and understanding its role as a potential stimulator and inhibitor of angiogenesis is critical in relation to its pathological consequences. With this knowledge, we can better recognize how its stimulatory effects influence pathological conditions as well as aid in countering its toxic outcomes. Recently, natural compounds and phytochemicals have been discussed for their protective

mechanisms in counteracting cadmium insult. Different studies focus on defence according to varying underlying mechanisms, such as antioxidant defence, mitochondrial protection, metal chelation, reduced uptake of cadmium and removal of cadmium (Sandbichler and Hockner, 2016). To elaborate, studies in adult mice have found that curcumin (Eybl et al., 2004; Eybl et al., 2006), grapefruit juice (Argüelles-Velázquez et al., 2012), farnesol (Jahangir et al., 2005), catechin (Choi et al., 2003), and sulforaphane (Jahan et al., 2014; Wang et al., 2015) prevent cadmium-induced genotoxic effects. Antioxidants have been demonstrated to be beneficial under ROS stress during hypoxic environments by counteracting mitochondrial-regulated cadmium-induced apoptosis (Poteet et al., 2014). Spirulina is another natural compound that has demonstrated preventative measures against the number of external visceral and skeletal malformations, exencephaly, micrognathia, lipid peroxidation and DNA oxidation against cadmium exposure for mice in utero (Argüelles-Velázquez et al., 2013; Paniagua-Castro et al., 2011). While natural compounds are promising in the treatment of cadmium toxicity, their use in pregnant women to prevent the teratogenic effects of cadmium exposure in utero needs to be carefully studied, as they may prove harmful to the fetus. Furthermore, P-glycoprotein (P-gp) is an ATP-dependent transmembrane transporter responsible for pumping cytotoxic substances out of cells. This transporter has been proven beneficial in removing cadmium ions; however, there are long-term effects of P-gp, demonstrating the importance of studying natural compounds in complement (Thévenod et al., 2000).

To conclude, cadmium exposure has implications in the development of pathological conditions and contributes to teratogenic assault on developing embryos. The results of this study suggest that low levels of cadmium may hinder the development of embryos, particularly the development of the yolk sac. More specifically, at low levels,

cadmium-exposed embryos experienced a significant increase in the number of vessels formed; however, they appeared to be slightly smaller in size. Furthermore, although the effects of cadmium on adult cells were insignificant, experimental evidence suggests that low cadmium concentrations upregulate angiogenic responses, more specifically, increase vessel length. Thus, it is important to establish the specific mechanisms of cadmium on cell proliferation, differentiation, and growth at a developmental and teratogenic level.

6 APPENDIX

Appendix A: Method of Mouse Embryo Culture and Histological Slide Fixation

Embryos exposed to cadmium chloride were examined histologically using cross-sections of mouse embryos prepared by a previous student (Scroggie, 1996). The slides were prepared from embryos grown in whole embryo culture, according to New's method (1978). Pregnant female mice from a population of random-bred Swiss albino mice housed at Trent University were sacrificed at day 8 of gestation, and embryos were carefully dissected from the uterus, leaving the ectoplacental cone and yolk sac intact. Embryos with 3 to 8 somites and no notable anomalies were selected for culture. The entire dissection was performed in Hank's Balanced Medium (HBS) under aseptic conditions.

The culture medium consisted of 90% rat serum/10% HBS, with 10 U/mL penicillin G and 10 µg/mL streptomycin. Embryos were placed in a sterile culture bottle with the prepared media and initially gassed with 5% O_2, 5% CO_2, and 90% N_2. The culture was incubated at 37 °C on a rotator at 30 rpm for 2 hours, allowing the embryos to equilibrate before cadmium chloride treatments. After the equilibration period, cadmium chloride in distilled water was applied at 1.25 µM and 1.75 µM concentrations, with the control group consisting solely of culture medium. The embryos were again gassed and incubated under the same conditions for 18 hours. At the 18-hour mark, the bottles were gassed with 20% O_2, 5% CO_2, and 75% N_2 and incubated under these conditions for 6 hours.

Upon culture termination, embryos were washed in HBS and fixed in acetone for 12 hours. Embryos were dehydrated through an increasing ethanol series and embedded in paraffin wax. Serial sections were taken both transversely and longitudinally at 6

microns, but I analyzed only the transverse sections. Sections were affixed to albumin-coated slides and stained in Harris' Hematoxylin and Eosin Y.

Appendix B: Data Points and Outliers for the Effects of Cadmium on Vessel Development in Day 8 of Gestation Mouse Embryos

Table 1. The effect of cadmium on the average number of blood vessels in mouse embryo yolk sacs.

CADMIUM CONCENTRATION		
0 μM	**1.25 μM**	**1.75 μM**
26.5	30.33	27
27.83	34.8	28.4
30.4	36.83	28.5
33	40.75	31.6
34.75	43	34
44	48.2	34.4
44.8	52.4	34.6
49.6	55.75	38.5
50.17	55.8	39.17
	63.5	43.17
	66.8	46.4

Table 2. The effect of cadmium on the total number of blood vessels in mouse embryo yolk sacs.

CADMIUM CONCENTRATION		
0 μM	**1.25 μM**	**1.75 μM**
132	174	114
139	182	135
152	221	142
159	223	158
167	241	170
220	258	172
224	262	173
248	279	231
301	326	232
	334	235
	381	259

Table 3. The effect of cadmium on yolk sac perimeter (µm) in mouse embryos.

CADMIUM CONCENTRATION		
0 μM	**1.25 μM**	**1.75 μM**
3518.54	3420.33	4359.14
4309.70	3630.20	4372.11
4327.01	3653.83	4926.57
4478.98	4117.86	4987.97
4506.01	4288.38	5365.09
4610.30	4474.00	5365.28
4849.64	4742.60	5616.16
4965.78 [OUTLIER]	4877.00	5652.77
	5142.00	5785.55
	5162.50	6012.71
	5702.80	6457.81

Table 4. The effect of cadmium on the cross-sectional area (μm^2) of the yolk sac in mouse embryos.

CADMIUM CONCENTRATION		
0 μM	**1.25 μM**	**1.75 μM**
804376.19	933539.50	1150929.83
807033.73	818122.17	1414178.14
1327700.32	919231	1670886.60
1471988.23	1061318.14	1700696.47
1487667.50	1331739.88	1705896.56
1594068.58	1334331.80	1820397.80
1884074.52	1582627.80	1876052.06
2258921.46	1722289.67	2184354.63
	1839594.50	2194288.89
	1884690.20	2228629.47
	2122073.00	2335345.56

Table 5. The effect of cadmium on the cross-sectional area (μm^2) of blood vessels in mouse embryo yolk sacs.

CADMIUM CONCENTRATION		
0 μM	**1.25 μM**	**1.75 μM**
1075.36	1390.40	1251.21
1184.16	1035.00	1300.98
1713.16	1212.90	1382.79
2149.23	1237.10	1437.07
2418.62	1386.60	1441.04
2804.88	1433.60	1508.15
3019.05	1516.70	1559.92
3406.83	1619.90	1642.93
6120.69 [OUTLIER]	1797.30	2357.11 [OUTLIER]
	2025.30	2383.86 [OUTLIER]
	2106.80	2780.83 [OUTLIER]

Table 6. The effect of cadmium on the perimeter (µm) of blood vessels in mouse embryo yolk sacs.

CADMIUM CONCENTRATION		
0 µM	**1.25 µM**	**1.75 µM**
176.27	194.70	178.98
185.09	153.80	195.32
208.86	164.50	206.73
255.41	165.30	213.08
272.10	187.00	218.79
275.02	189.20	252.29
322.07	196.40	255.16
361.03	202.00	276.09
416.34	217.30	282.19
	232.20	300.04
	243.70	308.28

Table 7. The effect of cadmium on the density of blood vessels per µm² in mouse embryo yolk sacs.

CADMIUM CONCENTRATION		
0 µM	**1.25 µM**	**1.75 µM**
1.54E-05	2.96E-05	1.30E-05
1.75E-05	3.03E-05	1.68E-05
1.75E-05	3.06E-05	1.70E-05
1.78E-05	3.15E-05	1.78E-05
2.22E-05	3.25E-05	1.85E-05
2.62E-05	3.31E-05	2.02E-05
3.37E-05	3.61E-05	2.03E-05
3.78E-05	3.69E-05	2.08E-05
5.55E-05	3.79E-05	2.11E-05
	4.05E-05	2.35E-05
	4.50E-05	2.40E-05

Appendix C: Raw values and outliers for the Effects of Cadmium on Blood Vessel Outgrowth from Aortic Rings in Culture

Table 8. The effect of cadmium on the number of blood vessels in aortic ring cultures.

CADMIUM CONCENTRATIONS				
0 μM	**0.5 μM**	**1 μM**	**5 μM**	**10 μM**
0	25	14	8	15
0	45	25	31	37
8	2	23	25	8
13		30	4	

Table 9. The effect of cadmium on the number of vessel branch points in aortic ring cultures.

CADMIUM CONCENTRATIONS				
0 μM	**0.5 μM**	**1 μM**	**5 μM**	**10 μM**
2	14	8	2	0
3	0	9	11	8
	15	23	18	19
		30	2	

Table 10. The effect of cadmium on vessel length (μm) in aortic ring cultures.

CADMIUM CONCENTRATIONS				
0 μM	**0.5 μM**	**1 μM**	**5 μM**	**10 μM**
85.64	74.74	33.64	21.70	31.99
92.38	76.66	45.24	33.64	51.09
93.23	76.86	47.45	38.67	75.32
94.88	78.72	52.34	43.98	77.13
101.05	90.72	59.92	44.39	78.24
103.75	93.05	60.25	65.91	81.45
106.39	103.06	66.61	69.15	92.45
113.41	107.24	66.61	70.00	102.13
114.04	113.95	69.39	70.50	115.07
140.46	115.07	69.70	76.86	118.47
165.40	116.08	72.37	86.66	130.23
166.00	120.65	73.84	87.94	132.50

166.74	120.70	79.95	94.50	137.23
179.09	125.23	86.82	96.77	138.45
183.92	126.46	88.68	97.67	142.78
209.39	128.21	90.97	100.92	147.12
214.50	130.41	91.59	120.96	154.42
223.51	130.54	92.55	121.32	155.83
239.89	143.12	92.61	121.45	165.74
259.44	147.12	94.24	122.32	168.24
271.19	147.85	102.77	123.94	168.49
	159.08	106.23	125.12	168.96
	159.80	106.67	129.15	169.00
	162.89	112.84	132.74	177.18
	164.95	115.90	133.32	183.73
	166.53	131.20	134.00	184.67
	167.95	135.89	137.09	189.86
	169.37	137.97	138.12	191.60
	176.30	141.69	140.21	192.82
	177.76	144.66	143.17	197.81
	180.85	149.13	147.54	200.01
	188.49	158.44	148.46	206.30
	195.84	159.51	158.71	213.84
	198.36	164.51	159.61	217.05
	200.00	164.88	161.99	220.15
	204.60	166.46	168.52	223.43
	206.38	169.90	171.07	225.97
	210.20	171.57	171.57	236.97
	217.57	171.75	176.26	237.02
	219.99	179.18	177.81	238.42
	226.35	181.39	182.92	243.68
	229.83	185.33	198.15	245.77
	232.65	194.92	201.06	248.36
	239.31	195.33	201.17	261.18
	240.01	197.88	205.57	264.70
	241.70	205.08	207.55	275.28
	242.22	206.29	210.27	284.54
	251.73	209.09	211.05	304.64
	267.80	212.45	218.45	305.92
	268.77	216.19	220.58	323.51
	270.77	217.30	226.15	324.98
	281.28	220.73	230.89	340.67
	288.49	222.01	236.36	362.09

	293.80	226.80	253.21	371.72
	312.47	239.94	262.40	373.81
	314.68	246.08	264.05	379.37
	319.10	257.05	271.95	418.96
	329.02	257.31	284.38	421.13
	338.61	266.60	285.83	438.12
	345.60	274.67	286.74	479.53
	348.87	296.96	290.58	494.42
	358.39	297.29	305.00	521.63
	367.68	298.88	307.61	557.05
	413.91	303.44	311.79	563.19
	437.52	324.70	321.93	621.24 [OUTLIER]
	457.14	334.97	330.63	644.22 [OUTLIER]
	475.39	340.77	338.43	763.91 [OUTLIER]
	493.61	340.95	339.26	
	565.73 [OUTLIER]	344.22	370.56	
	574.49 [OUTLIER]	373.45	384.32	
	632.28 [OUTLIER]	377.08	426.94	
	641.84 [OUTLIER]	394.17	443.54	
		404.35	457.23	
		407.48	563.51 [OUTLIER]	
		428.68	824.27 [OUTLIER]	
		437.65		
		451.16		
		504.30		
		615.44 [OUTLIER]		
		640.11 [OUTLIER]		
		666.83 [OUTLIER]		
		675.43 [OUTLIER]		
		706.90 [OUTLIER]		

		804.99 [OUTLIER]		
		845.35 [OUTLIER]		

Table 11. Raw values and outliers for the effect of cadmium on p-AKT amounts in aortic rings.

CADMIUM CONCENTRATIONS				
0 μM	**0.5 μM**	**1 μM**	**5 μM**	**10 μM**
0.94	0.34	0.93	0.32	0.43
1.37	0.61	1.03	0.73	0.57
1.47	0.77	1.07	1.14	0.68
1.86	1.00	2.61	1.31	1.42
1.41	1.10	2.78	1.63	1.83
0.89	1.70	4.04	1.68	3.23
0.24			7.12 [OUTLIERS]	
0.87				
0.99				
0.59				
1.23				

Table 12. Raw values and outliers for the effect of cadmium on p-PTEN amounts in aortic rings.

CADMIUM CONCENTRATIONS				
0 μM	**0.5 μM**	**1 μM**	**5 μM**	**10 μM**
1.89	0.34	0.29	0.35	0.31
0.65	0.60	0.72	0.42	0.45
0.82	0.64	1.17	0.61	0.61
1.60	1.17	1.28	1.01	0.84
0.68	1.23	1.58	2.61	0.99
0.77	1.44	1.74	3.24	1.25
0.92		12.60 [OUTLIER]	6.99 [OUTLIER]	3.59 [OUTLIER]
0.53				
0.78				
0.50				
2.30				
0.56				

Appendix D: One-way ANOVA and Tukey's Multiple Comparison Test Data for Aortic Ring Assay and Day 8 of Gestation Mouse Embryo Analysis

Table 13. Statistical analysis for the effect of cadmium on the average number of blood vessels in mouse embryo yolk sacs. **p<0.01.

TREATMENT	SUMMARY	ADJUSTED P VALUE
0 VS. 1.25 μM	ns	0.0612
0 VS. 1.75 μM	ns	0.7854
1.25 VS. 1.75 μM	**	0.0090

Table 14. Statistical analysis for the effect of cadmium on the total number of blood vessels in mouse embryo yolk sacs. *p<0.05 and **p<0.01.

TREATMENT	SUMMARY	ADJUSTED P VALUE
0 VS. 1.25 μM	*	0.0326
0 VS. 1.75 μM	ns	0.9223
1.25 VS. 1.75 μM	**	0.0089

Table 15. Statistical analysis for the effect of cadmium on the yolk sac perimeter (µm) in mouse embryos. *p<0.05 and **p<0.01.

TREATMENT	SUMMARY	ADJUSTED P VALUE
0 VS. 1.25 μM	ns	0.9951
0 VS. 1.75 μM	*	0.0129
1.25 VS. 1.75 μM	**	0.0085

Table 16. Statistical analysis for the effect of cadmium on the cross-sectional area (μm^2) of the yolk sac in mouse embryos.

TREATMENT	SUMMARY	ADJUSTED P VALUE
0 VS. 1.25 μM	ns	0.6528
0 VS. 1.75 μM	ns	0.5510
1.25 VS. 1.75 μM	ns	0.1203

Table 17. Statistical analysis for the effect of cadmium on the cross-sectional area (μm^2) of the blood vessels in mouse embryo yolk sacs. *p<0.05.

TREATMENT	SUMMARY	ADJUSTED P VALUE
0 VS. 1.25 μM	*	0.0196
0 VS. 1.75 μM	*	0.0150
1.25 VS. 1.75 μM	ns	0.9353

Table 18. Statistical analysis for the effect of cadmium on the perimeter of the blood vessels in mouse embryo yolk sacs. **p<0.01.

TREATMENT	SUMMARY	ADJUSTED P VALUE
0 VS. 1.25 μM	**	0.0069
0 VS. 1.75 μM	ns	0.4240
1.25 VS. 1.75 μM	ns	0.0956

Table 19. Statistical analysis for the effect of cadmium on the density of blood vessels per μm^2 in mouse embryo yolk sacs. ***p<0.001.

TREATMENT	SUMMARY	ADJUSTED P VALUE
0 VS. 1.25 μM	ns	0.0856
0 VS. 1.75 μM	ns	0.0939
1.25 VS. 1.75 μM	***	0.0002

Table 20. Statistical analysis for the effect of cadmium on the number of vessels in aortic ring cultures.

TREATMENT	SUMMARY	ADJUSTED P VALUE
0 VS. 0.5 μM	ns	0.3600
0 VS. 1 μM	ns	0.3400
0 VS. 5 μM	ns	0.7005
0 VS. 10 μM	ns	0.5791
0.5 VS. 1 μM	ns	>0.9999
0.5 VS. 5 μM	ns	0.9499
0.5 VS. 10 μM	ns	0.9950
1 VS. 5 μM	ns	0.9617
1 VS. 10 μM	ns	0.9979
5 VS. 10 μM	ns	0.9979

Table 21. Statistical analysis for the effect of cadmium on the number of vessel branch points in aortic ring cultures.

TREATMENT	SUMMARY	ADJUSTED P VALUE
0 VS. 0.5 μM	ns	0.8942
0 VS. 1 μM	ns	0.3409
0 VS. 5 μM	ns	0.9386
0 VS. 10 μM	ns	0.9226
0.5 VS. 1 μM	ns	0.7703
0.5 VS. 5 μM	ns	0.9995
0.5 VS. 10 μM	ns	>0.9999
1 VS. 5 μM	ns	0.5910
1 VS. 10 μM	ns	0.7169
5 VS. 10 μM	ns	>0.9999

Table 22. Statistical analysis for the effect of cadmium on vessel length (µm) in aortic ring cultures. *p<0.05.

TREATMENT	SUMMARY	ADJUSTED P VALUE
0 VS. 0.5 μM	ns	0.1942
0 VS. 1 μM	ns	0.5835
0 VS. 5 μM	ns	0.7719
0 VS. 10 μM	*	0.0368
0.5 VS. 1 μM	ns	0.8128
0.5 VS. 5 μM	ns	0.5612
0.5 VS. 10 μM	ns	0.8487
1 VS. 5 μM	ns	0.9917
1 VS. 10 μM	ns	0.2154
5 VS. 10 μM	ns	0.0909

Table 23. Statistical analysis for the effect of cadmium on p-AKT amounts in aortic ring cultures.

TREATMENT	SUMMARY	ADJUSTED P VALUE
0 VS. 0.5 μM	ns	>0.9999
0 VS. 1 μM	ns	0.0685
0 VS. 5 μM	ns	0.9930
0 VS. 10 μM	ns	0.8650
0.5 VS. 1 μM	ns	0.1116
0.5 VS. 5 μM	ns	0.9892
0.5 VS. 10 μM	ns	0.8719
1 VS. 5 μM	ns	0.2666
1 VS. 10 μM	ns	0.5280
5 VS. 10 μM	ns	0.9883

Table 24. Statistical analysis for the effect of cadmium on p-PTEN amounts in aortic ring cultures.

TREATMENT	SUMMARY	ADJUSTED P VALUE
0 VS. 0.5 μM	ns	0.9958
0 VS. 1 μM	ns	0.9986
0 VS. 5 μM	ns	0.8667
0 VS. 10 μM	ns	0.9219
0.5 VS. 1 μM	ns	0.9783
0.5 VS. 5 μM	ns	0.7646
0.5 VS. 10 μM	ns	0.9944
1 VS. 5 μM	ns	0.9732
1 VS. 10 μM	ns	0.8668
5 VS. 10 μM	ns	0.5247

Appendix E: Cohen's f Effect Size Statistics for Aortic Ring Assay and Day 8 of Gestation Mouse Embryo Analysis

Table 25. Cohen's f effect sizes for the effect of cadmium on the average number of blood vessels in mouse embryo yolk sacs. f = 0.1 – 0.24: small; and f ≥ 0.40: large.

TREATMENT	SUMMARY	ADJUSTED F VALUE
0 VS. 1.25 μM	Large effect size	0.43
0 VS. 1.75 μM	Small effect size	0.12
1.25 VS. 1.75 μM	Large effect size	0.58

Table 26. Cohen's f effect sizes for the effect of cadmium on the total number of blood vessels in mouse embryo yolk sacs. f < 0.1: trivial; and f ≥ 0.40: large.

TREATMENT	SUMMARY	ADJUSTED F VALUE
0 VS. 1.25 μM	Large effect size	0.48
0 VS. 1.75 μM	Trivial effect size	0.069
1.25 VS. 1.75 μM	Large effect size	0.58

Table 27. Cohen's f effect sizes for the effect of cadmium on yolk sac perimeter (µm) in mouse embryos. f < 0.1: trivial; and f ≥ 0.40: large.

TREATMENT	SUMMARY	ADJUSTED F VALUE
0 VS. 1.25 μM	Trivial effect size	0.018
0 VS. 1.75 μM	Large effect size	0.58
1.25 VS. 1.75 μM	Large effect size	0.61

Table 28. Cohen's f effect sizes for the effect of cadmium on the cross-sectional area (µm^2) of the yolk sac in mouse embryos. f = 0.1 – 0.24: small; and f = 0.25 – 0.39: medium.

TREATMENT	SUMMARY	ADJUSTED F VALUE
0 VS. 1.25 μM	Small effect size	0.16
0 VS. 1.75 μM	Small effect size	0.18
1.25 VS. 1.75 μM	Medium effect size	0.36

Table 29. Cohen's f effect sizes for the effect of cadmium on the cross-sectional area (μm^2) of the blood vessels in mouse embryo yolk. f < 0.1: trivial; and f ≥ 0.40: large.

TREATMENT	SUMMARY	ADJUSTED F VALUE
0 VS. 1.25 μM	Large effect size	0.54
0 VS. 1.75 μM	Large effect size	0.56
1.25 VS. 1.75 μM	Trivial effect size	0.065

Table 30. Cohen's f effect sizes for the effect of cadmium on the perimeter of the blood vessels in mouse embryo yolk sacs. f = 0.1 – 0.24: small; f = 0.25 – 0.39: medium; and f ≥ 0.40: large.

TREATMENT	SUMMARY	ADJUSTED F VALUE
0 VS. 1.25 μM	Large effect size	0.57
0 VS. 1.75 μM	Small effect size	0.22
1.25 VS. 1.75 μM	Medium effect size	0.37

Table 31. Cohen's f effect sizes for the effect of cadmium on the density of blood vessels per MM2 in mouse embryo yolk sacs. f = 0.25 – 0.39: medium; and f ≥ 0.40: large.

TREATMENT	SUMMARY	ADJUSTED F VALUE
0 VS. 1.25 μM	Medium effect size	0.39
0 VS. 1.75 μM	Medium effect size	0.39
1.25 VS. 1.75 μM	Large effect size	0.82

Table 32. Cohen's f effect sizes for the effect of cadmium on the number of vessels in aortic ring cultures. f < 0.1: trivial; f = 0.1 – 0.24: small; f = 0.25 – 0.39: medium; and f ≥ 0.40: large.

TREATMENT	SUMMARY	ADJUSTED F VALUE
0 VS. 0.5 μM	Large effect size	0.42
0 VS. 1 μM	Large effect size	0.43
0 VS. 5 μM	Medium effect size	0.28
0 VS. 10 μM	Medium effect size	0.33
0.5 VS. 1 μM	Trivial effect size	0.022
0.5 VS. 5 μM	Small effect size	0.16
0.5 VS. 10 μM	Trivial effect size	0.084
1 VS. 5 μM	Small effect size	0.15
1 VS. 10 μM	Trivial effect size	0.067
5 VS. 10 μM	Trivial effect size	0.067

Table 33. Cohen's f effect sizes for the effect of cadmium on the number of vessel branch points in aortic ring cultures. f < 0.1: trivial; f = 0.1 – 0.24: small; f = 0.25 – 0.39: medium; and f ≥ 0.40: large.

TREATMENT	SUMMARY	ADJUSTED F VALUE
0 VS. 0.5 μM	Small effect size	0.24
0 VS. 1 μM	Large effect size	0.53
0 VS. 5 μM	Small effect size	0.20
0 VS. 10 μM	Small effect size	0.22
0.5 VS. 1 μM	Medium effect size	0.31
0.5 VS. 5 μM	Trivial effect size	0.057
0.5 VS. 10 μM	Trivial effect size	0.025
1 VS. 5 μM	Large effect size	0.40
1 VS. 10 μM	Medium effect size	0.34
5 VS. 10 μM	Trivial effect size	0.030

Table 34. Cohen's f effect sizes for the effect of cadmium on vessel length (µm) in aortic ring cultures. f < 0.1: trivial; and f = 0.1 – 0.24: small.

TREATMENT	SUMMARY	ADJUSTED F VALUE
0 VS. 0.5 μM	Small effect size	0.13
0 VS. 1 μM	Trivial effect size	0.089
0 VS. 5 μM	Trivial effect size	0.070
0 VS. 10 μM	Small effect size	0.17
0.5 VS. 1 μM	Trivial effect size	0.066
0.5 VS. 5 μM	Trivial effect size	0.091
0.5 VS. 10 μM	Trivial effect size	0.061
1 VS. 5 μM	Trivial effect size	0.027
1 VS. 10 μM	Small effect size	0.13
5 VS. 10 μM	Small effect size	0.15

Table 35. Cohen's f effect sizes for the effect of cadmium on p-AKT amounts in aortic ring cultures. f < 0.1: trivial; f = 0.1 – 0.24: small; f = 0.25 – 0.39: medium; and f ≥ 0.40: large.

TREATMENT	SUMMARY	ADJUSTED F VALUE
0 VS. 0.5 μM	Trivial effect size	0.020
0 VS. 1 μM	Large effect size	0.44
0 VS. 5 μM	Trivial effect size	0.068
0 VS. 10 μM	Small effect size	0.16
0.5 VS. 1 μM	Large effect size	0.41
0.5 VS. 5 μM	Trivial effect size	0.078
0.5 VS. 10 μM	Small effect size	0.15
1 VS. 5 μM	Medium effect size	0.33
1 VS. 10 μM	Medium effect size	0.25
5 VS. 10 μM	Trivial effect size	0.077

Table 36. Cohen's f effect sizes for the effect of cadmium on p-PTEN amounts in aortic ring cultures. f < 0.1: trivial; f = 0.1 – 0.24: small; and f = 0.25 – 0.39: medium.

TREATMENT	SUMMARY	ADJUSTED F VALUE
0 VS. 0.5 μM	Trivial effect size	0.047
0 VS. 1 μM	Trivial effect size	0.061
0 VS. 5 μM	Small effect size	0.17
0 VS. 10 μM	Small effect size	0.12
0.5 VS. 1 μM	Trivial effect size	0.095
0.5 VS. 5 μM	Small effect size	0.19
0.5 VS. 10 μM	Trivial effect size	0.066
1 VS. 5 μM	Trivial effect size	0.099
1 VS. 10 μM	Small effect size	0.16
5 VS. 10 μM	Medium effect size	0.26

Appendix F: Phase Contrast Images from the Aortic Ring Assay

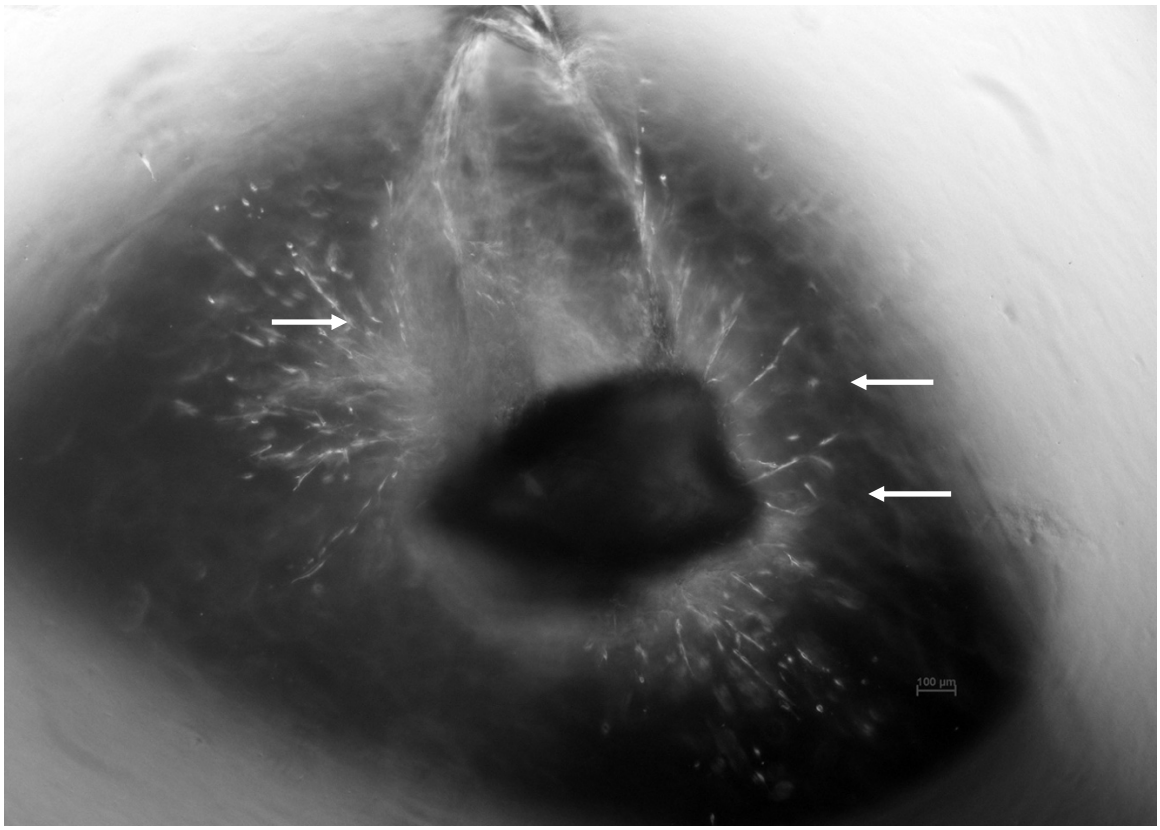

Figure 25. Phase contrast aortic ring microvessel outgrowth embedded in collagen. Scale bar 100 μm. The arrows highlight some of the vessel outgrowth.

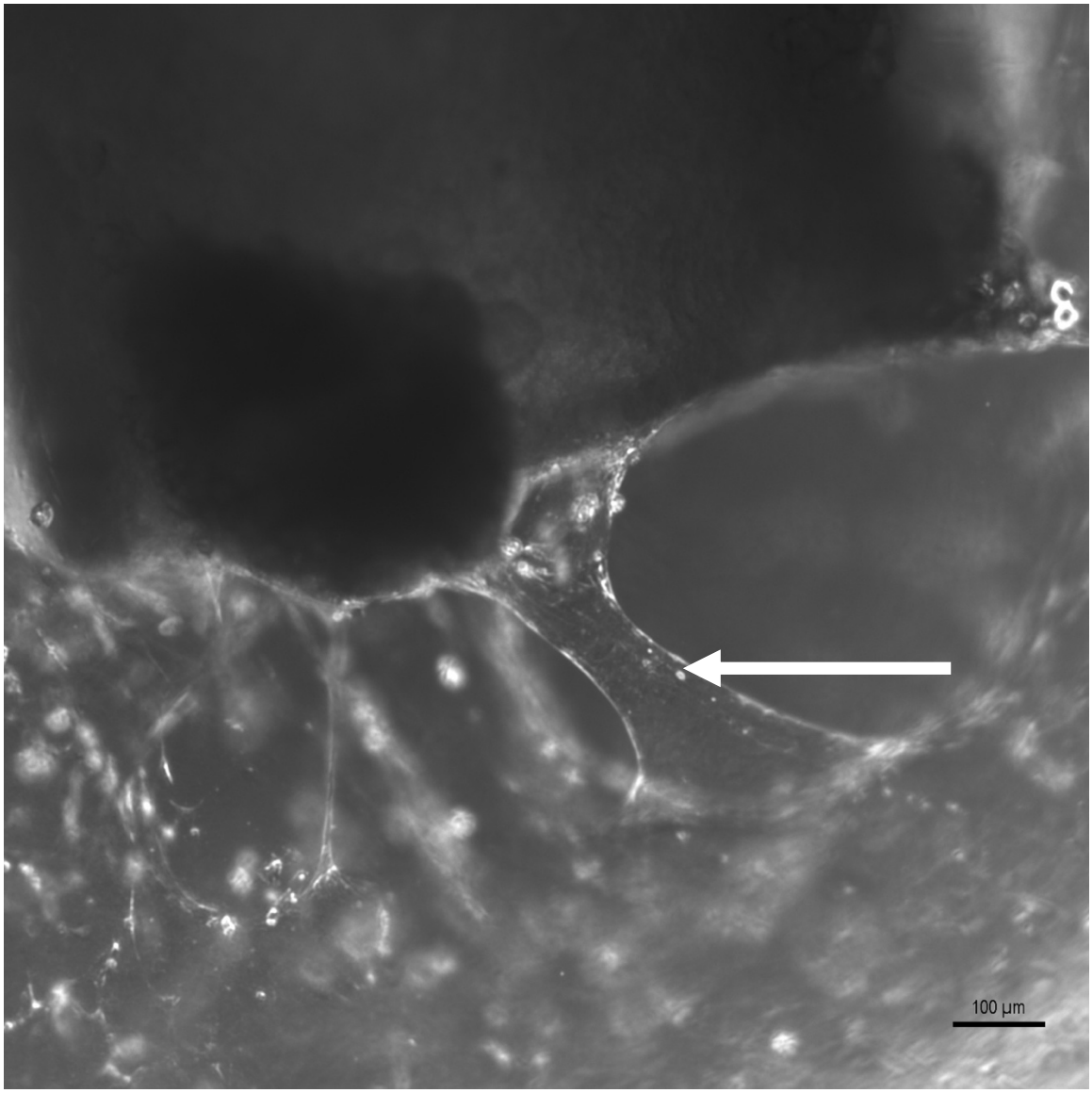

Figure 26. Phase contrast aortic ring microvessel outgrowth embedded in collagen. Scale bar 100 μm. The arrow highlights some of the vessel outgrowth.

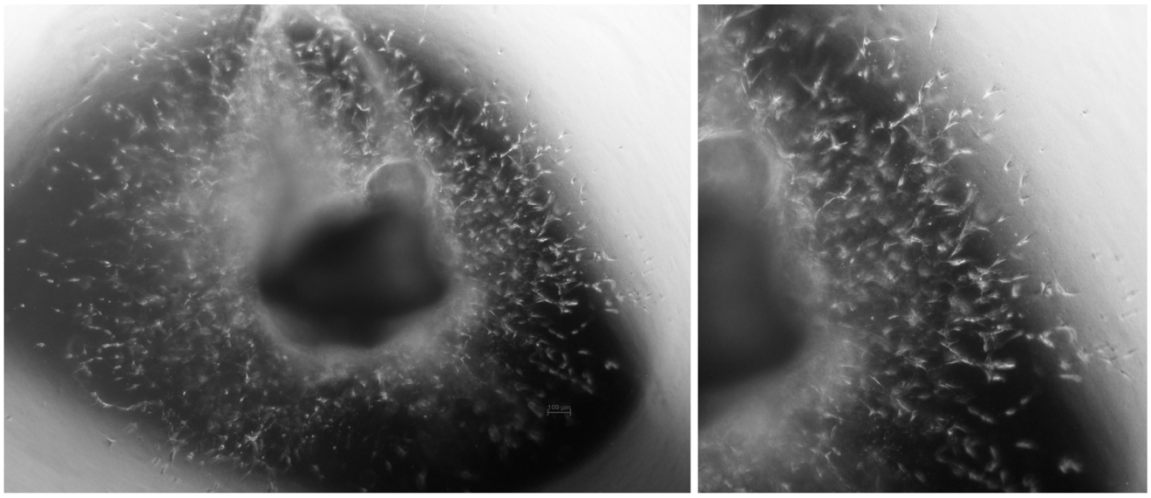

Figure 27. Phase contrast aortic ring microvessel and fibroblast outgrowth embedded in collagen.

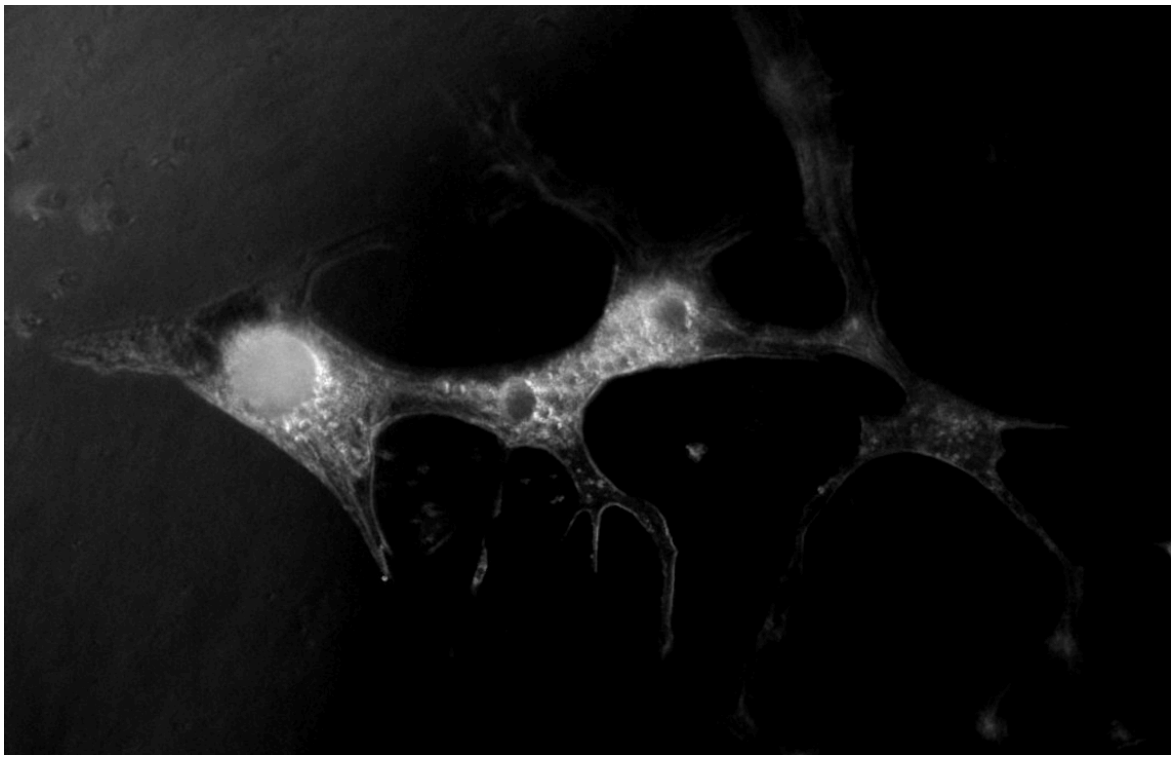

Figure 28. Phase contrast image of a fibroblast cell grown in the aortic ring culture, embedded in collagen.

Appendix G: Western Blotting – GAPDH Band Inconsistency

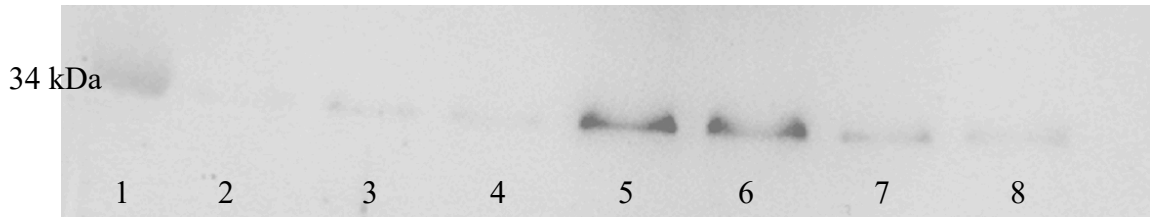

Figure 29. Western blot showing the amounts of GAPDH. Samples were resolved on a 10% polyacrylamide gel and transferred to a nitrocellulose membrane. Primary rabbit monoclonal antibodies to GAPDH were used for protein identification.

Appendix H: Western Blotting – p-AKT and p-PTEN

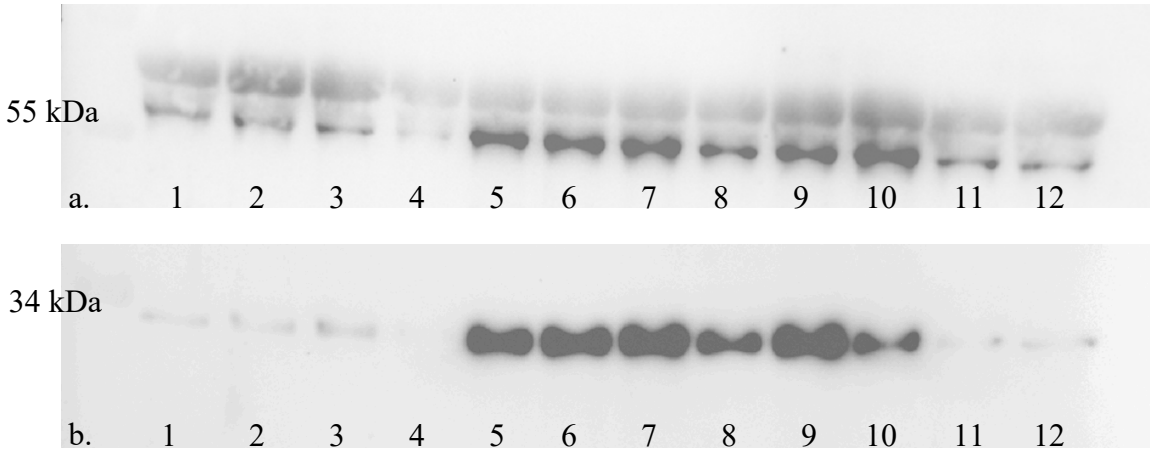

Figure 30. Western blot showing the amounts of p-PTEN and GAPDH. Samples were resolved on a 10% polyacrylamide gel and transferred to a nitrocellulose membrane. Primary rabbit monoclonal antibodies to PTEN and GAPDH were used for protein identification. Molecular weight ladder was used for protein identification. Phosphorylated PTEN was identified at a kDA of 54 (a) and GAPDH at 37 (b). Lanes 1-4 represent samples collected from mouse one embryos exposed to 0 μM, 1 μM, 5 μM, and 10 μM cadmium chloride, respectively. Lanes 5-9 represent samples collected from mouse two embryos exposed to 0 μM, 0.5 μM, 1 μM, 5 μM, and 10 μM cadmium chloride, respectively. Lanes 10-12 represent samples collected from mouse three embryos exposed to 0 μM, 1 μM, and 5 μM cadmium chloride, respectively.

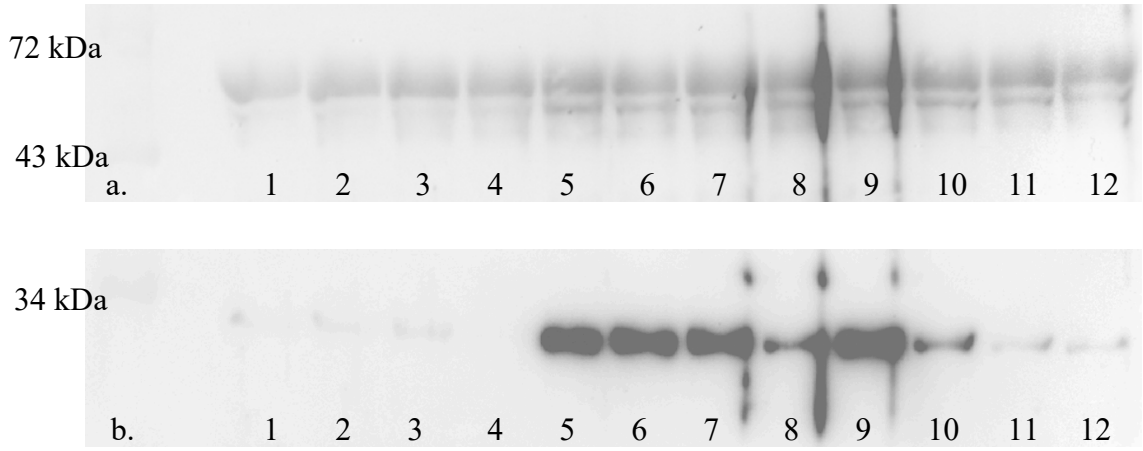

Figure 31. Western blot showing the amounts of p-AKT and GAPDH. Samples were resolved on a 10% polyacrylamide gel and transferred to a nitrocellulose membrane. Primary rabbit monoclonal antibodies to AKT and GAPDH were used for protein identification. Molecular weight ladder was used for protein identification. Phosphorylated AKT was identified at a kDA of 60 (a) and GAPDH at 37 (b). Lanes 1-4 represent samples collected from mouse one embryos exposed to 0 μM, 1 μM, 5 μM, and 10 μM cadmium chloride, respectively. Lanes 5-9 represent samples collected from mouse two embryos exposed to 0 μM, 0.5 μM, 1 μM, 5 μM, and 10 μM cadmium chloride, respectively. Lanes 10-12 represent samples collected from mouse three embryos exposed to 0 μM, 1 μM, and 5 μM cadmium chloride, respectively.

7 REFERENCES

Abeyrathna, P., & Su, Y. (2015). The critical role of Akt in cardiovascular function. *Vascular Pharmacology*, *74*, 38–48. https://doi.org/10.1016/j.vph.2015.05.008

Adair, T. H., & Montani, J.-P. (2010). Overview of Angiogenesis. In *Angiogenesis*. Morgan & Claypool Life Sciences. https://www.ncbi.nlm.nih.gov/books/NBK53238/

Akesson, A., Berglund, M., Schütz, A., Bjellerup, P., Bremme, K., & Vahter, M. (2002). Cadmium exposure in pregnancy and lactation in relation to iron status. *American Journal of Public Health*, *92*(2), 284–287. https://doi.org/10.2105/ajph.92.2.284

Aldavood, S. J., Abbott, L. C., Evans, Z. R., Griffin, D. J., Lee, M. D., Quintero-Arevalo, N. M., & Villalobos, A. R. (2020). Effect of cadmium and nickel exposure on early development in zebrafish *(Danio rerio)* embryos. *Water*, *12*(11), 3005. https://doi.org/10.3390/w12113005

Araújo, I. C. S., Café, M. B., Mesquita, M. A., Caiado, B. N., Faria, A. M., Mello, H. H. C., Stringhini, J. H., & Leandro, N. S. M. (2020). Effect of a commercial product containing canthaxanthin for in ovo feeding to broiler embryos on hatchability, chick quality, oxidation status, and performance. *Poultry Science*, *99*(11), 5598–5606. https://doi.org/10.1016/j.psj.2020.08.044

Argüelles, N., Álvarez-González, I., Chamorro, G., & Madrigal-Bujaidar, E. (2012). Protective effect of grapefruit juice on the teratogenic and genotoxic damage induced by cadmium in mice. *Journal of Medicinal Food*, *15*(10), 887–893. https://doi.org/10.1089/jmf.2012.0023

Argüelles-Velázquez, N., Alvarez-González, I., Madrigal-Bujaidar, E., & Chamorro-Cevallos, G. (2013). Amelioration of cadmium-produced teratogenicity and genotoxicity in mice given *Arthrospira maxima* (spirulina) treatment. *Evidence-Based Complementary and Alternative Medicine*, *2013*, e604535. https://doi.org/10.1155/2013/604535

Auerbach, R., Akhtar, N., Lewis, R. L., & Shinners, B. L. (2000). Angiogenesis assays: Problems and pitfalls. *Cancer Metastasis Reviews*, *19*(1–2), 167–172. https://doi.org/10.1023/a:1026574416001

Awad, N. S., Salkho, N. M., Abuwatfa, W. H., Paul, V., AlSawaftah, N. M., & Husseini, G. A. (2023). Tumor vasculature vs tumor cell targeting: Understanding the latest trends in using functional nanoparticles for cancer treatment. *OpenNano*, *11*, 100136. https://doi.org/10.1016/j.onano.2023.100136

Bachelder, R. E., Wendt, M. A., Fujita, N., Tsuruo, T., & Mercurio, A. M. (2001). The cleavage of Akt/protein kinase B by death receptor signaling is an important event in detachment-induced apoptosis. *The Journal of Biological Chemistry*, *276*(37), 34702–34707. https://doi.org/10.1074/jbc.M102806200

Baker, M., Robinson, S. D., Lechertier, T., Barber, P. R., Tavora, B., D'Amico, G., Jones, D. T., Vojnovic, B., & Hodivala-Dilke, K. (2012). Use of the mouse aortic ring assay to study angiogenesis. *Nature Protocols*, *7*, 89-104. https://doi.org/10.1038/nprot.2011.435

Baluk, P., Hashizume, H., & McDonald, D. M. (2005). Cellular abnormalities of blood vessels as targets in cancer. *Current Opinion in Genetics & Development*, *15*(1), 102–111. https://doi.org/10.1016/j.gde.2004.12.005

Baluk, P., Morikawa, S., Haskell, A., Mancuso, M., & McDonald, D. M. (2003). Abnormalities of basement membrane on blood vessels and endothelial sprouts in tumors. *The American Journal of Pathology*, *163*(5), 1801–1815.

Basagiannis, D., & Christoforidis, S. (2016). Constitutive endocytosis of VEGFR2 protects the receptor against shedding. *The Journal of Biological Chemistry*, *291*(32), 16892–16903. https://doi.org/10.1074/jbc.M116.730309

Benbrahim-Tallaa, L., Waterland, R. A., Dill, A. L., Webber, M. M., & Waalkes, M. P. (2007). Tumor suppressor gene inactivation during cadmium-induced malignant transformation of human prostate cells correlates with overexpression of *de Novo* DNA methyltransferase. *Environmental Health Perspectives*, *115*(10), 1454–1459. https://doi.org/10.1289/ehp.10207

Berglund, M., Akesson, A., Nermell, B., & Vahter, M. (1994). Intestinal absorption of dietary cadmium in women depends on body iron stores and fiber intake. *Environmental Health Perspectives*, *102*(12), 1058–1066. https://doi.org/10.1289/ehp.941021058

Beyersmann, D., & Hechtenberg, S. (1997). Cadmium, gene regulation, and cellular signalling in mammalian cells. *Toxicology and Applied Pharmacology*, *144*(2), 247–261. https://doi.org/10.1006/taap.1997.8125

Bharathiraja, K., Hari Babu, L., Vijayaprakash, S., Tamilselvan, P., & Balasubramanian, M. P. (2013). Fucoxanthin, a marine carotenoid protects cadmium-induced oxidative renal dysfunction in rats. *Biomedicine & Preventive Nutrition*, *3*(3), 201–207. https://doi.org/10.1016/j.bionut.2013.04.005

Blanco, R., & Gerhardt, H. (2013). VEGF and notch in tip and stalk cell selection. *Cold Spring Harbor Perspectives in Medicine*, *3*(1). https://doi.org/10.1101/cshperspect.a006569

Branca, J. J. V., Morucci, G., & Pacini, A. (2018). Cadmium-induced neurotoxicity: Still much ado. *Neural Regeneration Research*, *13*(11), 1879–1882. https://doi.org/10.4103/1673-5374.239434

Bremnes, R. M., Camps, C., & Sirera, R. (2006). Angiogenesis in non-small cell lung cancer: The prognostic impact of neoangiogenesis and the cytokines VEGF and bFGF in tumours and blood. *Lung Cancer (Amsterdam, Netherlands)*, *51*(2), 143–158. https://doi.org/10.1016/j.lungcan.2005.09.005

Brooks, S. A., & Fry, R. C. (2017). Cadmium inhibits placental trophoblast cell migration via miRNA regulation of the transforming growth factor beta (TGF-β) pathway. *Food and Chemical Toxicology : An International Journal Published for the British Industrial Biological Research Association*, *109*(Pt 1), 721–726. https://doi.org/10.1016/j.fct.2017.07.059

Buée, L., Hof, P. R., Bouras, C., Delacourte, A., Perl, D. P., Morrison, J. H., & Fillit, H. M. (1994). Pathological alterations of the cerebral microvasculature in Alzheimer's disease and related dementing disorders. *Acta Neuropathologica*, *87*(5), 469–480. https://doi.org/10.1007/BF00294173

Buée, L., Hof, P. R., & Delacourte, A. (1997). Brain microvascular changes in alzheimer's disease and other dementias. *Annals of the New York Academy of Sciences*, *826*(1), 7–24. https://doi.org/10.1111/j.1749-6632.1997.tb48457.x

Burri, P. H., & Djonov, V. (2002). Intussusceptive angiogenesis—The alternative to capillary sprouting. *Molecular Aspects of Medicine*, *23*(6S), S1-27. https://doi.org/10.1016/s0098-2997(02)00096-1

Cao, J., Spielmann, M., Qiu, X., Huang, X., Ibrahim, D. M., Hill, A. J., Zhang, F., Mundlos, S., Christiansen, L., Steemers, F. J., Trapnell, C., & Shendure, J. (2019). The single cell transcriptional landscape of mammalian organogenesis. *Nature*, *566*(7745), 496–502. https://doi.org/10.1038/s41586-019-0969-x

Carmeliet, P. (2005). Angiogenesis in life, disease and medicine. *Nature*, *438*(7070), 932–936. https://doi.org/10.1038/nature04478

Carmeliet, P., & Jain, R. K. (2000). Angiogenesis in cancer and other diseases. *Nature*, *407*, 429-257. https://doi.org/10.1038/35025220

Carracedo, A., Alimonti, A., & Pandolfi, P. P. (2011). PTEN level in tumor suppression: How much is too little? *Cancer Research*, *71*(3), 629–633. https://doi.org/10.1158/0008-5472.CAN-10-2488

Chávez, M. N., Aedo, G., Fierro, F. A., Allende, M. L., & Egaña, J. T. (2016). Zebrafish as an emerging model organism to study angiogenesis in development and regeneration. *Frontiers in Physiology*, *7*. https://www.frontiersin.org/articles/10.3389/fphys.2016.00056

Chen, W., Xia, P., Wang, H., Tu, J., Liang, X., Zhang, X., & Li, L. (2019). The endothelial tip-stalk cell selection and shuffling during angiogenesis. *Journal of Cell Communication and Signaling*, *13*(3), 291–301. https://doi.org/10.1007/s12079-019-00511-z

Cheng, S. H., Wai, A. W. K., So, C. H., & Wu, R. S. S. (2000). Cellular and molecular basis of cadmium-induced deformities in zebrafish embryos. *Environmental*

Toxicology and Chemistry, *19*(12), 3024–3031. https://doi.org/10.1002/etc.5620191223

Choi, J.-H., Rhee, I.-K., Park, K.-Y., Park, K.-Y., Kim, J.-K., & Rhee, S.-J. (2003). Action of green tea catechin on bone metabolic disorder in chronic cadmium-poisoned rats. *Life Sciences*, *73*(12), 1479–1489. https://doi.org/10.1016/S0024-3205(03)00433-8

Chunhabundit, R. (2016). Cadmium exposure and potential health risk from foods in contaminated area, Thailand. *Toxicological Research*, *32*(1), 65–72. https://doi.org/10.5487/TR.2016.32.1.065

Cullinane, J., Bannigan, J., & Thompson, J. (2009). Cadmium teratogenesis in the chick: Period of vulnerability using the early chick culture method, and prevention by divalent cations. *Reproductive Toxicology*, *28*(3), 335–341. https://doi.org/10.1016/j.reprotox.2009.05.069

Dash, Ch. S. K., Behera, A. K., Dehuri, S., & Ghosh, A. (2023). An outliers detection and elimination framework in classification task of data mining. *Decision Analytics Journal*, *6*, 100164. https://doi.org/10.1016/j.dajour.2023.100164

De Spiegelaere, W., Casteleyn, C., Van den Broeck, W., Plendl, J., Bahramsoltani, M., Simoens, P., Djonov, V., & Cornillie, P. (2012). Intussusceptive angiogenesis: A biologically relevant form of angiogenesis. *Journal of Vascular Research*, *49*(5), 390–404. https://doi.org/10.1159/000338278

Dejana, E., Orsenigo, F., & Lampugnani, M. G. (2008). The role of adherens junctions and VE-cadherin in the control of vascular permeability. *Journal of Cell Science*, *121*(13), 2115–2122. https://doi.org/10.1242/jcs.017897

Dencker, L. (1975). Possible mechanisms of cadmium fetotoxicity in golden hamsters and mice: Uptake by the embryo, placenta and ovary. *Reproduction*, *44*(3), 461–471. https://doi.org/10.1530/jrf.0.0440461

Djonov, V., Baum, O., & Burri, P. H. (2003). Vascular remodeling by intussusceptive angiogenesis. *Cell and Tissue Research*, *314*(1), 107–117. https://doi.org/10.1007/s00441-003-0784-3

Djonov, V. G., Kurz, H., & Burri, P. H. (2002). Optimality in the developing vascular system: Branching remodeling by means of intussusception as an efficient adaptation mechanism. *Developmental Dynamics: An Official Publication of the American Association of Anatomists*, *224*(4), 391–402. https://doi.org/10.1002/dvdy.10119

Djonov, V., & Makanya, A. N. (2005). New insights into intussusceptive angiogenesis. *EXS*, *94*, 17–33. https://doi.org/10.1007/3-7643-7311-3_2

Domingues, I., Rino, J., Demmers, J. A. A., De Lanerolle, P., & Santos, S. C. R. (2011). VEGFR2 translocates to the nucleus to regulate its own transcription. *PLOS ONE*, *6*(9), e25668. https://doi.org/10.1371/journal.pone.0025668

Dong, S., Shen, H.-M., & Ong, C.-N. (2001). Cadmium-induced apoptosis and phenotypic changes in mouse thymocytes. In X. Shi, V. Castranova, V. Vallyathan, & W. G. Perry (Eds.), *Molecular Mechanisms of Metal Toxicity and Carcinogenesis* (pp. 11–20). Springer US. https://doi.org/10.1007/978-1-4615-0793-2_2

Donovan, D., Brown, N. J., Bishop, E. T., & Lewis, C. E. (2001). Comparison of three in vitro human 'angiogenesis' assays with capillaries formed in vivo. *Angiogenesis*, *4*(2), 113–121. https://doi.org/10.1023/A:1012218401036

Drake, C. J., & Fleming, P. A. (2000). Vasculogenesis in the day 6.5 to 9.5 mouse embryo. *Blood*, *95*(5), 1671–1679. https://doi.org/10.1182/blood.V95.5.1671.005k39_1671_1679

Đukić-Ćosić, D., Baralić, K., Javorac, D., Djordjevic, A. B., & Bulat, Z. (2020). An overview of molecular mechanisms in cadmium toxicity. *Current Opinion in Toxicology*, *19*, 56–62. https://doi.org/10.1016/j.cotox.2019.12.002

Edelberg, J. M., & Reed, M. J. (2003). Aging and angiogenesis. *Frontiers in Bioscience: A Journal and Virtual Library*, *8*, s1199-1209. https://doi.org/10.2741/1166

Eliceiri, B. P. (2001). Integrin and growth factor receptor crosstalk. *Circulation Research*, *89*(12), 1104–1110. https://doi.org/10.1161/hh2401.101084

Elshabrawy, H. A., Chen, Z., Volin, M. V., Ravella, S., Virupannavar, S., & Shahrara, S. (2015). The pathogenic role of angiogenesis in rheumatoid arthritis. *Angiogenesis*, *18*(4), 433–448. https://doi.org/10.1007/s10456-015-9477-2

Emerich, D. F., Schneider, P., Bintz, B., Hudak, J., & Thanos, C. G. (2007). Aging reduces the neuroprotective capacity, VEGF secretion, and metabolic activity of rat choroid plexus epithelial cells. *Cell Transplantation*, *16*(7), 697–705. https://doi.org/10.3727/000000007783465145

Eybl, V., Kotyzová, D., & Bludovská, M. (2004). The effect of curcumin on cadmium-induced oxidative damage and trace elements level in the liver of rats and mice. *Toxicology Letters*, *151*(1), 79–85. https://doi.org/10.1016/j.toxlet.2004.02.019

Eybl, V., Kotyzova, D., & Koutensky, J. (2006). Comparative study of natural antioxidants—Curcumin, resveratrol and melatonin—In cadmium-induced oxidative damage in mice. *Toxicology*, *225*(2–3), 150–156. https://doi.org/10.1016/j.tox.2006.05.011

Fagerberg, B., Bergström, G., Borén, J., & Barregard, L. (2012). Cadmium exposure is accompanied by increased prevalence and future growth of atherosclerotic plaques in 64-year-old women. *Journal of Internal Medicine*, *272*(6), 601–610. https://doi.org/10.1111/j.1365-2796.2012.02578.x

Falk, W., Goodwin, R. H., & Leonard, E. J. (1980). A 48-well micro chemotaxis assembly for rapid and accurate measurement of leukocyte migration. *Journal of Immunological Methods*, *33*(3), 239–247. https://doi.org/10.1016/0022-1759(80)90211-2

Fang, M.-Z., Mar, W., & Cho, M.-H. (2002). Cadmium affects genes involved in growth regulation during two-stage transformation of Balb/3T3 cells. *Toxicology*, *177*(2), 253–265. https://doi.org/10.1016/S0300-483X(02)00229-9

FAO/WHO (Food and Agriculture Organization; World Health Organization). (2021). *Evaluation of certain food additives and contaminants: ninety-first report of the Joint FAO/WHO Expert Committee on Food Additives.* WHO Technical Report Series No. 1036. https://iris.who.int/bitstream/handle/10665/364702/9789240054585-eng.pdf?sequence=1

Fende, P. L., & Niewenhuis, R. J. (1977). An electron microscopic study of the effects of cadmium chloride on cryptorchid testes of the rat. *Biology of Reproduction*, *16*(3), 298–305. https://doi.org/10.1095/biolreprod16.3.298

Ferkowicz, M. J., & Yoder, M. C. (2005). Blood island formation: Longstanding observations and modern interpretations. *Experimental Hematology*, *33*(9), 1041–1047. https://doi.org/10.1016/j.exphem.2005.06.006

Ferraro, P. M., Costanzi, S., Naticchia, A., Sturniolo, A., & Gambaro, G. (2010). Low level exposure to cadmium increases the risk of chronic kidney disease: Analysis of the NHANES 1999-2006. *BMC Public Health*, *10*(1), 304. https://doi.org/10.1186/1471-2458-10-304

Fish, J. E., Santoro, M. M., Morton, S. U., Yu, S., Yeh, R.-F., Wythe, J. D., Ivey, K. N., Bruneau, B. G., Stainier, D. Y. R., & Srivastava, D. (2008). Mir-126 regulates angiogenic signaling and vascular integrity. *Developmental Cell*, *15*(2), 272–284. https://doi.org/10.1016/j.devcel.2008.07.008

Fisher, A. B., Chien, S., Barakat, A. I., & Nerem, R. M. (2001). Endothelial cellular response to altered shear stress. *American Journal of Physiology-Lung Cellular and Molecular Physiology*, *281*(3), L529–L533. https://doi.org/10.1152/ajplung.2001.281.3.L529

Forsythe, J. A., Jiang, B. H., Iyer, N. V., Agani, F., Leung, S. W., Koos, R. D., & Semenza, G. L. (1996). Activation of vascular endothelial growth factor gene transcription by hypoxia-inducible factor 1. *Molecular and Cellular Biology*, *16*(9), 4604–4613.

Freeman, D. J., Li, A. G., Wei, G., Li, H.-H., Kertesz, N., Lesche, R., Whale, A. D., Martinez-Diaz, H., Rozengurt, N., Cardiff, R. D., Liu, X., & Wu, H. (2003). PTEN tumor suppressor regulates p53 protein levels and activity through phosphatase-dependent and -independent mechanisms. *Cancer Cell*, *3*(2), 117–130. https://doi.org/10.1016/S1535-6108(03)00021-7

Garcia, M. D., & Larina, I. V. (2014). Vascular development and hemodynamic force in the mouse yolk sac. *Frontiers in Physiology*, *5*. https://www.frontiersin.org/articles/10.3389/fphys.2014.00308

Garcia-Morales, P., Saceda, M., Kenney, N., Kim, N., Salomon, D. S., Gottardis, M. M., Solomon, H. B., Sholler, P. F., Jordan, V. C., & Martin, M. B. (1994). Effect of cadmium on estrogen receptor levels and estrogen-induced responses in human breast cancer cells. *The Journal of Biological Chemistry*, *269*(24), 16896–16901.

Genchi, G., Sinicropi, M. S., Lauria, G., Carocci, A., & Catalano, A. (2020). The effects of cadmium toxicity. *International Journal of Environmental Research and Public Health*, *17*(11), 3782. https://doi.org/10.3390/ijerph17113782

Geng, H.-X., & Wang, L. (2019). Cadmium: Toxic effects on placental and embryonic development. *Environmental Toxicology and Pharmacology*, *67*, 102–107. https://doi.org/10.1016/j.etap.2019.02.006

Gheorghescu, A. K., Tywoniuk, B., Duess, J., Buchete, N.-V., & Thompson, J. (2015). Exposure of chick embryos to cadmium changes the extra-embryonic vascular branching pattern and alters expression of VEGF-A and VEGF-R2. *Toxicology and Applied Pharmacology*, *289*(1), 79–88. https://doi.org/10.1016/j.taap.2015.09.004

Gheorghescu, A., & Thompson, J. (2016). Delayed vasculogenesis and impaired angiogenesis due to altered Ang-2 and VE-cadherin levels in the chick embryo model following exposure to cadmium. *Pediatric Surgery International*, *32*(2), 175–186. https://doi.org/10.1007/s00383-015-3830-9

Gilbert, S. F. (2000). Lateral Plate Mesoderm. In *Developmental Biology. 6th edition*. Sinauer Associates. https://www.ncbi.nlm.nih.gov/books/NBK9982/

Gilbert, S. F. (2022). *Developmental Biology* (Ninth edition). Sinauer Associates, Inc.

Gobe, G., & Crane, D. (2010). Mitochondria, reactive oxygen species and cadmium toxicity in the kidney. *Toxicology Letters*, *198*(1), 49–55. https://doi.org/10.1016/j.toxlet.2010.04.013

Goodwin, A. M. (2007). In vitro assays of angiogenesis for assessment of angiogenic and anti-angiogenic agents. *Microvascular Research*, *74*(2–3), 172–183. https://doi.org/10.1016/j.mvr.2007.05.006

Graham, E., Moss, J., Burton, N., Roochun, Y., Armit, C., Richardson, L., & Baldock, R. (2015). The atlas of mouse development eHistology resource. *Development (Cambridge, England)*, *142*(11), 1909–1911. https://doi.org/10.1242/dev.124917

Grammas, P., Sanchez, A., Tripathy, D., Luo, E., & Martinez, J. (2011). Vascular signaling abnormalities in Alzheimer disease. *Cleveland Clinic Journal of Medicine*, *78 Suppl 1*, S50-53. https://doi.org/10.3949/ccjm.78.s1.09

Grunewald, M., Kumar, S., Sharife, H., Volinsky, E., Gileles-Hillel, A., Licht, T., Permyakova, A., Hinden, L., Azar, S., Friedmann, Y., Kupetz, P., Tzuberi, R., Anisimov, A., Alitalo, K., Horwitz, M., Leebhoff, S., Khoma, O. Z., Hlushchuk, R., Djonov, V., … Keshet, E. (2021). Counteracting age-related VEGF signaling insufficiency promotes healthy aging and extends life span. *Science*, *373*(6554), eabc8479. https://doi.org/10.1126/science.abc8479

Gundacker, C., & Hengstschläger, M. (2012). The role of the placenta in fetal exposure to heavy metals. *Wiener Medizinische Wochenschrift*, *162*(9), 201–206. https://doi.org/10.1007/s10354-012-0074-3

Haberstroh, K. M. W., & Kapron, C. M. (2006). Activation of c-Jun N-terminal kinase by cadmium in mouse embryo neural cells in vitro. *Environmental Toxicology and Pharmacology*, *22*(1), 1–7. https://doi.org/10.1016/j.etap.2005.10.004

Hanson, M. L., Holásková, I., Elliott, M., Brundage, K. M., Schafer, R., & Barnett, J. B. (2012). Prenatal cadmium exposure alters postnatal immune cell development and

function. *Toxicology and Applied Pharmacology*, *261*(2), 196–203. https://doi.org/10.1016/j.taap.2012.04.002

Helmestam, M., Stavreus-Evers, A., & Olovsson, M. (2010). Cadmium chloride alters mRNA levels of angiogenesis related genes in primary human endometrial endothelial cells grown in vitro. *Reproductive Toxicology*, *30*(3), 370–376. https://doi.org/10.1016/j.reprotox.2010.05.003

Hendriks, M., & Ramasamy, S. K. (2020). Blood vessels and vascular niches in bone development and physiological remodeling. *Frontiers in Cell and Developmental Biology*, *8*, 602278. https://doi.org/10.3389/fcell.2020.602278

Hopkins, B. D., Hodakoski, C., Barrows, D., Mense, S., & Parsons, R. E. (2014). PTEN function, the long and the short of it. *Trends in Biochemical Sciences*, *39*(4), 183–190. https://doi.org/10.1016/j.tibs.2014.02.006

Hovland, D. N., Machado, A. F., Scott, W. J., & Collins, M. D. (1999). Differential sensitivity of the SWV and C57BL/6 mouse strains to the teratogenic action of single administrations of cadmium given throughout the period of anterior neuropore closure. *Teratology*, *60*(1), 13–21. https://doi.org/10.1002/(SICI)1096-9926(199907)60:1<13::AID-TERA6>3.0.CO;2-B

Jacobson, M. D. (1997). Apoptosis: Bcl-2-related proteins get connected. *Current Biology*, *7*(5), R277–R281. https://doi.org/10.1016/S0960-9822(06)00136-9

Jahan, S., Khan, M., Ahmed, S., & Ullah, H. (2014). Comparative analysis of antioxidants against cadmium induced reproductive toxicity in adult male rats. *Systems Biology in Reproductive Medicine*, *60*(1), 28–34. https://doi.org/10.3109/19396368.2013.843039

Jahangir, T., Khan, T. H., Prasad, L., & Sultana, S. (2005). Alleviation of free radical mediated oxidative and genotoxic effects of cadmium by farnesol in Swiss albino mice. *Redox Report: Communications in Free Radical Research*, *10*(6), 303–310. https://doi.org/10.1179/135100005X83671

Jakob, W., Jentzsch, K. D., Mauersberger, B., & Heder, G. (1978). The chick embryo choriallantoic membrane as a bioassay for angiogenesis factors: Reactions induced by carrier materials. *Experimentelle Pathologie*, *15*(5), 241–249. https://doi.org/10.1016/s0014-4908(78)80064-7

Järup, L. (2002). Cadmium overload and toxicity. *Nephrology, Dialysis, Transplantation: Official Publication of the European Dialysis and Transplant Association - European Renal Association*, *17 Suppl 2*, 35–39. https://doi.org/10.1093/ndt/17.suppl_2.35

Jellinger, K. A. (2002). Alzheimer disease and cerebrovascular pathology: An update. *Journal of Neural Transmission*, *109*(5–6), 813–836. https://doi.org/10.1007/s007020200068

Jensen, L. D., Honek, J., Hosaka, K., Rouhi, P., Lim, S., Ji, H., Cao, Z., Hedlund, E. M., Zhang, J., Cao, Y., Jensen, L. D., Honek, J., Hosaka, K., Rouhi, P., Lim, S., Ji, H., Cao, Z., Hedlund, E. M., Zhang, J., & Cao, Y. (2012). Animal models of angiogenesis and lymphangiogenesis. In *Biomedical Science, Engineering and Technology*. IntechOpen. https://doi.org/10.5772/20211

Jiang, B.-H., & Liu, L.-Z. (2009). PI3K/PTEN signaling in angiogenesis and tumorigenesis. *Advances in Cancer Research*, *102*, 19–65. https://doi.org/10.1016/S0065-230X(09)02002-8

Jiang, G., Xu, L., Song, S., Zhu, C., Wu, Q., Zhang, L., & Wu, L. (2008). Effects of long-term low-dose cadmium exposure on genomic DNA methylation in human embryo lung fibroblast cells. *Toxicology*, *244*(1), 49–55. https://doi.org/10.1016/j.tox.2007.10.028

Jing, Y., Liu, L.-Z., Jiang, Y., Zhu, Y., Guo, N. L., Barnett, J., Rojanasakul, Y., Agani, F., & Jiang, B.-H. (2012). Cadmium increases HIF-1 and VEGF expression through ROS, ERK, and AKT signaling pathways and induces malignant transformation of human bronchial epithelial cells. *Toxicological Sciences*, *125*(1), 10–19. https://doi.org/10.1093/toxsci/kfr256

Johnson, M. D., Kenney, N., Stoica, A., Hilakivi-Clarke, L., Singh, B., Chepko, G., Clarke, R., Sholler, P. F., Lirio, A. A., Foss, C., Reiter, R., Trock, B., Paik, S., & Martin, M. B. (2003). Cadmium mimics the in vivo effects of estrogen in the uterus and mammary gland. *Nature Medicine*, *9*(8), 1081–1084. https://doi.org/10.1038/nm902

Kafer, G. R., & Cesare, A. J. (2020). A survey of essential genome stability genes reveals that replication stress mitigation is critical for peri-implantation embryogenesis. *Frontiers in Cell and Developmental Biology*, *8*, 416. https://doi.org/10.3389/fcell.2020.00416

Kalaria, R. N., Cohen, D. L., Premkumar, D. R. D., Nag, S., LaManna, J. C., & Lust, W. D. (1998). Vascular endothelial growth factor in Alzheimer's disease and experimental cerebral ischemia. *Molecular Brain Research*, *62*(1), 101–105. https://doi.org/10.1016/S0169-328X(98)00190-9

Kapoor, A., Chen, C. G., & Iozzo, R. V. (2020). A simplified aortic ring assay: A useful ex vivo method to assess biochemical and functional parameters of angiogenesis. *Matrix Biology Plus*, *6–7*, 100025. https://doi.org/10.1016/j.mbplus.2020.100025

Kapron-Brás, C. M., & Hales, B. F. (1991). Heat-shock induced tolerance to the embryotoxic effects of hyperthermia and cadmium in mouse embryos in vitro. *Teratology*, *43*(1), 83–94. https://doi.org/10.1002/tera.1420430110

Karar, J., & Maity, A. (2011). PI3K/AKT/mTOR pathway in angiogenesis. *Frontiers in Molecular Neuroscience*, *4*, 51. https://doi.org/10.3389/fnmol.2011.00051

Karthik, S., Djukic, T., Kim, J.-D., Zuber, B., Makanya, A., Odriozola, A., Hlushchuk, R., Filipovic, N., Jin, S. W., & Djonov, V. (2018). Synergistic interaction of sprouting and intussusceptive angiogenesis during zebrafish caudal vein plexus development. *Scientific Reports*, *8*, Article 9840. https://doi.org/10.1038/s41598-018-27791-6

Kim, J., Lim, W., Ko, Y., Kwon, H., Kim, S., Kim, O., Park, G., Choi, H., & Kim, O. (2012). The effects of cadmium on VEGF-mediated angiogenesis in HUVECs. *Journal of Applied Toxicology*, *32*(5), 342–349. https://doi.org/10.1002/jat.1677

Kim, J., Tchernyshyov, I., Semenza, G. L., & Dang, C. V. (2006). HIF-1-mediated expression of pyruvate dehydrogenase kinase: A metabolic switch required for cellular adaptation to hypoxia. *Cell Metabolism*, *3*(3), 177–185. https://doi.org/10.1016/j.cmet.2006.02.002

Kim, K., Melough, M. M., Vance, T. M., Noh, H., Koo, S. I., & Chun, O. K. (2018). Dietary cadmium intake and sources in the US. *Nutrients*, *11*(1), 2. https://doi.org/10.3390/nu11010002

Kippler, M., Engström, K., Mlakar, S. J., Bottai, M., Ahmed, S., Hossain, M. B., Raqib, R., Vahter, M., & Broberg, K. (2013). Sex-specific effects of early life cadmium exposure on DNA methylation and implications for birth weight. *Epigenetics*, *8*(5), 494–503. https://doi.org/10.4161/epi.24401

Klaassen, C. D., & Liu, J. (1997). Role of metallothionein in cadmium-induced hepatotoxicity and nephrotoxicity. *Drug Metabolism Reviews*, *29*(1–2), 79–102. https://doi.org/10.3109/03602539709037574

Klaassen, C. D., Liu, J., & Diwan, B. A. (2009). Metallothionein protection of cadmium toxicity. *Toxicology and Applied Pharmacology*, *238*(3), 215–220. https://doi.org/10.1016/j.taap.2009.03.026

Klein, R. (2012). Eph/ephrin signalling during development. *Development (Cambridge, England)*, *139*(22), 4105–4109. https://doi.org/10.1242/dev.074997

Kleinzeller, A., & Werner, H. (1939). Catalase activity during the development of the chick embryo. *Biochemical Journal*, *33*(3), 291–292.

Knighton, D. R., Fiegel, V. D., & Phillips, G. D. (1991). The assay of angiogenesis. *Progress in Clinical and Biological Research*, *365*, 291–299.

Kozlosky, D., Lu, A., Doherty, C., Buckley, B., Goedken, M. J., Miller, R. K., Barrett, E. S., & Aleksunes, L. M. (2023). Cadmium reduces growth of male fetuses by impairing development of the placental vasculature and reducing expression of nutrient transporters. *Toxicology and Applied Pharmacology*, *475*, 116636. https://doi.org/10.1016/j.taap.2023.116636

Kubier, A., Wilkin, R. T., & Pichler, T. (2019). Cadmium in soils and groundwater: A review. *Applied Geochemistry : Journal of the International Association of*

Geochemistry and Cosmochemistry, *108*, 1–16. https://doi.org/10.1016/j.apgeochem.2019.104388

Lähteenvuo, J., & Rosenzweig, A. (2012). Effects of aging on angiogenesis. *Circulation Research*, *110*(9), 1252–1264. https://doi.org/10.1161/CIRCRESAHA.111.246116

Lamalice, L., Le Boeuf, F., & Huot, J. (2007). Endothelial cell migration during angiogenesis. *Circulation Research*, *100*(6), 782–794. https://doi.org/10.1161/01.RES.0000259593.07661.1e

le Noble, F., Moyon, D., Pardanaud, L., Yuan, L., Djonov, V., Matthijsen, R., Bréant, C., Fleury, V., & Eichmann, A. (2004). Flow regulates arterial-venous differentiation in the chick embryo yolk sac. *Development (Cambridge, England)*, *131*(2), 361–375. https://doi.org/10.1242/dev.00929

Leazer, T. (2002). Cadmium absorption and its relationship to divalent metal transporter-1 in the pregnant rat. *Toxicology and Applied Pharmacology*, *185*(1), 18–24. https://doi.org/10.1006/taap.2002.9505

Leslie, N. R., Yang, X., Downes, C. P., & Weijer, C. J. (2007). PtdIns(3,4,5)P(3)-dependent and -independent roles for PTEN in the control of cell migration. *Current Biology: CB*, *17*(2), 115–125. https://doi.org/10.1016/j.cub.2006.12.026

Li, X., Yang, T., & Sun, Z. (2019). Hormesis in health and chronic diseases. *Trends in Endocrinology & Metabolism*, *30*(12), 944–958. https://doi.org/10.1016/j.tem.2019.08.007

Liao, D., & Johnson, R. S. (2007). Hypoxia: A key regulator of angiogenesis in cancer. *Cancer Metastasis Reviews*, *26*(2), 281–290. https://doi.org/10.1007/s10555-007-9066-y

Liu, F., Wang, B., Li, L., Dong, F., Chen, X., Li, Y., Dong, X., Wada, Y., Kapron, C. M., & Liu, J. (2015). Low-dose cadmium upregulates VEGF expression in lung adenocarcinoma cells. *International Journal of Environmental Research and Public Health*, *12*(9), 10508–10521. https://doi.org/10.3390/ijerph120910508

Liu, Y., Xiao, T., Perkins, R. B., Zhu, J., Zhu, Z., Xiong, Y., & Ning, Z. (2017). Geogenic cadmium pollution and potential health risks, with emphasis on black shale. *Journal of Geochemical Exploration*, *176*, 42–49. https://doi.org/10.1016/j.gexplo.2016.04.004

López Fernández de Villaverde, E. (2005). *Mechanisms behind cadmium-induced teratogenicity* [Doctoral, Uppsala University]. https://urn.kb.se/resolve?urn=urn:nbn:se:uu:diva-6223

Lugano, R., Ramachandran, M., & Dimberg, A. (2020). Tumor angiogenesis: Causes, consequences, challenges and opportunities. *Cellular and Molecular Life Sciences: CMLS*, *77*(9), 1745–1770. https://doi.org/10.1007/s00018-019-03351-7

Mahalik, M. P., Hitner, H. W., & Prozialeck, W. C. (1995). Teratogenic effects and distribution of cadmium (Cd2+) administered via osmotic minipumps to gravid CF-1 mice. *Toxicology Letters*, *76*(3), 195–202. https://doi.org/10.1016/0378-4274(95)80003-V

Majumder, S., Gupta, R., Reddy, H., Sinha, S., Muley, A., Kolluru, G. K., & Chatterjee, S. (2009). Cadmium attenuates bradykinin-driven nitric oxide production by interplaying with the localization pattern of endothelial nitric oxide synthase. *Biochemistry and Cell Biology = Biochimie Et Biologie Cellulaire*, *87*(4), 605–620. https://doi.org/10.1139/o09-018

Majumder, S., Muley, A., Kolluru, G. K., Saurabh, S., Tamilarasan, K. P., Chandrasekhar, S., Reddy, H. B., Purohit, S., & Chatterjee, S. (2008). Cadmium reduces nitric oxide production by impairing phosphorylation of endothelial nitric oxide synthase. *Biochemistry and Cell Biology = Biochimie Et Biologie Cellulaire*, *86*(1), 1–10. https://doi.org/10.1139/o07-146

Makanya, A. N., Hlushchuk, R., & Djonov, V. G. (2009). Intussusceptive angiogenesis and its role in vascular morphogenesis, patterning, and remodeling. *Angiogenesis*, *12*(2), 113–123. https://doi.org/10.1007/s10456-009-9129-5

Manickam, V., Tiwari, A., Jung, J.-J., Bhattacharya, R., Goel, A., Mukhopadhyay, D., & Choudhury, A. (2011). Regulation of vascular endothelial growth factor receptor 2 trafficking and angiogenesis by Golgi localized t-SNARE syntaxin 6. *Blood*, *117*(4), 1425–1435. https://doi.org/10.1182/blood-2010-06-291690

Mao, W. P., Zhang, N. N., Zhou, F. Y., Li, W. X., Liu, H. Y., Feng, J., Zhou, L., Wei, C. J., Pan, Y. B., & He, Z. J. (2011). Cadmium directly induced mitochondrial dysfunction of human embryonic kidney cells. *Human & Experimental Toxicology*, *30*(8), 920–929. https://doi.org/10.1177/0960327110384286

Marmé, D., & Fusenig, N. (2007). *Tumor Angiogenesis: Basic Mechanisms and Cancer Therapy*. Springer Berlin, Heidelberg.

Marrelli, A., Cipriani, P., Liakouli, V., Carubbi, F., Perricone, C., Perricone, R., & Giacomelli, R. (2011). Angiogenesis in rheumatoid arthritis: A disease specific process or a common response to chronic inflammation? *Autoimmunity Reviews*, *10*(10), 595–598. https://doi.org/10.1016/j.autrev.2011.04.020

May, D., Gilon, D., Djonov, V., Itin, A., Lazarus, A., Gordon, O., Rosenberger, C., & Keshet, E. (2008). Transgenic system for conditional induction and rescue of

chronic myocardial hibernation provides insights into genomic programs of hibernation. *Proceedings of the National Academy of Sciences of the United States of America*, *105*(1), 282–287. https://doi.org/10.1073/pnas.0707778105

Mayo, L. D., & Donner, D. B. (2001). A phosphatidylinositol 3-kinase/Akt pathway promotes translocation of Mdm2 from the cytoplasm to the nucleus. *Proceedings of the National Academy of Sciences of the United States of America*, *98*(20), 11598–11603. https://doi.org/10.1073/pnas.181181198

Medina-Leyte, D. J., Domínguez-Pérez, M., Mercado, I., Villarreal-Molina, M. T., & Jacobo-Albavera, L. (2020). Use of human umbilical vein endothelial cells (HUVEC) as a model to study cardiovascular disease: A review. *Applied Sciences*, *10*(3), Article 938. https://doi.org/10.3390/app10030938

Méndez-Armenta, M., & Ríos, C. (2007). Cadmium neurotoxicity. *Environmental Toxicology and Pharmacology*, *23*(3), 350–358. https://doi.org/10.1016/j.etap.2006.11.009

Mezynska, M., & Brzóska, M. M. (2018). Environmental exposure to cadmium-a risk for health of the general population in industrialized countries and preventive strategies. *Environmental Science and Pollution Research International*, *25*(4), 3211–3232. https://doi.org/10.1007/s11356-017-0827-z

Mikhailova, M. V., Littlefield, N. A., Hass, B. S., Poirier, L. A., & Chou, M. W. (1997). Cadmium-induced 8-hydroxydeoxyguanosine formation, DNA strand breaks and antioxidant enzyme activities in lymphoblastoid cells. *Cancer Letters*, *115*(2), 141–148. https://doi.org/10.1016/s0304-3835(97)04720-4

Milkiewicz, M., Uchida, C., Gee, E., Fudalewski, T., & Haas, T. L. (2008). Shear stress–induced Ets-1 modulates protease inhibitor expression in microvascular endothelial

cells. *Journal of Cellular Physiology*, *217*(2), 502–510. https://doi.org/10.1002/jcp.21526

Miotla, J., Maciewicz, R., Kendrew, J., Feldmann, M., & Paleolog, E. (2000). Treatment with soluble VEGF receptor reduces disease severity in murine collagen-induced arthritis. *Laboratory Investigation; a Journal of Technical Methods and Pathology*, *80*(8), 1195–1205. https://doi.org/10.1038/labinvest.3780127

Molina-Mesa, S., Martínez-Cendán, J. P., Moyano-Rubiales, D., Cubillas-Rodríguez, I., Molina-García, J., & González-Mesa, E. (2022). Detection of relevant heavy metal concentrations in human placental tissue: Relationship between the concentrations of Hg, As, Pb and Cd and the diet of the pregnant woman. *International Journal of Environmental Research and Public Health*, *19*(22), 14731. https://doi.org/10.3390/ijerph192214731

Nagarajan, S., Rajendran, S., Saran, U., Priya, M. K., Swaminathan, A., Siamwala, J. H., Sinha, S., Veeriah, V., Sonar, P., Jadhav, V., Jaffar Ali, B. M., & Chatterjee, S. (2013). Nitric oxide protects endothelium from cadmium mediated leakiness. *Cell Biology International*, *37*(5), 495–506. https://doi.org/10.1002/cbin.10070

Nakanishi, A., Kitagishi, Y., Ogura, Y., & Matsuda, S. (2014). The tumor suppressor PTEN interacts with p53 in hereditary cancer (Review). *International Journal of Oncology*, *44*(6), 1813–1819. https://doi.org/10.3892/ijo.2014.2377

Nakashima, K., Wakisaka, T., & Fujiki, Y. (1987). Dose-response relationship of cadmium embryotoxicity in cultured mouse embryos. *Reproductive Toxicology*, *1*(4), 293–298. https://doi.org/10.1016/0890-6238(87)90021-9

Nemmiche, S. (2017). Oxidative signaling response to cadmium exposure. *Toxicological Sciences*, *156*(1), 4–10. https://doi.org/10.1093/toxsci/kfw222

New, D. A. (1978). Whole-embryo culture and the study of mammalian embryos during organogenesis. *Biological Reviews of the Cambridge Philosophical Society*, *53*(1), 81–122. https://doi.org/10.1111/j.1469-185x.1978.tb00993.x

New, D. A., Coppola, P. T., & Cockroft, D. L. (1976). Comparison of growth in vitro and in vivo of post-implantation rat embryos. *Journal of Embryology and Experimental Morphology*, *36*(1), 133–144.

Niewenhuis, R. J., Dimitriu, C., & Prozialeck, W. C. (1997). Ultrastructural characterization of the early changes in intercellular junctions in response to cadmium (Cd2+) exposure in LLC-PK1cells. *Toxicology and Applied Pharmacology*, *142*(1), 1–12. https://doi.org/10.1006/taap.1996.8026

Nishida, N., Yano, H., Nishida, T., Kamura, T., & Kojiro, M. (2006). Angiogenesis in cancer. *Vascular Health and Risk Management*, *2*(3), 213–219.

Nishijo, M., Nakagawa, H., Suwazono, Y., Nogawa, K., & Kido, T. (2017). Causes of death in patients with Itai-itai disease suffering from severe chronic cadmium poisoning: A nested case–control analysis of a follow-up study in Japan. *BMJ Open*, *7*(7), e015694. https://doi.org/10.1136/bmjopen-2016-015694

Nordberg, M., & Nordberg, G. F. (2022). Metallothionein and cadmium toxicology—Historical review and commentary. *Biomolecules*, *12*(3), Article 360. https://doi.org/10.3390/biom12030360

Norrby, K. (2006). In vivo models of angiogenesis. *Journal of Cellular and Molecular Medicine*, *10*(3), 588–612. https://doi.org/10.1111/j.1582-4934.2006.tb00423.x

Notarachille, G., Arnesano, F., Calò, V., & Meleleo, D. (2014). Heavy metals toxicity: Effect of cadmium ions on amyloid beta protein 1-42. Possible implications for Alzheimer's disease. *Biometals: An International Journal on the Role of Metal Ions*

in Biology, Biochemistry, and Medicine, *27*(2), 371–388. https://doi.org/10.1007/s10534-014-9719-6

Ogawara, Y., Kishishita, S., Obata, T., Isazawa, Y., Suzuki, T., Tanaka, K., Masuyama, N., & Gotoh, Y. (2002). Akt enhances Mdm2-mediated ubiquitination and degradation of p53. *The Journal of Biological Chemistry*, *277*(24), 21843–21850. https://doi.org/10.1074/jbc.M109745200

Oh, S.-H., & Lim, S.-C. (2006). A rapid and transient ROS generation by cadmium triggers apoptosis via caspase-dependent pathway in HepG2 cells and this is inhibited through N-acetylcysteine-mediated catalase upregulation. *Toxicology and Applied Pharmacology*, *212*(3), 212–223. https://doi.org/10.1016/j.taap.2005.07.018

Osawa, M., Masuda, M., Kusano, K., & Fujiwara, K. (2002). Evidence for a role of platelet endothelial cell adhesion molecule-1 in endothelial cell mechanosignal transduction: Is it a mechanoresponsive molecule? *The Journal of Cell Biology*, *158*(4), 773–785. https://doi.org/10.1083/jcb.200205049

Pacyna, J. M., & Pacyna, E. G. (2001). An assessment of global and regional emissions of trace metals to the atmosphere from anthropogenic sources worldwide. *Environmental Reviews*, *9*(4), 269–298. https://doi.org/10.1139/a01-012

Paleolog, E. M. (2002). Angiogenesis in rheumatoid arthritis. *Arthritis Research*, *4 Suppl 3*(Suppl 3), S81-90. https://doi.org/10.1186/ar575

Palis, J., & Yoder, M. C. (2001). Yolk-sac hematopoiesis: The first blood cells of mouse and man. *Experimental Hematology*, *29*(8), 927–936. https://doi.org/10.1016/S0301-472X(01)00669-5

Paniagua-Castro, N., Escalona-Cardoso, G., Hernández-Navarro, D., Pérez-Pastén, R., & Chamorro-Cevallos, G. (2011). *Spirulina (Arthrospira)* protects against cadmium-

induced teratogenic damage in mice. *Journal of Medicinal Food*, *14*(4), 398–404. https://doi.org/10.1089/jmf.2010.0070

Paniagua-Castro, N., Escalona-Cardoso, G., Madrigal-Bujaidar, E., Martínez-Galero, E., & Chamorro-Cevallos, G. (2008). Protection against cadmium-induced teratogenicity in vitro by glycine. *Toxicology in Vitro*, *22*(1), 75–79. https://doi.org/10.1016/j.tiv.2007.08.005

Paplomata, E., & O'Regan, R. (2014). The PI3K/AKT/mTOR pathway in breast cancer: Targets, trials and biomarkers. *Therapeutic Advances in Medical Oncology*, *6*(4), 154–166. https://doi.org/10.1177/1758834014530023

Pappas, R. S., Fresquez, M. R., Martone, N., & Watson, C. H. (2014). Toxic metal concentrations in mainstream smoke from cigarettes available in the USA. *Journal of Analytical Toxicology*, *38*(4), 204–211. https://doi.org/10.1093/jat/bku013

Parenti, A., Morbidelli, L., Ledda, F., Granger, H. J., & Ziche, M. (2001). The bradykinin/B1 receptor promotes angiogenesis by up-regulation of endogenous FGF-2 in endothelium via the nitric oxide synthase pathway. *FASEB Journal: Official Publication of the Federation of American Societies for Experimental Biology*, *15*(8), 1487–1489.

Paris, D., Patel, N., DelleDonne, A., Quadros, A., Smeed, R., & Mullan, M. (2004). Impaired angiogenesis in a transgenic mouse model of cerebral amyloidosis. *Neuroscience Letters*, *366*(1), 80–85. https://doi.org/10.1016/j.neulet.2004.05.017

Peana, M., Pelucelli, A., Chasapis, C. T., Perlepes, S. P., Bekiari, V., Medici, S., & Zoroddu, M. A. (2023). Biological Effects of Human Exposure to Environmental Cadmium. *Biomolecules*, *13*(1), Article 36. https://doi.org/10.3390/biom13010036

Pedersen, M., Giorgis-Allemand, L., Bernard, C., Aguilera, I., Andersen, A.-M. N., Ballester, F., Beelen, R. M. J., Chatzi, L., Cirach, M., Danileviciute, A., Dedele, A., Eijsden, M. van, Estarlich, M., Fernández-Somoano, A., Fernández, M. F., Forastiere, F., Gehring, U., Grazuleviciene, R., Gruzieva, O., … Slama, R. (2013). Ambient air pollution and low birthweight: A European cohort study (ESCAPE). *The Lancet Respiratory Medicine*, *1*(9), 695–704. https://doi.org/10.1016/S2213-2600(13)70192-9

PI3K Akt Pathway. (2016). Cell Signaling Technology. Retrieved January 28, 2024, from https://www.cellsignal.com/pathways/pathways-akt-signaling

Piersma, A. H. (1993). Whole embryo culture and toxicity testing. *Toxicology in Vitro: An International Journal Published in Association with BIBRA*, *7*(6), 763–768. https://doi.org/10.1016/0887-2333(93)90079-k

Poteet, E., Winters, A., Xie, L., Ryou, M., Liu, R., & Yang, S. (2014). *In vitro* protection by pyruvate against cadmium-induced cytotoxicity in hippocampal HT-22 cells. *Journal of Applied Toxicology*, *34*(8), 903–913. https://doi.org/10.1002/jat.2913

Prozialeck, W. C., & Edwards, J. R. (2012). Mechanisms of cadmium-induced proximal tubule injury: New insights with implications for biomonitoring and therapeutic interventions. *The Journal of Pharmacology and Experimental Therapeutics*, *343*(1), 2–12. https://doi.org/10.1124/jpet.110.166769

Prozialeck, W. C., Edwards, J. R., Nebert, D. W., Woods, J. M., Barchowsky, A., & Atchison, W. D. (2008). The vascular system as a target of metal toxicity. *Toxicological Sciences*, *102*(2), 207–218. https://doi.org/10.1093/toxsci/kfm263

Prozialeck, W. C., Edwards, J. R., & Woods, J. M. (2006). The vascular endothelium as a target of cadmium toxicity. *Life Sciences*, *79*(16), 1493–1506. https://doi.org/10.1016/j.lfs.2006.05.007

Qubit protein assay user guide, ThermoFisher Scientific, Leederville, WA, Australia, 2022. Accessed: Nov. 17, 2023. [Online]. Available: https://assets.fishersci.com/TFS-Assets/LSG/manuals/Qubit_Protein_Assay_UG.pdf

Rafati Rahimzadeh, M., Rafati Rahimzadeh, M., Kazemi, S., & Moghadamnia, A. (2017). Cadmium toxicity and treatment: An update. Caspian Journal of Internal Medicine, 8(3), 135–145. https://doi.org/10.22088/cjim.8.3.135

Raftopoulou, M., Etienne-Manneville, S., Self, A., Nicholls, S., & Hall, A. (2004). Regulation of cell migration by the C2 domain of the tumor suppressor PTEN. *Science (New York, N.Y.)*, *303*(5661), 1179–1181. https://doi.org/10.1126/science.1092089

Rajabi, M., & Mousa, S. A. (2017). The role of angiogenesis in cancer treatment. *Biomedicines*, *5*(2), 34. https://doi.org/10.3390/biomedicines5020034

Rengel, Z. (1999). Heavy Metals as Essential Nutrients. In *Heavy Metal Stress in Plants* (pp. 231–251). Springer Berlin, Heidelberg. https://doi-org.proxy1.lib.trentu.ca/10.1007/978-3-662-07745-0_11

Richter, P., Faroon, O., & Pappas, R. S. (2017). Cadmium and cadmium/zinc ratios and tobacco-related morbidities. *International Journal of Environmental Research and Public Health*, *14*(10), 1154. https://doi.org/10.3390/ijerph14101154

Risau, W. (1998). Development and differentiation of endothelium. *Kidney International. Supplement*, *67*, S3-6. https://doi.org/10.1046/j.1523-1755.1998.06701.x

Risau, W., & Flamme, I. (1995). Vasculogenesis. *Annual Review of Cell and Developmental Biology*, *11*, 73–91. https://doi.org/10.1146/annurev.cb.11.110195.000445

Rivera-Pérez, J. A., & Hadjantonakis, A.-K. (2015). The dynamics of morphogenesis in the early mouse embryo. *Cold Spring Harbor Perspectives in Biology*, *7*(11), a015867. https://doi.org/10.1101/cshperspect.a015867

Robertson, J. D., & Orrenius, S. (2000). Molecular mechanisms of apoptosis induced by cytotoxic chemicals. *Critical Reviews in Toxicology*, *30*(5), 609–627. https://doi.org/10.1080/10408440008951122

Rodriguez, S., & Huynh-Do, U. (2012). The role of PTEN in tumor angiogenesis. *Journal of Oncology*, *2012*, 141236. https://doi.org/10.1155/2012/141236

Rousseau, S., Houle, F., & Huot, J. (2000). Integrating the VEGF signals leading to actin-based motility in vascular endothelial cells. *Trends in Cardiovascular Medicine*, *10*(8), 321–327. https://doi.org/10.1016/S1050-1738(01)00072-X

Roy, A., Nethi, S. K., Suganya, N., Raval, M., Chatterjee, S., & Patra, C. R. (2020). Attenuation of cadmium-induced vascular toxicity by pro-angiogenic nanorods. *Materials Science and Engineering: C*, *115*, 111108. https://doi.org/10.1016/j.msec.2020.111108

Sabolić, I., Breljak, D., Škarica, M., & Herak-Kramberger, C. M. (2010). Role of metallothionein in cadmium traffic and toxicity in kidneys and other mammalian organs. *BioMetals*, *23*(5), 897–926. https://doi.org/10.1007/s10534-010-9351-z

Saedi, S., Watson, S. E., Young, J. L., Tan, Y., Wintergerst, K. A., & Cai, L. (2023). Does maternal low-dose cadmium exposure increase the risk of offspring to develop

metabolic syndrome and/or type 2 diabetes? *Life Sciences*, *315*, 121385. https://doi.org/10.1016/j.lfs.2023.121385

San Roman, A. K., Kim, T.-H., & Shivdasani, R. A. (2016). 5—The Alimentary Canal. In R. Baldock, J. Bard, D. R. Davidson, & G. Morriss-Kay (Eds.), *Kaufman's Atlas of Mouse Development Supplement* (pp. 77–84). Academic Press. https://doi.org/10.1016/B978-0-12-800043-4.00005-1

Sandbichler, A., & Höckner, M. (2016). Cadmium protection strategies—A hidden trade-off? *International Journal of Molecular Sciences*, *17*(1), 139. https://doi.org/10.3390/ijms17010139

Sant, K. E., & Timme-Laragy, A. R. (2018). Zebrafish as a model for toxicological perturbation of yolk and nutrition in the early embryo. *Current Environmental Health Reports*, *5*(1), 125–133. https://doi.org/10.1007/s40572-018-0183-2

Schindelin, J., Arganda-Carreras, I., Frise, E., Kaynig, V., Longair, M., Pietzsch, T., Preibisch, S., Rueden, C., Saalfeld, S., Schmid, B., Tinevez, J.-Y., White, D. J., Hartenstein, V., Eliceiri, K., Tomancak, P., & Cardona, A. (2012). Fiji: An open-source platform for biological-image analysis. *Nature Methods*, *9*(7), 676–682. https://doi.org/10.1038/nmeth.2019

Scroggie, M. (1996) Histological analysis of the effects of cadmium chloride on Day-8 Swiss mice embryos. Thesis. (BSc). Trent University.

Sewduth, R., & Santoro, M. M. (2016). "Decoding" angiogenesis: New facets controlling endothelial cell behavior. *Frontiers in Physiology*, *7*, 306. https://doi.org/10.3389/fphys.2016.00306

Shalaby, F., Ho, J., Stanford, W. L., Fischer, K. D., Schuh, A. C., Schwartz, L., Bernstein, A., & Rossant, J. (1997). A requirement for Flk1 in primitive and definitive

hematopoiesis and vasculogenesis. *Cell*, *89*(6), 981–990. https://doi.org/10.1016/s0092-8674(00)80283-4

Shi, Z., Carey, M., Meharg, C., Williams, P. N., Signes-Pastor, A. J., Triwardhani, E. A., Pandiangan, F. I., Campbell, K., Elliott, C., Marwa, E. M., Jiujin, X., Farias, J. G., Nicoloso, F. T., De Silva, P. M. C. S., Lu, Y., Norton, G., Adomako, E., Green, A. J., Moreno-Jiménez, E., … Meharg, A. A. (2020). Rice grain cadmium concentrations in the global supply-chain. *Exposure and Health*, *12*(4), 869–876. https://doi.org/10.1007/s12403-020-00349-6

Shibuya, M. (2011). Vascular endothelial growth factor (VEGF) and its receptor (VEGFR) signaling in angiogenesis. *Genes & Cancer*, *2*(12), 1097–1105. https://doi.org/10.1177/1947601911423031

Shiojima, I., & Walsh, K. (2002). Role of Akt signaling in vascular homeostasis and angiogenesis. *Circulation Research*, *90*(12), 1243–1250. https://doi.org/10.1161/01.res.0000022200.71892.9f

Silva, R., D'Amico, G., Hodivala-Dilke, K. M., & Reynolds, L. E. (2008). Integrins: The keys to unlocking angiogenesis. *Arteriosclerosis, Thrombosis, and Vascular Biology*, *28*(10), 1703–1713. https://doi.org/10.1161/ATVBAHA.108.172015

Simons, M. (2012). An inside view: VEGF receptor trafficking and signaling. *Physiology*, *27*(4), 213–222. https://doi.org/10.1152/physiol.00016.2012

Sionov, R. V., & Haupt, Y. (1999). The cellular response to p53: The decision between life and death. *Oncogene*, *18*, 6145-6157. https://doi.org/10.1038/sj.onc.1203130

Smereczański, N. M., & Brzóska, M. M. (2023). Current levels of environmental exposure to cadmium in industrialized countries as a risk factor for kidney damage

in the general population: A comprehensive review of available data. *International Journal of Molecular Sciences*, *24*(9), 8413. https://doi.org/10.3390/ijms24098413

Smolders, E., & Mertens, J. (2013). Cadmium. In B. J. Alloway (Ed.), *Heavy Metals in Soils* (3rd ed., Vol. 22, pp. 283–311). Springer Netherlands. https://doi.org/10.1007/978-94-007-4470-7_10

Song, W., Fhu, C., Ang, K. H., Liu, C., Johari, N. A., Lio, D., Abraham, S., Hong, W., Moss, S., Greenwood, J., & Wang, X. (2015). The fetal mouse metatarsal bone explant as a model of angiogenesis. *Nature Protocols*, *10*, 1459–1473. https://doi.org/10.1038/nprot.2015.097

Staton, C. A., Stribbling, S. M., Tazzyman, S., Hughes, R., Brown, N. J., & Lewis, C. E. (2004). Current methods for assaying angiogenesis in vitro and in vivo. *International Journal of Experimental Pathology*, *85*(5), 233–248. https://doi.org/10.1111/j.0959-9673.2004.00396.x

Stoica, A., Katzenellenbogen, B. S., & Martin, M. B. (2000). Activation of estrogen receptor-alpha by the heavy metal cadmium. *Molecular Endocrinology (Baltimore, Md.)*, *14*(4), 545–553. https://doi.org/10.1210/mend.14.4.0441

Sudhakar, M., Silambanan, S., Prabhakaran, A. A., & Ramakrishnan, R. (2021). Angiogenic potential, circulating angiogenic factors and insulin resistance in subjects with obesity. *Indian Journal of Clinical Biochemistry: IJCB*, *36*(1), 43–50. https://doi.org/10.1007/s12291-019-0816-8

Taft, R. A. (2008). Virtues and limitations of the preimplantation mouse embryo as a model system. *Theriogenology*, *69*(1), 10–16. https://doi.org/10.1016/j.theriogenology.2007.09.032

Tallkvist, J., Bowlus, C. L., & Lönnerdal, B. (2001). DMT1 gene expression and cadmium absorption in human absorptive enterocytes. *Toxicology Letters*, *122*(2), 171–177. https://doi.org/10.1016/s0378-4274(01)00363-0

Tamura, M., Gu, J., Matsumoto, K., Aota, S., Parsons, R., & Yamada, K. M. (1998). Inhibition of cell migration, spreading, and focal adhesions by tumor suppressor PTEN. *Science (New York, N.Y.)*, *280*(5369), 1614–1617. https://doi.org/10.1126/science.280.5369.1614

Thévenod, F., Fels, J., Lee, W.-K., & Zarbock, R. (2019). Channels, transporters and receptors for cadmium and cadmium complexes in eukaryotic cells: Myths and facts. *Biometals: An International Journal on the Role of Metal Ions in Biology, Biochemistry, and Medicine*, *32*(3), 469–489. https://doi.org/10.1007/s10534-019-00176-6

Thévenod, F., Friedmann, J. M., Katsen, A. D., & Hauser, I. A. (2000). Up-regulation of multidrug resistance P-glycoprotein via nuclear factor-kappaB activation protects kidney proximal tubule cells from cadmium- and reactive oxygen species-induced apoptosis. *The Journal of Biological Chemistry*, *275*(3), 1887–1896. https://doi.org/10.1074/jbc.275.3.1887

Thompson, J., & Bannigan, J. (2008). Cadmium: Toxic effects on the reproductive system and the embryo. *Reproductive Toxicology*, *25*(3), 304–315. https://doi.org/10.1016/j.reprotox.2008.02.001

Thompson, S. (2009). Immunoprecipitation and Blotting. In J. M. Walker (Ed.), *The Protein Protocols Handbook* (pp. 1845–1858). Humana Press. https://doi.org/10.1007/978-1-59745-198-7_196

Tobwala, S., Wang, H.-J., Carey, J. W., Banks, W. A., & Ercal, N. (2014). Effects of lead and cadmium on brain endothelial cell survival, monolayer permeability, and crucial oxidative stress markers in an in vitro model of the blood-brain barrier. *Toxics*, *2*(2), 258-275. https://doi.org/10.3390/toxics2020258

Tonini, T., Rossi, F., & Claudio, P. P. (2003). Molecular basis of angiogenesis and cancer. *Oncogene*, *22*, 6549–6556. https://doi.org/10.1038/sj.onc.1206816

Trotman, L. C., & Pandolfi, P. P. (2003). PTEN and p53: Who will get the upper hand? *Cancer Cell*, *3*(2), 97–99. https://doi.org/10.1016/S1535-6108(03)00022-9

Tymchuk, T. K., Abramov, S. V., Kryzhanovsky, D. G., Fedchenko, M. P., Filipenko, V. V., Chernenko, G. P., & Myakushko, V. A. (2022). Embryotoxic effect of cadmium chloride and cuprum during the entire pregnancy period in white rats. *Ukrainian Medical Stomatological Academy*, *1*(3), 115–119.

Vahter, M., Åkesson, A., Lidén, C., Ceccatelli, S., & Berglund, M. (2007). Gender differences in the disposition and toxicity of metals. *Environmental Research*, *104*(1), 85–95. https://doi.org/10.1016/j.envres.2006.08.003

Vailhé, B., Vittet, D., & Feige, J.-J. (2001). In vitro models of vasculogenesis and angiogenesis. *Laboratory Investigation*, *81*(4), 439-452. https://doi.org/10.1038/labinvest.3780252

van Royen, N., Piek, J. J., Buschmann, I., Hoefer, I., Voskuil, M., & Schaper, W. (2001). Stimulation of arteriogenesis; a new concept for the treatment of arterial occlusive disease. *Cardiovascular Research*, *49*(3), 543–553. https://doi.org/10.1016/S0008-6363(00)00206-6

Vasudev, N. S., & Reynolds, A. R. (2014). Anti-angiogenic therapy for cancer: Current progress, unresolved questions and future directions. *Angiogenesis*, *17*(3), 471–494. https://doi.org/10.1007/s10456-014-9420-y

Veeriah, V., Saran, U., Swaminathan, A., Balaguru, U. M., Thangaraj, P., Nagarajan, S., Rajendran, V. K., & Chatterjee, S. (2015). Cadmium-induced embryopathy: Nitric oxide rescues teratogenic effects of cadmium. *Toxicological Sciences*, *144*(1), 90–104. https://doi.org/10.1093/toxsci/kfu258

Vilahur, N., Vahter, M., & Broberg, K. (2015). The epigenetic effects of prenatal cadmium exposure. *Current Environmental Health Reports*, *2*(2), 195–203. https://doi.org/10.1007/s40572-015-0049-9

Villar-Cheda, B., Sousa-Ribeiro, D., Rodriguez-Pallares, J., Rodriguez-Perez, A. I., Guerra, M. J., & Labandeira-Garcia, J. L. (2009). Aging and sedentarism decrease vascularization and vegf levels in the rat substantia nigra. Implications for parkinson's disease. *Journal of Cerebral Blood Flow and Metabolism: Official Journal of the International Society of Cerebral Blood Flow and Metabolism*, *29*(2), 230–234. https://doi.org/10.1038/jcbfm.2008.127

Viotti, M., Nowotschin, S., & Hadjantonakis, A.-K. (2011). Afp::mCherry, a red fluorescent transgenic reporter of the mouse visceral endoderm. *Genesis (New York, N.Y.: 2000)*, *49*(3), 124–133. https://doi.org/10.1002/dvg.20695

Waalkes, M. P., & Poirier, L. A. (1984). In vitro cadmium-DNA interactions: Cooperativity of cadmium binding and competitive antagonism by calcium, magnesium, and zinc. *Toxicology and Applied Pharmacology*, *75*(3), 539–546. https://doi.org/10.1016/0041-008x(84)90190-x

Waisberg, M., Joseph, P., Hale, B., & Beyersmann, D. (2003). Molecular and cellular mechanisms of cadmium carcinogenesis. *Toxicology*, *192*(2–3), 95–117. https://doi.org/10.1016/s0300-483x(03)00305-6

Wang, D., Sun, H., Wu, Y., Zhou, Z., Ding, Z., Chen, X., & Xu, Y. (2016). Tubular and glomerular kidney effects in the Chinese general population with low environmental cadmium exposure. *Chemosphere*, *147*, 3–8. https://doi.org/10.1016/j.chemosphere.2015.11.069

Wang, H. U., Chen, Z. F., & Anderson, D. J. (1998). Molecular distinction and angiogenic interaction between embryonic arteries and veins revealed by ephrin-B2 and its receptor Eph-B4. *Cell*, *93*(5), 741–753. https://doi.org/10.1016/s0092-8674(00)81436-1

Wang, H., Xu, X., Yin, Y., Yu, S., Ren, H., Xue, Q., & Xu, X. (2020a). Catalpol protects vascular structure and promotes angiogenesis in cerebral ischemic rats by targeting HIF-1α/VEGF. *Phytomedicine*, *78*, 153300. https://doi.org/10.1016/j.phymed.2020.153300

Wang, W., He, Y., Yu, G., Li, B., Sexton, D. W., Wileman, T., Roberts, A. A., Hamilton, C. J., Liu, R., Chao, Y., Shan, Y., & Bao, Y. (2015). Sulforaphane protects the liver against CdSe quantum dot-induced cytotoxicity. *PLOS ONE*, *10*(9), e0138771. https://doi.org/10.1371/journal.pone.0138771

Wang, X., Bove, A. M., Simone, G., & Ma, B. (2020b). Molecular bases of VEGFR-2-mediated physiological function and pathological role. *Frontiers in Cell and Developmental Biology*, *8*. https://www.frontiersin.org/articles/10.3389/fcell.2020.599281

Warner, C. W., Sadler, T. W., Tulis, S. A., & Smith, M. K. (1984). Zinc amelioration of cadmium-induced teratogenesis in vitro. *Teratology*, *30*(1), 47–53. https://doi.org/10.1002/tera.1420300107

Watanabe, C., Imaizumi, T., Kawai, H., Suda, K., Honma, Y., Ichihashi, M., Ema, M., & Mizutani, K. (2020). Aging of the vascular system and neural diseases. *Frontiers in Aging Neuroscience*, *12*, 557384. https://doi.org/10.3389/fnagi.2020.557384

Waterston, R. H., Lander, E. S., & Sulston, J. E. (2002). On the sequencing of the human genome. *Proceedings of the National Academy of Sciences of the United States of America*, *99*(6), 3712–3716. https://doi.org/10.1073/pnas.042692499

Webster, W. S., Brown-Woodman, P. D., & Ritchie, H. E. (1997). A review of the contribution of whole embryo culture to the determination of hazard and risk in teratogenicity testing. *The International Journal of Developmental Biology*, *41*(2), 329–335.

Wei, T., Jia, J., Wada, Y., Kapron, C. M., & Liu, J. (2017). Dose dependent effects of cadmium on tumor angiogenesis. *Oncotarget*, *8*(27), 44944–44959. https://doi.org/10.18632/oncotarget.16572

Welsh, S. J., Dale, A. G., Lombardo, C. M., Valentine, H., de la Fuente, M., Schatzlein, A., & Neidle, S. (2013). Inhibition of the hypoxia-inducible factor pathway by a G-quadruplex binding small molecule. *Scientific Reports*, *3*, Article 2799. https://doi.org/10.1038/srep02799

Williams, M. R., Arthur, J. S., Balendran, A., van der Kaay, J., Poli, V., Cohen, P., & Alessi, D. R. (2000). The role of 3-phosphoinositide-dependent protein kinase 1 in activating AGC kinases defined in embryonic stem cells. *Current Biology: CB*, *10*(8), 439–448. https://doi.org/10.1016/s0960-9822(00)00441-3

Woods, J. M., Leone, M., Klosowska, K., Lamar, P. C., Shaknovsky, T. J., & Prozialeck, W. C. (2008). Direct antiangiogenic actions of cadmium on human vascular endothelial cells. *Toxicology in Vitro: An International Journal Published in Association with BIBRA*, *22*(3), 643–651. https://doi.org/10.1016/j.tiv.2007.12.009

Xiong, Y.-W., Xu, X.-F., Zhu, H.-L., Cao, X.-L., Yi, S.-J., Shi, X.-T., Zhu, K.-H., Nan, Y., Zhao, L.-L., Zhang, C., Gao, L., Chen, Y.-H., Xu, D.-X., & Wang, H. (2021). Environmental exposure to cadmium impairs fetal growth and placental angiogenesis via GCN-2-mediated mitochondrial stress. *Journal of Hazardous Materials*, *401*, 123438. https://doi.org/10.1016/j.jhazmat.2020.123438

Xu, P., Wu, Z., Xi, Y., & Wang, L. (2016). Epigenetic regulation of placental glucose transporters mediates maternal cadmium-induced fetal growth restriction. *Toxicology*, *372*, 34–41. https://doi.org/10.1016/j.tox.2016.10.011

Xu, Z., Liu, M., Gao, C., Kuang, W., Chen, X., Liu, F., Ge, B., Yan, X., Zhou, T., & Xie, S. (2021). Centrosomal protein FOR20 knockout mice display embryonic lethality and left-right patterning defects. *FEBS Letters*, *595*(10), 1462–1472. https://doi.org/10.1002/1873-3468.14071

Yang, P.-M., Chiu, S.-J., Lin, K.-A., & Lin, L.-Y. (2004a). Effect of cadmium on cell cycle progression in chinese hamster ovary cells. *Chemico-Biological Interactions*, *149*(2), 125–136. https://doi.org/10.1016/j.cbi.2004.08.001

Yang, S.-H., Chen, S.-T., Liang, C., Shi, Y.-H., & Chen, Q.-S. (2022). Effects of cadmium exposure on leydig cells and blood vessels in mouse testis. *International Journal of Environmental Research and Public Health*, *19*(4), 2416. https://doi.org/10.3390/ijerph19042416

Yang, S.-P., Bae, D.-G., Kang, H. J., Gwag, B. J., Gho, Y. S., & Chae, C.-B. (2004b). Co-accumulation of vascular endothelial growth factor with beta-amyloid in the brain of patients with Alzheimer's disease. *Neurobiology of Aging*, *25*(3), 283–290. https://doi.org/10.1016/S0197-4580(03)00111-8

Zakrzewicz, A., Secomb, T. W., & Pries, A. R. (2002). Angioadaptation: Keeping the vascular system in shape. *Physiology*, *17*(5), 197–201. https://doi.org/10.1152/nips.01395.2001

Zhang, H., Gao, P., Fukuda, R., Kumar, G., Krishnamachary, B., Zeller, K. I., Dang, C. V., & Semenza, G. L. (2007). HIF-1 inhibits mitochondrial biogenesis and cellular respiration in VHL-deficient renal cell carcinoma by repression of C-MYC activity. *Cancer Cell*, *11*(5), 407–420. https://doi.org/10.1016/j.ccr.2007.04.001

Zhang, Y., Xu, X., Chen, A., Davuljigari, C. B., Zheng, X., Kim, S. S., Dietrich, K. N., Ho, S.-M., Reponen, T., & Huo, X. (2018). Maternal urinary cadmium levels during pregnancy associated with risk of sex-dependent birth outcomes from an e-waste pollution site in China. *Reproductive Toxicology*, *75*, 49–55. https://doi.org/10.1016/j.reprotox.2017.11.003

Zhao, H.-F., Wang, J., & Tony To, S.-S. (2015). The phosphatidylinositol 3-kinase/Akt and c-Jun N-terminal kinase signaling in cancer: Alliance or contradiction? (Review). *International Journal of Oncology*, *47*(2), 429–436. https://doi.org/10.3892/ijo.2015.3052

Zhu, S., Li, X., Dai, X., & Li, J. (2024). Prenatal cadmium exposure impairs neural tube closure via inducing excessive apoptosis in neuroepithelium. *Journal of Environmental Sciences*, *138*, 572–584. https://doi.org/10.1016/j.jes.2023.03.036

Zhu, W.-H., Iurlaro, M., MacIntyre, A., Fogel, E., & Nicosia, R. F. (2003). The mouse aorta model: Influence of genetic background and aging on bFGF- and VEGF-induced angiogenic sprouting. *Angiogenesis*, *6*(3), 193–199. https://doi.org/10.1023/B:AGEN.0000021397.18713.9c

Zhu, Y., Zhao, Y., Chai, X.-X., Zhou, J., Shi, M.-J., Zhao, Y., Tian, Y., Wang, X.-M., Ying, T.-X., Feng, Q., Sheng, J., & Luo, C. (2022). Chronic exposure to low-dose cadmium facilitated nonalcoholic steatohepatitis in mice by suppressing fatty acid desaturation. *Ecotoxicology and Environmental Safety*, *233*, 113306. https://doi.org/10.1016/j.ecoenv.2022.113306